

**SULPHONATION OF SYNTHETIC RUBBER AS AN
ALTERNATIVE MEMBRANE FOR PROTON EXCHANGE
MEMBRANE FUEL CELL**

CHRISTOPHER AVWOGHOKOGHENE IDIBIE

**A Thesis Submitted to the Faculty of Engineering and the Built Environment,
University of the Witwatersrand, in Fulfillment of the requirement for the Degree of
Doctor of Philosophy in Engineering.**

Johannesburg, 2009.

DECLARATION

I declare that this thesis is my own, unaided work. It is being submitted for the degree of Doctor of Philosophy in the University of Witwatersrand, Johannesburg. It has not been submitted before for any degree or examination in any other University.

(Signature of candidature)

_____ Day of _____

ABSTRACT

Synthesis and characterisation of PEM using aryl backbone commercial polystyrene-butadiene rubber (locally sourced) were carried out by sulphonation with chlorosulphonic acid, and assessed for its potential to serve as possible PEMFC application. The effect of weight of the polystyrene-butadiene rubber (PSBR), sulphonation time, stirring speed, concentration of sulphonation agent and sulphonation temperature on the degree of sulphonation (DS), ion exchange capacity (IEC) and viscosity of the resulting sulphonated material were investigated. Synthesized membranes were thus characterized by Fourier Transform Infra-red (FT-IR) and Proton Nuclear Magnetic Resonance (^1H NMR) to confirm sulphonation. Thermal Gravimetric Analysis (TGA) and Differential Scanning Calorimetry (DSC) were used to verify the thermal stability of the membrane, while impedance spectroscopy was used to measure the proton conductivity of the membrane. The results obtained revealed that the weight of the rubber, sulphonation time, stirring speed, concentration of sulphonating agent and the sulphonation temperature affect the DS, IEC, viscosity, thermal stability and proton conductivity of the membrane, such that, sulphonation time of 24 hrs and acid concentration of 1.6 M/ml gave the best DS, with IEC ranging from 0.23 to 2.36 mmol/g. Conductivities were in the range of 10^{-3} – 10^{-2} S/cm. However, over 2 folds increase in ion exchange capacity and degree of sulphonation was achieved on the effect of temperature. The sulphonation kinetic of PSBR was studied in $0.0016 \text{ mol L}^{-1}$ of chlorosulphonic acid where first-order kinetic model; without the effect of HCl and the effect of HCl were investigated. The reaction rate was found to obey the first-order model with the HCl produced having a desulphonation effect on the reaction. A predictive model

developed is able to predict degree of sulphonation at different initial concentration of acid. The thermodynamic study showed that the reaction is non-spontaneous, and as temperature increases the reaction system experienced phase change from liquid to solid at temperature above 328 K. The DSC and TGA analysis showed that polystyrene-butadiene rubber is a thermo stable polymer for PEM fuel cell application with a glass transition temperature (T_g) of about 198°C. Porosity of the membrane and uptake of solvent per sulphonic groups at different thickness of membrane were also calculated. The porosity of the membrane to methanol increased with a decrease in membrane thickness and increased with an increase in methanol concentration. Based on the results obtained from the porosity of the membrane to methanol and methanol up take, it can be inferred that the membrane is less permeable to methanol than water. In comparism, the porosity of the synthesised membrane to methanol was less than that of Nafion[®] which was in the range of 0.40-0.51. The results also showed that water uptake increases as the thickness of the membrane decreases. However, the membrane was found to exhibit a moderately water absorption and desorption capacity. But considering the effect of temperature, the membrane will require proper humidification especially if the fuel cell where the membrane will be used will be operated above room temperature. The electrochemical activity test was performed on a single fuel cell fed with H₂/O₂ at room temperature. An open circuit voltage (OCV) of 718.75 mV was achieved with electrode 40 wt % loaded with catalyst, while a maximum power density of 73.68 mW/cm² was recorded at 199.68 mA/cm². The effect of degree of sulphonation resulted in 3.8 fold increase in performance of the cell potential. This study therefore shows that it is feasible to synthesize an alternative PEM to Nafion[®] that will be efficient for fuel cell application from a locally available polystyrene-butadiene rubber that is of commercial quantity.

DEDICATION

This thesis is exclusively dedicated to our Lord Jesus Christ who is, who was and who is to come in the glory of God the Father, forever and ever. Amen.

ACKNOWLEDGEMENTS

I give all praise, glory and thanks to the Almighty, wonderful, miracle working and self sufficient God, who enabled me to complete this study against all odds. His grace is truly 'all sufficient'.

I wish to express my appreciation to my supervisors, Prof. S. E. Iyuke and Dr L. vanDyk for their guidance, suggestions, and encouragement throughout the period of this research.

I also wish to express my sincere appreciation to TATA Africa, University of the Witwatersrand, Johannesburg, South Africa, for the scholarship they provided to support this study.

Many thanks too to Professor Emeritus, W. Neuse, who granted me free access to his equipment to perform some of my laboratory experiments in polymer chemistry laboratory at the School of Chemistry, the University of the Witwatersrand. God bless you. The assistance of Mrs. Blessing Aderigbe, and Mr Eli in this same polymer chemistry laboratory, and Mr Kalala Mbuyi of the School of Chemical Engineering can not be forgotten. May the good Lord Jesus Christ bless you richly.

Special thanks and sincere appreciation go to my loving parents Mr. and Mrs. Sunday Ufuoma Idibie and the entire family members, for all their prayers, support, love and encouragement. May our Jehovah God cause His face to shine on you and be gracious to everyone in Jesus name. Amen.

Special appreciation is extended also to different individuals that have at one point or the other inspired me academically. I sincerely recognise the person of Emmanuel

Omudu who contributed to my academic at the early days. A big thank goes to Mr. Eric Efurhievwe and family.

I also express my candid appreciation to Dr. Mulenga Bwalya for being there for me at a critical time of this research, Dr. Olubambi Peter and his family, Mr. and Mrs. Adewale, Dr Ilemobade and family, Ndidi Ngwuluka, Leonard Okonye, Pius Fasinu, Busuyi Mekusi, Jendele Hungbo, Maria Modiba, Gladys Mabasa, Mr. and Mrs. Meswanganye and family, Holy Trinity Young Adult Family, the Kingdom Heritage fellowship faithfuls, students and staff of School of Chemical and Metallurgical Engineering, WITS University and to those whose names are too many to mention are also appreciated. Many thanks to you for touching my life positively in one way or the other during this research. God bless you all richly in Jesus' name.

My best regards and thanks also go to Willie and Diamond Akele for their strong support on every side. May the Almighty God bless you.

I also wish to recognise my research group members, Saka Abdulkareem and Samuel Afolabi. Thank you for demonstrating a high sense of trust, understanding and togetherness for us to be able to surmount every academic and emotional challenge during this study.

Furthermore, I cannot but acknowledge the laudable moral, physical and financial support of Chief Ama Johnson, the Adjere 1 of Agbarho Kingdom. Your good deeds towards me will provoke good results in your life. God bless you and members of your family richly in Jesus' name. Amen.

CONFERENCE ATTENDED

Idibie C. A, Abdulkareem A. S, Iyuke S. E, Van Dyk, L and Piennar, .H.C.vZ (2009). Modification of Polystyrene-butadiene Rubber for Proton Exchange Membrane Fuel cell. First International Conference on Multifunctional, Hybrid and Nanomaterials, 15 – 19th March, 2009. Tours, France.

JOURNAL PAPERS PUBLISHED AND PAPERS SUBMITTED

Idibie, C. A; Abdulkareem, A. S; Pienaar, H. C. vZ; Iyuke S. E and Van Dyk, L. Synthesis of Low Methanol Permeation Polymer Electrolyte Membrane from Polystyrene-butadiene Rubber. Journal of Polymer Plastic Technology and Engineering. 48: 1121–1129, 2009

Abdulkareem, A. S; Idibie, C. A; Piennar, H. C. vZ; Iyuke, S. E and Van Dyk, L. Synthesis and characterization of proton exchange membrane using Polystyrene-Butadiene Rubber. Journal of Energy and Environment. (Accepted)

Abdulkareem .A.S, Idibie .C.A, Afolabi A.S, Piennar .H.C.vZ, Iyuke S.E. and vanDyk, L. Synthesis of proton conducting membrane from polystyrene butadiene rubber for fuel cell application: The effect of sulphonating agents on the membrane characteristics. Journal of Energy Source, Part A: Recovery, Utilization, and Environmental Effect. (Accepted for publication)

Idibie C.A, Abdulkareem A.S, Piennar .H.C.vZ and Iyuke S.E. Vandyk, L. Mechanism and Kinetics of Sulphonation of Polystyrene-butadiene Rubber with Chlorosulphonic Acid. Journal of Industrial & Engineering Chemistry Research. (Accepted for publication)

Idibie C.A, Abdulkareem A.S, Piennar .H.C.vZ and Iyuke S.E. Vandyk, L. Sulphonation of Polystyrene-butadiene Rubber with Chlorosulphonic Acid for Proton Exchange Membrane: Kinetic Study. Journal of Applied Polymer Scienc. (Submitted and under review)

Idibie C.A, Abdulkareem A.S, Piennar .H.C.vZ and Iyuke S.E. Vandyk, L. Thermodynamic Study of the Sulphonation of Polystyrene-butadiene Rubber for Proton Exchange Membrane with Chlorosulphonic Acid. Journal of Applied Polymer Science. (Submitted and under review)

PATENT WORK IN PROGRESS

Iyuke S.E, Idibie C.A, Abdulkareem A.S and Piennar .H.C.vZ. Ion Exchange Membrane (provisional patent number 2009/04368)

TABLE OF CONTENTS

	Page
DECLARATION	ii
ABSTRACT	iii
DEDICATION	v
ACKNOWLEDGEMENTS	vi
CONFERENCE ATTENDED/JOURNAL PAPERS SUBMITTED	viii
TABLE OF CONTENTS	x
LIST OF FIGURES	xvi
LIST OF SCHEMES	xx
LIST OF TABLES	xxi
LIST OF ABBREVIATIONS AND SYMBOLS	xxiv
CHAPTER ONE: INTRODUCTION	1
1.1 Background and Motivations	1
1.2 Research Problem	5
1.3 Hypothesis	6
1.4 Justification of the Study	7
1.5 Scope of the Project	7
1.6 Research Question	8
1.7 Purpose and Aims	7
1.8 Expected Contribution to Knowledge	9
1.9 Thesis Outline	9

	Page
CHAPTER TWO: LITERATURE REVIEW	11
2.1 FUEL CELLS TECHNOLOGY	11
2.1.1 Functioning of Fuel Cells	12
2.1.2 General Fuel Cell Performance	14
2.1.3 Types of Fuel Cell	17
2.2 POLYMER ELECTROLYTE MEMBRANE (PEM)	18
2.3 SULPHONATION OF POLYMERIC MATERIALS FOR PEM	21
2.4 ION EXCHANGE CAPACITY AND PROTON CONDUCTIVITY OF A MEMBRANE	28
CHAPTER THREE: EXPERIMENTAL	31
3.1 Materials and Method	31
3.2 Solubility Determination	31
3.3 Sulphonation of Polystyrene-butadiene Rubber (PSBR)	32
3.4 Fourier Transform (FT) Infra-red (IR) Studies of Polymer	33
3.5 Proton Nuclear Magnetic Resonance (¹ H NMR) Studies of Polymer	33
3.6 Viscosity Measurement of Unsulphonated and Sulphonated PSBR	34
3.7 Thermal Analysis of Polymer	34
3.8 Determination of Ion Exchange Capacity (IEC) and Degree of Sulphonation (DS)	34
3.9 Quantification of HCl in Aqueous Solution of the Copolymer	35
3.10 Casting of Membrane into a Thin Film	36
3.11 Water Uptake Capacity of the Cast Membrane	37
3.12 Scanning Electron Microscopy Studies of PSBR	38

	Page
3.13 Total Solvent Uptake Determination and Porosity of Synthesised Membrane	39
3.14 Measurement of the Proton Conductivity of the Synthesised Membrane	40
3.15 Methanol Permeability Measurement	40
CHAPTER FOUR: SULPHONATION OF PLYSTYRENE-BUTADIENE RUBBER	42
4.1 The Choice of Polystyrene-butadiene Rubber	42
4.2 Preliminary Investigation	
4.2.1 Identification of a Suitable Solvent for PSBR and SPSBR	43
4.2.2 Choice of Sulphonating Agent	44
4.2.3 IR Analysis of Sulphonated PSBR with Different Sulphonating Agents	48
4.2.4 ¹ H NMR Analysis of Sulphonated PSBR with Different Sulphonating Agents	48
4.3 Sulphonation of PSBR with Chlorosulphonic Acid	52
4.3.1 Effect of the weight of polymer and sulphonation time	52
4.3.2 FT – IR and ¹ H NMR Studies	56
4.3.3 Effect of concentration of acid on the sulphonation of PSBR	58
4.3.4 Effect of stirring speed	62
4.3.5 Effect of time on sulphonation of PSBR	64
4.3.6 FT- IR analysis of effect of time on SPSBR	67
4.3.7 Effect of temperature on ion exchange capacity and degree of	

	Page
Sulphonation	70
CHAPTER FIVE: KINETIC STUDY OF THE SULPHONATION OF POLYSTYRENEBUTADIEN RUBBER	73
5.1 Kinetic Study of Aromatic Sulphonation of PSBR with Chlorosulphonic Acid	73
5.2 Reaction Mechanism of Polystyrene-butadiene Rubber with Chlorosulphonic acid	
5.3 IR and ¹ HNMR Studies of Sulphonated rubber	78
5.4 Rate of Sulphonation of PSBR	79
5.4.1 The kinetic treatment of case (A) mechanism	79
5.4.2. Rate of reaction in case (B) mechanism	82
5.5 Thermodynamic Study of PSBR Sulphonation	88
CHAPTER SIX: MEMBRANE CASTING AND CHARACTERISATION	94
6.1 Membrane Casting	94
6.2 Thermal Stability of Synthesised Membranes	94
6.3 Morphology of Unsulphonated and Sulphonated PSBR	101
6.4 Proton Conductivity of Synthesised Membranes	103
6.5 Porosity and Total Solvent Uptake	106
6.6 Methanol Crossover Study	110
6.7 Water Uptake and Water Desorption Capacity of the Membranes	117
6.8 PSBR Related Problem of Brittleness and Cure	123
6.9 Performance Testing of Synthesised Memebrane in PEMFC	124

	Page
6.9.1 Effect of degree of sulphonation on the SPSBR membrane performance	128
6.9.2 Fuel cell durability test	130
CHAPTER SEVEN: CONCLUSION AND RECOMMENDATION	132
7.1 Conclusion	132
7.2 Recommendation	135
REFERENCES	136
APPENDICES	157
1	157
2	158
3	159
4	160
5	161
6	163
7	164
8	166
9	167
10	168
11	169
12	170

	Page
13	172
14	174

LIST OF FIGURES

Figure	Page
1.1: Typical fuel cell picture	3
2.1: Schematic of a typical acid electrolyte fuel cell	13
2.2: Schematic of MEA in a single-cell testing apparatus	15
2.3: Typical polarisation curve	16
2.4: Chemical structure of Nafion	19
2.5: Poly (styrene-butadiene) rubber repeat unit structure	28
3.1: Experimental set up of chlorosulphonation of polystyrene-butadiene rubber	32
3.2: Sulphonation reaction of PSBR in chlorosulphonic acid	35
3.3: Laboratory scale tape caster	37
3.4: Schematic of two identical chamber containers for solvent permeability determination	41
4.1: IR spectra of different sulphonating agents	50
4.2: ¹ HNMR of different sulphonating agents	51
4.3: FT-IR spectra of: unsulphonated PSBR and sulphonated PSBR	57
4.4: ¹ HNMR spectra of: unsulphonated PSBR and sulphonated PSBR	58
4.5: Lump formation as a result of acid over concentration	59
4.6: SEM images of over concentration of chlorosulphonic acid	60
4.7: Effect of increasing acid concentration on sulphonation of PSBR	61
4.8: Relationship between ion exchange capacity, degree of sulphonation and viscosity	61
4.9: Effect of stirring speed on sulphonation of PSBR	63
4.10: Degree of sulphonation and ion exchange capacity as a function	

Figure	Page
of optimum reaction time	65
4.11: A graph of viscosity against degree of sulphonation and ion exchange capacity	66
4.12: IR spectra of SPSBR on the effect of sulphonation time	69
4.13: ¹ HNMR spectra of SPSBR on the effect of sulphonation time	70
4.14: Effect of temperature on the ion exchange capacity of PSBR	71
4:15: Effect of temperature on the degree of sulphonation	72
5.1: Reaction mechanism of polystyrene-butadiene rubber in chlorosulphonic acid	76
5.2: IR of short time (A) and at sulphonation > 1hr	
5.3 Kinetic of PSBR sulphonation in chlorosulphonic acid in different initial concentration of acid	80
5:4: Kinetics of PSBR sulphonation in chlorosulphonic acid: the first-order irreversible rate treatment with respect to the substrate concentration	81
5.5: First-order reversible treatment of PSBR in chlorosulphonic acid	84
5.6: A plot of degree of sulphonation against time: smooth lines represent model while marked lines represent experiment	86
5.7: Kinetics of PSBR sulphonation in chlorosulphonic acid: the effect of temperature	87
5.8: Logarithm of equilibrium constant versus the reciprocal temperature	89
5.9: Entropy plot against temperature	93
6.1: DSC curves of the unsulphonated and sulphonated rubber at	

Figure	Page
different sulphonation time	96
6.2: DSC curves of the unsulphonated and sulphonated rubber at different degree of sulphonation	96
6.3: TGA curve of the unsulphonated and sulphonated rubber at different degree of sulphonation	97
6.4: TGA curve of the unsulphonated and sulphonated rubber at different sulphonation time	98
6.5: Experimental and theoretical degree of sulphonation at different concentration of acid	100
6.6: Differential thermal curve of sulphonated and unsulphonated polystyrene butadiene-rubber at different sulphonation time	101
6.7: SEM images of (a) unsulphonated and (b-d) sulphonated rubber at DS = 2.31 %, 7.54 % and > 10 % respectively	102
6.8: Protons conductivity of the membrane at different degree of sulphonation and temperature	104
6.9: Effect of membrane thickness on the proton conductivity of the membrane at different degrees of sulphonation	105
6.10: Methanol molecule uptake per sulphonic group at different Concentration of methanol and degree of sulphonation	107
6.11: Effect of membrane thickness on the porosity of the membrane at different concentrations of methanol	108
6.12: Uptake of solution molecule per sulphonic group	109

Figure	Page
6.13: Methanol crossover concentration at different degree of sulphonation	110
6.14: Plot of $\frac{\frac{1}{2} \ln C_{A0}}{C_{A0} - 2C_B}$ against time at different degree of sulphonation	113
6.15: Methanol permeation at different degree of sulphonation and membrane thickness	115
6.16: Theoretically calculated methanol permeation	116
6.17: Water uptake at different degree of sulphonation	118
6.18: Water uptake at different membrane thickness	119
6.19: Effect of temperature and membrane thickness on water uptake and swelling ratio	120
6.20: SEM images of (g) DS < 2.5 %; (h) DS = > 7 %; (i) DS > 10 %; (j) DS > 55 %, respectively	124
6.21: Cell potential Vs current density for a single cell (25 cm ²) for electrodes operated at 25°C with H ₂ :O ₂ ratio of 1:2	126
6.22: Power density Vs current density for a single cell (25 cm ²) for electrodes operated at 25°C with H ₂ :O ₂ ratio of 1:2	127
6.23: Plot of cell potential as a function of current density drawn from experimental data and calculated	128
6.24: Plot of the power density as a function of current density drawn from experimental data and calculated	129
6.25: Performance durability for a single cell (25 cm ²) for electrode operated at 25°C	131
xiv i: A graph of Proton Conductivity Measurement of the	

Figure	Page
synthesised membrane from impedance spectroscopy	174

LIST OF SCHEMES

Scheme

5.1: Sulphonation reaction mechanism of polystyrene-butadiene rubber	75
6.1: Sulphonated PSBR	99

LIST OF TABLES

Table	Page
2.1: Various fuel cell types and their characteristics	17
4.1: Solubility determination of PSBR and SPSBR	44
4.2: Results of investigated different sulphonating agents	46
4.2 continue: Results of investigated different sulphonating agents	46
4.3: Effect of weight of polymer rubber and sulphonation time on the ion exchange capacity of the sulphonated rubber at constant stirring speed of 1000 rpm	53
4.4: Effect of sulphonation time and weight of polymer rubber on the degree of sulphonation (DS) and viscosity (η) of the sulphonated rubber carried out at a constant stirring speed of 1000 rpm	55
4.5: Results of Sulphur content analysis (%), ion exchange capacity and degree of sulphonation at varying concentration of chlorosulphuric acid	60
5.1: Amount of HCl produced alongside sulphonation of PSBR	85
5.2: K values at different sulphonation temperatures	88
5.3: Heats of different reactants and products at different temperatures	90
5.4: The heat change of different reactants at different temperature	91
5.5: ΔG_R , ΔH_R and ΔS_R at different temperatures	92
6.1: Overall diffusion coefficient of the membrane at different thickness and degree of sulphonation	114
6.2: Effect of time and temperature on the water desorption	

Table	Page
capacity of the membrane	122
i: Effect of Acid Concentration on the DS and IEC of PSBR	157
ii: Effect of Acid Concentration on DS, IEC and Viscosity on PSBR	157
iii: Effect of Time on DS and IEC of PSBR	158
iv: Effect of Time on the DS and Viscosity of PSBR	158
v: Effect of Stirring Speed on DS and IEC	159
vi: Effect of Temperature on % Sulphure (S)	160
vii: Effect of Temperature on IEC	160
viii: Effect of Temperature on DS	160
ix: Kinetics of PSBR Conversion at Different Concentrations of acid	161
x: $-\ln(1-X)$ as a Function of Time	161
xi: $C_0\{-X-\ln(1-X)\}$ as a function of Time	162
xii: Model data	162
xiii: Water Uptake at Different Degrees of Sulphonation and Constant Membrane Thickness of 350 μ m	163
xiv: Water Uptake at Different Membrane Thickness and Constant Degree of Sulphonation (9.4%)	163
xv: Effect of Hydration and Temperature on Proton Conductivity at Different Degrees of Sulphonation	164
xvi: Effect of Membrane Thickness on the Proton conductivity of the Membrane at Different degree of Sulphonation	165
xvii: Methanol Molecule Uptake Per Sulphonic Group at Different	

Table	Page
Concentration of Methanol	166
xviii: Effects of Membrane Thickness on the Porosity of the Membrane at Different Concentration of Methanol	167
xix: Uptake of Solution Per Sulphonic Group	168
xx: Methanol Crossover Concentration at Different Degree of Sulphonation	169
xxi: Performance of MEA at Different Weight of Catalyst, Constant Membrane DS (39.38%) and Nafion 112	170
xxii: Power Density at Different Weight of Catalyst, Constant Membrane DS (39.38%) and Nafion 112	171

LIST OF ABBREVIATIONS AND SYMBOLS

ABBREVIATIONS

AFCs	Alkaline fuel cells
APUs	Auxiliary power units
AcSO ₄ H	Acetylsuphate
BaCl ₂	Barium chloride
BaSO ₃	Barium sulphite
<i>C</i>	Concentration
<i>C</i> ₀	Initial concentration
<i>C</i> _A	Concentration of methanol in compartment A
<i>C</i> _B	Concentration of methanol in compartment B
CDCl ₃	Chloroform
C ₂ H ₄ Cl ₂	1, 2 dichloromethane
CH ₂ Cl ₂	Dichloromethane
CHCl ₃	Trichloromethane
ClSO ₃ H	Chlorosulphonic acid
CO	Carbon monoxide
<i>d</i> _m	Membrane thickness.
DMFCs	Direct methanol fuel cells
DMF	Dimethylformamide
DMAc	Dimethylacetemide
DMSO	Dimethylsulphoxide
DS	Degree of sulphonation
DSC	Differential scanning calorimetric
DTA	Differential thermal analysis

GDL	Gas diffusion layers
<i>EW</i>	Equivalent weight
E_T	Theoretical voltage
F-H ₂ SO ₄ H	Fuming sulphuric acid
FTIR	Fourier transform infra-red
¹ H NMR	Proton nuclear magnetic resonance
HCl	Hydrochloric acid
H/F	Mixture of sulphuric acid and fuming sulphuric acid
IEC	Ion exchange capacity
IEMFC	Exchange membrane fuel cells
kPa	Kilopascal
kW	Kilowatts
mA	Miliampere
mW	Miliwatt
MEA	Membrane electrode assembling
MCFCs	Molten carbonate fuel cells
M_{PSBR}	Molecular weight of polystyrene butadiene
$M_{W_{SO_3H}}$	Molecular weight of SO ₃ H
Mw	Molecular weight
mV	Milivolt
NaOH	Sodium hydroxide
NO _x	Nitric oxide
OCV	Open circuit voltage
PAFCs	Phosphoric Acid Fuel Cells

PE	Petroleum ether
PEEK	polyether-ether-keton
PEMFCs	Proton exchange membrane fuel cells
PTFE	polytetrafluorethelene
PSBR	Polystyrene-butadiene rubber
PSS	Polystyrene sulphonate
RD&D	Research, development and demonstration
rpm	Revolution per minutes
Sc	Sulphur content
SEM	Scanning electron microscopy
SOFCs	Solid Oxide Fuel Cells
SO _x	Sulphide oxides
SPEFCs	Solid polymer electrolyte fuel cells
SPSBR	Sulphonated polyetyrene-btadiene rubber
T_{dry}	The thickness of dry membranes
TGA	Thermo gravimetric analysis
T_g	Transition temperature
T_{wet}	Thickness of wet membranes
UV	Ultraviolet
W_{wet}	Weight of wet membranes of dry membrane
W_{dry}	Weight of dry membranes

SYMBOLS

\mathcal{D}_{Am}	Diffusion coefficient
K^m	Proportional constant

\mathcal{D}_m	Overall methanol diffusion coefficient
J	Methanol permeation
V	Voltage
V_o	Initial volume
ρ_{dry}	Density of dry membrane
ρ_{sol}	Density of the methanol solution
ε	Porosity of the wet membrane
x_{water}	Molar fraction of water in the solution
λ_{total}	Overall uptake of solvent molecules
σ	proton conductivity
T	Thickness
R	Resistance
η	Inherent viscosity
X	conversion
t	Time
k_I	First-order rate constant
$S\text{ cm}^{-1}$	proton conductivity
Ω	total cell resistance
F	Faraday's constant
ΔG	Free energy of the fuel
η	Over potential or over voltage
E	Ideal equilibrium potential
E°	Ideal standard potential
E_a	Activation energy

CHAPTER ONE

1.0 INTRODUCTION

1.1 Background and Motivations

Attaining sustainable energy development is posing a major challenge globally as a result of over-dependence on fossil fuel, resulting in energy crises due to a shortage in supply, price instability (Wonbong et al., 2006; Edward, 1987) and incessant adjustment of energy policies. In practical terms, fossil fuels are finite in nature and its reserves have shrunk in recent years. As of today, oil is the major source of energy, and on the average, the world uses more than 26 billion barrels of oil yearly (Campbell 2004). The growth of human population globally is also on the increase. The increasing energy demands all over the world, the depleting reserves of fossil fuels and the reliance on uranium based fuel have necessitated serious effort to engage and develop alternative sources of energy in order to bridge the current inevitable gap between energy supply and demand (Schwarz, 2006; Yi and Nguyen, 1999; Lee et al., 2004). This indicates that failure to balance energy production with increasing energy demand may threaten economic security.

In fact according to the General Energy Council (Algeniene Energieraad, AER), there is the likelihood that a large scale exploration and production of oil will diminish significantly after the first few decades of this century. This problem can occur as early as 2030 because world oil stocks do not cover expected needs and as such, the high cost of exploring the remaining oil stocks will therefore lead to high prices of oil and oil based materials and products (Heijden and Baarle, 2002).

In another vein, the impact of burning fossil fuel on the earth biosphere can not be ignored since human life is largely dependent on the ecosystem. Urgent ways of providing energy with zero or less greenhouse effect have gained momentum in recent times due to the large scale effect of carbon emissions on the atmosphere. Though there is no energy source that is completely environmentally safe, energy must be generated and used more wisely in order to reduce environmental hazards and optimize the efficiency with which it is produced (Kevin and Lewis, 1984). It therefore becomes imperative to improve the quality of life through the development of highly efficient, cleaner and more environmental friendly energy devices and utilization systems, which possess the virtues of sustainability and low environmental impact. As a result, the fuel cell is recognised as a promising alternative (Wonbong et al., 2005; Xianguo, 2006).

A fuel cell (Figure 1.1) is an electrochemical device that converts the chemical energy of the reactants (both fuel and oxidant) directly into electrical energy (Xianguo, 2006). Typical fuel cells include Alkaline Fuel Cells (AFCs), Phosphoric Acid Fuel Cells (PAFCs), Proton Exchange Membrane Fuel Cells (PEMFCs), Molten Carbonate Fuel Cells (MCFCs), Solid Oxide Fuel Cells (SOFCs) and Direct Methanol Fuel Cells (DMFCs). However, the PEMFC happens to be one of the most efficient, portable power sources convenient for vehicular transportation, residences and home devices, institutions, mobile electronic devices and industrial applications (Gao et al., 2003; Steele and Heinzl., 2001; Quan et al., 2005; Chedie and Munroe, 2003). This is as a result of their high-power density which makes them compact and lightweight, coupled with their rapid response to varying load, relatively quick start up, low operating temperature and approximately zero emission which makes them more environmentally friendly (Quan et al., 2005; Shibasaki et al., 2005).

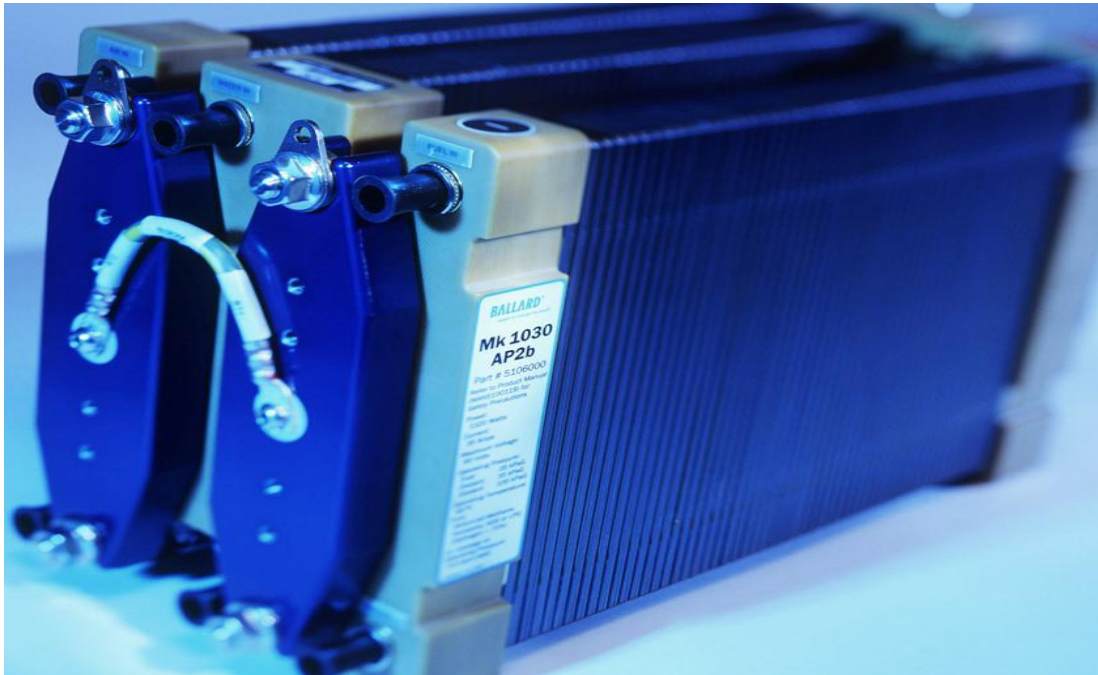


Figure 1.1: Typical fuel cell picture (Ballard[®] Fuel Cells, 2007)

The fundamental structure of the PEMFC is two electrodes, an anode and a cathode separated by a solid membrane that acts as an electrolyte (Maher and Sandi, 2005; Hogarth et al., 2005; Iyuke et al., 2002). The membrane functions as an ionic conductor between the two electrodes, a barrier for passage of electron and gas cross leakage between electrodes (Gao et al., 2003; Xing et al., 2004). The electrodes provide active surface sites for ionization and de-ionization of the fuel and oxidant, it acts as a physical barrier between ions in the gaseous stream and liquid electrolyte, and it provides a porous interface between ions in the gaseous stream and ions conducting electrolyte (Hays, 2005; Song et al., 2002).

The polymer membrane which is recognised as one of the key components in PEMFC has a principal function to conduct or rather allow the transport of protons generated at the anode, and simultaneously opposing direct contact between the fuel and the oxidant (Bai et al., 2006). The heart of the fuel cell is the membrane electrode assembling (MEA), which

consists of a proton exchange membrane, a catalyst layer, and gas diffusion layers (GDL). The structure and composition of the MEA are of vital importance (Costamagna and Srinivasan, 2000) in order to: minimise all forms of over-potential and maximise power density; minimise the noble metal loading (and thus, the cost per kW of the PEMFC) in the gas diffusion electrodes by high utilisation of the surface areas of nanosized particles of the electrocatalyst; effective thermal and water management and; to attain the lifetime of the PEMFC as necessary for power generation, transportation and portable power application.

Since PEMFCs function electrochemically, the performance of the PEM used as an electrolyte and separator, therefore, becomes very crucial to the functioning of these types of fuel cells (Kerres, 2001). But in order to qualify for fuel cell application, the PEM should possess some salient properties such as excellent chemical stability especially against the attack of oxygen and strong acids, high proton conductivity, suitable water uptake, resistance to fuel crossover and adequate mechanical properties (Gao et al., 2003). At present, the only commercially available PEM in use is the perfluorinated ionomer Nafion[®]. Though it guarantees high proton conductivity ($\sigma \geq 10^{-2} \text{ S cm}^{-1}$) and excellent durability under the fuel cell operating conditions (a life time of 50,000 hrs) (Ralp, 1997), the large scale application is limited by the high cost of the membranes. This membrane type also exhibits some other serious drawbacks such as high methanol permeation and dehydration at high temperature (> 80°C) (Gao et al., 2003) and therefore loss of conductivity. These negative features hinder their further application (Savadogo, 1998; Inzelt et al., 2000).

Therefore, in order to develop a cheaper and a possible alternative to the perfluorinated ionomer Nafion[®] membranes that would not exhibit the same disadvantageous properties, sulphonation of polystyrene-butadiene rubber (readily available locally) will be carried out to

synthesise PEM. Sulfonation in this context is a practical means of modifying the structure and properties of the polymers to serve as ion exchange membranes by tailoring the degree of sulphonation with sulphonating agent(s).

1.2 Research Problem

The strong need to improve the quality of life by developing highly efficient, cleaner and more environmental friendly energy generators and utilization systems other than fossil fuel brings about the drive for sustainable energy development systems (Song, 2002). Fuel cells have been suggested as a more feasible alternative energy source because they are free from undesirable emissions (Costamanga and Srinivasan, 2001; Steele and Heinzel, 2001; Larminie and Dicks 2000). At present, the PEM fuel cell has gained recognition as the most promising of all the fuel cell systems, based on their potential for portable power systems, sustainability and reliability (Jang et al., 2005; Sopian and Wan Daud, 2006; Smitha et al., 2005; Li et al., 2005).

Nafion[®], which is based on a perfluorinated ionomer produced by DuPont, is the only commercially available PEM for PEMFC (Gao et al., 2003; Wilson and Gottesfeld, 1992; Zawodzinski et al., 1993; Ren et al., 1996). Although Nafion[®] has been widely used due to its attractive properties such as high mechanical strength, high oxidative and hydrolytic stability and high ionic conductivity (Xing et al., 2004; Wang et al., 2005; Song et al., 2005), it is known to be faced with very serious drawbacks such as loss of conductivity at high temperature (> 80 °C), high permeability to the fuel, as well as, extremely high cost and monopoly of few nations and companies that supply the membrane. These factors hinder the development of perfluorinated polymer membranes for full commercial application (Song et al., 2002; Chen et al., 2005; Dimitrova et al., 2002; Zongwu et al., 2006; Bahir et al., 2001).

In an attempt to reduce the high cost of polymer membrane, research and development of novel polymer electrolyte membranes have been intensified in recent times in order to provide alternatives to Nafion[®]. However, the problems associated with it remain that of lower proton attraction, low electrical conductivity and contact area, higher permeability to the fuel and excessive swelling (Chen et al., 2005). These problems are attributed to the process route(s) used in introducing the sulphonated graft chain into highly chemically stable fluorinated polymers, which result in poor bonding of the catalyst layer to the grafted membrane, leading to excessive use of catalyst with very high cost. Therefore they are not suitable for commercial realization of PEM (Chen et al., 2005; Lee, 2004). Hence the world's biggest challenges in relation to efficient and clean energy consumption are to reduce the cost of the membrane for PEMFC and the upscaling of laboratory findings into commercial benefit. Because of the rising awareness and interest in PEMFC as a promising alternative source of energy, the need to reduce the cost of the membrane is therefore very crucial. This could be achieved by using a non-fluorinated membrane by sulphonating a polymer backbone of polystyrene-butadiene rubber that is cheap and readily available locally.

1.3 Hypothesis

An alternative membrane for PEM fuel cell could be synthesised through sulphonation process using polystyrene-butadiene rubber. This rubber has excellent mechanical properties arising from the two-phase microstructure (polystyrene which is a thermoplastic domain dispersed in a rubbery butadiene continuous phase). Controlling the degree of sulphonation during modification of the polymer should produce a polymer electrolyte membrane that is proton conductive with the required mechanical properties suitable for PEM fuel cell application.

1.4 Justification of the Study

Efforts are being made to develop alternative and more economical membranes from perfluorinated and non – perfluorinated polymer materials globally. The results appear promising, but with some lapses in properties under fuel cell consideration. The first membrane employed in the Gemini program was a crosslinked polystyrene sulphonic acid used as both an auxiliary power source and a source of water for the astronauts (William, 2002). This membrane generated one kilowatt (1 kW) in a fuel cell stack (Liebhafsky and Cairns, 1968; Okada and Yokoyama, 2001). However, the monomer polystyrene sulphonic acid membrane was not durable enough under actual PEM fuel cell operating conditions. The initial poor performance of this polystyrene has not deterred other researchers from continuing research on modifying polystyrene materials (Williams, 2002) due to its promising nature. Polystyrene-Butadiene Rubber (PSBR), a high-breed of polystyrene has not been investigated sufficiently in view of fuel cell application, and precisely no work has been done on the kinetic study of sulphonated aromatic PSBR. This research, therefore, addresses the development of PEM that could serve as an alternative to Nafion[®]. This will be achieved by synthesising ion exchange membranes that are proton conductive from locally available material such as PSBR. PSBR is readily available in South Africa, it is, therefore, an adequate resource material for the preparation of this polymer membrane, even at a reduced cost. Kinetic study of the synthesised membrane will also be considered.

1.5 Scope of the Project

Synthesis of a polymer electrolyte membrane for fuel cell application is the main focus of this study. Achieving the required properties will thus depend on the type of materials, method of fabrication, degree of sulphonation, phase separation into hydrophobic – hydrophilic domains, etc., hence the scope of this research will encompass sulphonation of polystyrene-

butadiene rubber, membrane fabrication for fuel cell application, characterisation, conductivity measurement and testing of MEA in PEM fuel cell stack.

1.6 Research Question

Is it possible to synthesise PEM for fuel cells application that would not suffer the major drawbacks inherent in the currently available membranes from a low cost and locally available polystyrene-butadiene rubber?

1.7 Purpose and Aims

The main purpose of the research is to develop a possible alternative PEM for PEM fuel cell using locally available polystyrene-butadiene rubber. The research will be achieved from the following objectives:

- ✚ Sulphonation of the polystyrene-butadiene rubber (phenyl group) at various concentrations of sulphonic agent, reaction times, stirring rates and temperatures.
- ✚ To study the kinetics of aromatic sulphonation of the PSBR for PEM synthesis.
- ✚ Analysis of the chemical and physical properties of the sulphonated polymer
- ✚ To cast thin film membranes from sulphonated polystyrene - butadiene-rubber solution
- ✚ Membrane characterization to determine the thermal stability, degree of sulphonation, water uptake and swelling, methanol permeation, diffusion coefficient, ion exchange capacity and proton conductivity
- ✚ Comparison of the properties of the synthesised membrane with the required properties for PEMs.
- ✚ Membrane-electrode-assembling (MEA) test in a fuel cell stack

1.8 Expected Contribution to Knowledge

This work aims at synthesising a possible alternative PEM for fuel cell application because one of the major challenges in PEM fuel cell research and development is to reduce the production cost of the fuel cell by reducing PEM cost for economic effectiveness. This research is therefore not only going to synthesise PEM from a low cost base material but is also expected to:

- ✚ Provide the necessary background for the development of a non-polyfluoro membrane using polystyrene-butadiene rubber easily sourced within South Africa.
- ✚ Provide knowledge on the kinetics of aromatic sulphonation of PSBR using chlorosulphonic acid
- ✚ Tailoring the degree of sulphonation for PEM synthesis suitable for PEM fuel cell, and coupled with its kinetic study, this work will therefore be useful for engineering design and application of PEM.
- ✚ This work will provide useful information on the output testing of the MEA in PEMFC stacks.
- ✚ As a means of advancing the science of fuel cell technology.

1.9 Thesis Outline

The outline of the entire thesis will include:

Chapter one

This chapter discusses the background and motivation of the study, research problem, hypothesis, justification of the study, scope of the project, research questions, purpose and aims and the expected contribution to knowledge.

Chapter two

This chapter, which contains the literature review, will be structured into three parts: The first part gives an overview of fuel cell and their types, the second part focuses mainly on PEM fuel cell while the third part discusses the sulphonation process of polymeric materials for PEM fuel cell application.

Chapter three

This chapter explains the experimental procedure of polymer electrolyte membrane synthesis from polystyrene-butadiene rubber, methods of characterisation and physico-chemical test.

Chapter four

Chapter four discusses experimental results of the rubber sulphonation in terms of degree of sulphonation, ion exchange capacity and its viscosity.

Chapter five

This chapter deals with the kinetic study of polystyrene-butadiene rubber.

Chapter six

Chapter six discusses the membrane casting and characterisation, the ionic conductivity and the electrochemical performance of the membrane-electrode- assembly test.

Chapter seven

Chapter seven is the concluding part of the thesis, which gives a summation of the research and the recommendations for further development of the process used in the study.

CHAPTER TWO

2.0 LITERATURE REVIEW

2.1 FUEL CELL TECHNOLOGY

Fuel cells are electrochemical devices that convert the chemical energy of reactants (both fuel and oxidant) directly into electrical energy (Xianguo, 2006). The direct chemical conversion into electricity and heat does not involve combustion cycles. Therefore, the use of the thermal-mechanical-electric sequence with Carnot's theorem limitation in the conventional indirect technology is avoided (Kordesh and Simader, 1996). Although heat engines and fuel cells are both energy conversion devices that require reactants being stored externally, fuel cells on the other hand have the overall efficiency to produce profitable energy which is about twice that obtainable by means of conventional combustion engines (Alcaide et al, 2006). This is because, the operation of fuel cells at a known temperature generates electrical energy by electrochemical process of the reactants in one step without any intermediate form of energy.

Fuel cells are also like dry cell batteries in terms of construction, but unlike batteries, fuel cells do not require recharging because they do not run down or undergo material changes. They have unlimited lifetime in principle, as long as the reactants are supplied and products removed continuously. In addition, fuel cells are generally identified as one of the most promising and potential energy technologies which meet the requirements for energy security, economic growth and environmental sustainability arising from zero emission (Xianguo, 2006). Although fuel cells are few years behind other competitive technologies (steam turbine and internal combustion engines) in terms of development and use, this concept was first introduced by Sir W. R Grove in 1839 (Larminie and Dicks, 2000). He

demonstrated the direct conversion of chemical energy to electrical energy in a hydrogen/oxygen fuel cell.

The first PEM fuel cell was developed by General Electric in the US in the 1960's for auxiliary power sources for the Gemini space missions (Bockris and Srinivasan, 1969). This early version is known to have a life time of 500 hours though still considered sufficient for the early missions (Warshay and Prokopius, 1990; Larminie and Dicks, 2000). As development of the PEM fuel cell continued, a major breakthrough became evident in 1966 with the introduction of a new polymer membrane in 1967 known as Nafion, a registered trademark of Dupont de Nemours Company as an electrolyte for PEM fuel cell (Larminie and Dicks, 2000). This is the only commercially available, state-of-the-art membrane that is successfully employed in PEM fuel cell (Zongwu et al., 2006). However in the 1970's and early 1980's the development of PEM fuel cell went into abeyance and in the 1980's PEM fuel cell indeed experienced a renaissance in the areas of low platinum loading electrodes (reduction factor of 100 for platinum loading), the use of thin film electrodes and increase in current density to around 1 A.cm^2 or more (Larminie and Dicks, 2000). Currently fuel cells are coming into the market and one of their promising areas of application is the automotive industry, where cars and buses are already running on fuel cells. Fuel cells, intended to power stationary and portable electronic devices such as cell phones, personal digital assistants and laptop computers on micro power, are seen to be the key technical and economical driver for the entire fuel cell market (Atkinson, 2005).

2.1.1 Functioning of Fuel Cells

A fuel cell is made up of three active components namely; a fuel electrode (anode), oxidant electrode (cathode), and an electrolyte in-between the electrodes as shown in Figure 2.1.

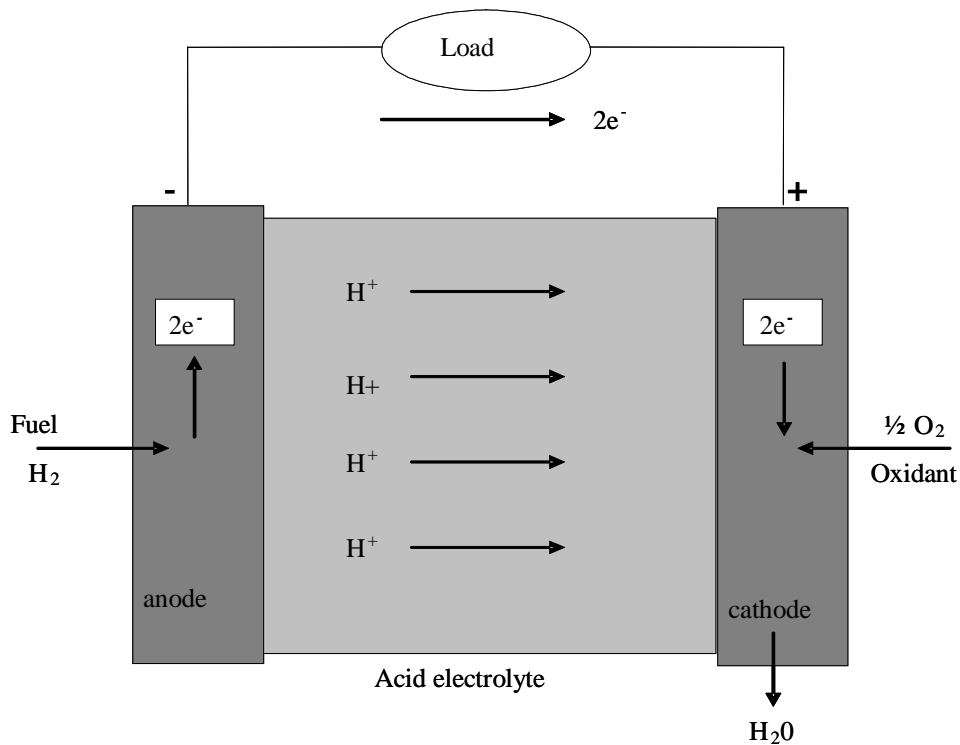
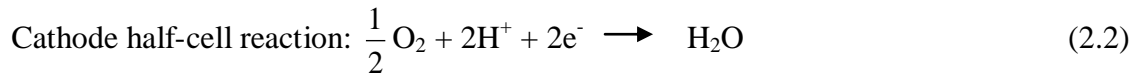


Figure 2.1: Schematic of a typical acid electrolyte fuel cell (Xianguo, 2006)

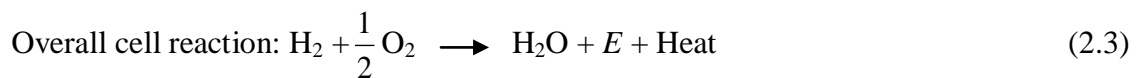
The functioning of fuel cell involves the molecular hydrogen being delivered from a gas stream to the anode and then reacts electrochemically in the anode as in equation (2.1). Generally the hydrogen is oxidised at the anode/electrolyte interface into a hydrogen ion or proton H⁺ and gives up an electron e⁻ (Xianguo, 2006).



The proton migrates through the electrolyte, while the electrons flow through the electrode and to an external circuit. Both the electron and proton arriving at the cathode react with the oxidant which is usually oxygen supplied from an external gas flow stream and thus reduces oxygen to form water as illustrated in equation (2.2).



It is important to know that both the electric current and mass transfer of the H^+ ion form a complete circuit, where the electrons migrate through the external electrical circuit, do work on the electric load and thus, representing the useful output of electrical energy (E) from the fuel cell. Simultaneously, waste heat is generated due to; electrochemical reactions taking place at the anode and the cathode, the migration of protons through the electrolyte as well as electron transporting in the solid portion of the electrodes to the external circuit (Xianguo, 2006). Thus the two half-cell reactions give an overall cell reaction as:



In order to maintain a continuous isothermal operation for electric power generation, it is important to remove the by-product of heat and water continuously. This is known as water and thermal management (Larminie and Dicks, 2000; Xianguo, 2006). The half-cell reactions may vary with fuel cell types but the overall cell reaction is the same for all types of fuel cells.

2.1.2 General Fuel Cell Performance

A typical fuel cell usually produces a high current and low voltage (Nazan, 2001) as a result of polarisation effect. But a practical voltage of 0.9 Volts/cell can be realised by connecting many individual cells in series or in parallel to form what is known as a cell stack (Figure 2.2). The use of a 'bipolar plate' is an important method of cell interconnection. While series connection yields high voltage, parallel connection allows a stronger current to be drawn.

This, in turn, increases losses in the fuel cell and results in less efficiency. However, the output voltage depends not only on the voltage of each cell but the number of cells making the stack.

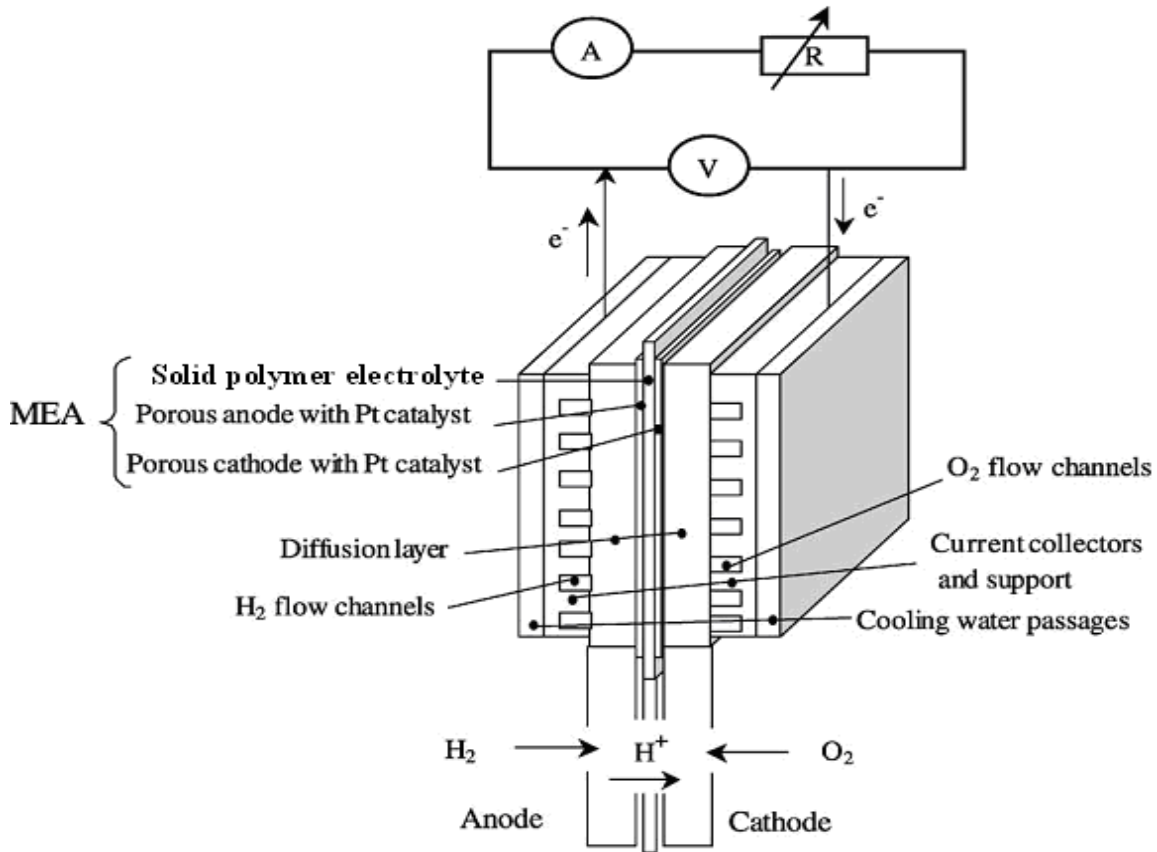


Figure 2.2: Schematic of MEA in a single-cell testing apparatus (Iyuke et al., 2003)

In the operation of fuel cells, generally, the anode is known to have lower electric potential, the cathode a higher electric potential, and the difference in their electric potential constitutes what is known as the actual cell potential (Xianguo, 2006). However, fuel cells always experience energy losses in terms of potential losses as a result of many irreversible reactions which have the tendency of reducing the cell potential difference to about 0.7 V. If no loss is experienced in the fuel cell, then, a reversible process where all the Gibbs free energy is converted into electrical energy is achieved (Larminie and Dicks, 2000). The efficiency of a

cell is almost proportional to its voltage since most losses can be attributed to voltage drop in the cell. The phenomena of voltage loss, often called overpotential or overvoltage, is referred to as polarisation and the plot of cell voltage change as a function of cell current density is called the polarisation curve (Figure 2.3).

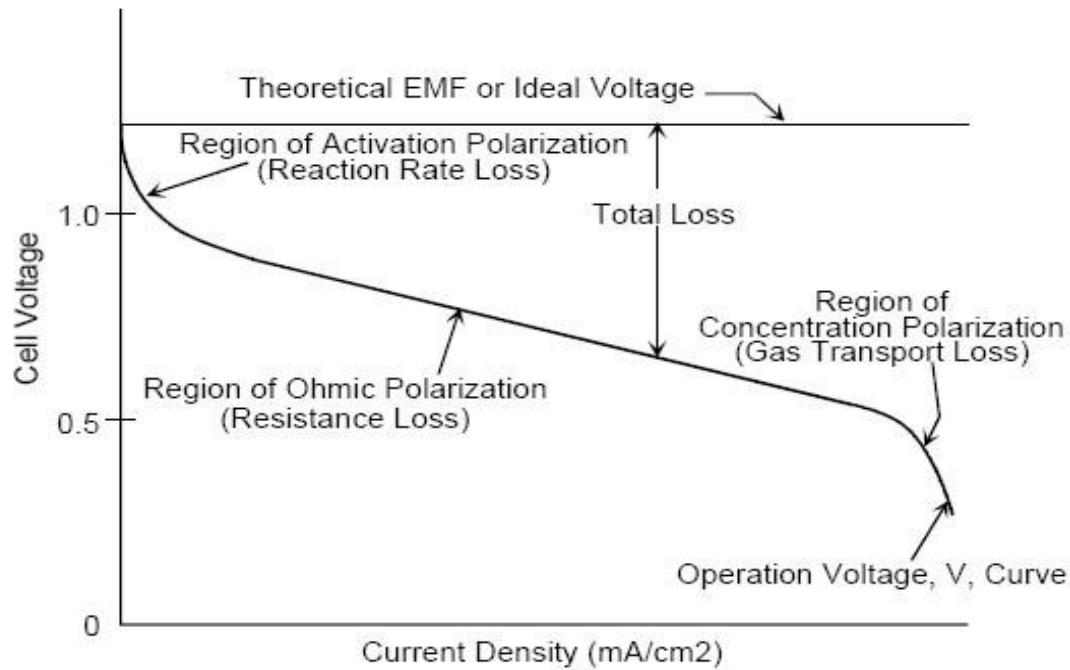


Figure 2.3: Typical polarisation curve (Clauwaert et al., 2008)

Figure 2.3 is a polarisation curve which shows the relationship between the voltage and current density when an external load is connected to the cell. The three regions of voltage losses are indicated on the curve: ohmic, activation and mass transport or concentration polarization which can as well be investigated with the polarization curve.

In fuel cells, direct current is produced which may not be suitable for direct connection to an electrical load and, hence, an inverter is required to convert the output to alternating current. However, there are some areas of concern in fuel cell technology. One of such is the slow

reaction rate that constitutes low currents and power as a result of low probability of molecule not having enough energy to overcome the energy hill (classical) poses some degree of concern in fuel cell technology. As a result, the use of catalyst, raising the temperature and increasing the electrode surface area of the system are given a robust attention. Another area of concern is that hydrogen as a fuel is not readily available (Larminie and Dicks, 2000). It is true that the by-products of fuel cells are water and heat, making it environmentally friendly, but if sources of fuel are not pure (natural gas, low-sulphur distillate, methyl fuel, heavy oils, coal, solid waste, biomass, off-gas etc) unwanted substances may be emitted into the environment, and as such, draw some level of concern for the environment.

2.1.3 Types of Fuel Cell

Table 2.1 shows the various fuel cell types and their characteristics.

Table 2.1: Various fuel cell types and their characteristics

Type of Fuel Cells	Mobile Ion	Operating Temperature	Fuel Efficiency	Applications
AFCs	OH ⁻	50 - 200 °C	40-60	Space, mobile
PAFCs	H ⁺	~200 °C	55	Dispersed and distributed power
PEMFCs	H ⁺	50 -100 °C	45-60	Portable, mobile, space, stationary
MCFCs	CO ₃ ²⁻	~650 °C	60-65	Distributed power generation
SOFCs	O ²⁻	500 -1000 °C	55-65	Base load power generation
DMFCs	Varies	90 °C	34	Portable, mobile

where AFCs = Alkaline fuel cells, PAFCs = Phosphoric acid fuel cells, PEMFCs = Proton exchange membrane fuel cells, MCFCs = Molten carbonate fuel cells = SOFCs = Solid oxide fuel cells, DMFCs = Direct methanol fuel cells

2.2 POLYMER ELECTROLYTE MEMBRANE (PEM)

The central component of the PEM fuel cell is the polymer electrolyte membrane which is also called the proton exchange membrane. It functions both as an electrolyte for transporting protons from the anode to the cathode and as a barrier to the passage of electrons as well as a gas cross-leak between the electrodes (Xing et al., 2004). The type of electrolyte used determines the characteristics of any PEM fuel cell including its construction, material selection and operation. In order for any polymer membrane to qualify for fuel cell application, it must possess some salient properties such as excellent chemical stability (especially against the attack of oxygen and strong acids), high proton conductivity ($> 10^{-2}$ S/cm), suitable water uptake, resistance to fuel crossover and adequate mechanical properties (Gao et al., 2003; Kreuer, 2001). However, the polymer electrolyte membrane will only be conductive when it is hydrated. This, therefore, limits the operating temperature of PEM fuel cells to that of boiling point of water, which makes water management a serious issue in PEM fuel cell technology (Mikkola, 2001). Although some membranes are self humidifying, these are membrane types which make use of small fuel and oxidant with little fuel crossover (Balkin, 2002).

The polymeric structure of the electrolyte membrane contains ionisable groups or functional groups such as SO_3H (sulphonic acid) or any salt of alkali cations like SO_3Na , SO_3Li , SO_3K , SO_3Rb etc, which upon dissociation produces two ionic components of its kind. As one of the components (SO_3^-) is retained in the structure the other component is a mobile or replaceable, simple ion known as the counter ion (H^+ , Li^+ , Na^+ , K^+ , Rb^+ etc) which is electrostatically related to the fixed ion. The counter ion freely undergoes exchange with ions of same sign from the solution (in the presence of water), hence it is called ion exchange membrane (Xianguo, 2006).

The present state-of-the-art membrane (Figure 2.4) which is a perfluorinated ionomer Nafion, successfully employed in PEM fuel cell (Zawodzinski et al., 1993; Yan et al., 2006) due to their excellent chemical and mechanical stabilities as well as high proton conductivity (Yan et al., 2006). These qualities are attributed to the three regions that it is composed of: region one is the hydrophobic semi crystal ionic (poly – tetrafluoroethylene), that is primarily made up of the backbone chains.

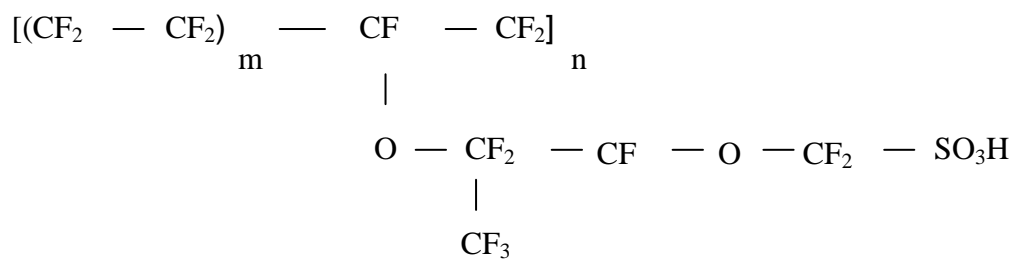


Figure 2.4: Chemical structure of Nafion

This provides structural stability to the membrane and prevents it from dissolving in water; region two is largely empty and amorphous, made up of side chains (normally spaced with perfluoro vinyl ether) and some sulphonic acid groups and; region three is made up of strong clusters of hydrophilic sulphonate ionic groups that are used for conducting proton across the membrane (Haubold et al., 2001; Dhar, 2005). However, they have three major drawbacks: very high cost; loss of conductivity at high temperature (> 80°C); and high methanol crossover. These negative characteristics result in dramatic loss of proton conductivity due to dehydration of the membrane and thus hinder their further application (Zonqwu et al., 2006; Savadog and Mater, 1998; Inzelt et al., 2000). In fact, on the very high cost of Nafion[®], existing literature has it to be U.S\$ 700 m⁻² corresponding to U.S\$ 135 kW⁻¹ at 0.65 V, which is known to be closer to the operating potential of a stationary power plant. This is considered

to be too costly, particularly for widespread application of PEMFCs in passenger cars (Ralp, 1997). As a result of the crucial disadvantages associated with these membranes, huge efforts are put into developing alternative more economical non-perfluorinated polymers that can be used as PEM for high temperature use (Xing et al., 2004).

Homopolymer, random copolymers and block, as well as graft copolymers containing aromatic rings or double bonds, have been recognized as suitable materials for PEMs in fuel cell application (Smitha et al., 2003). Hydrocarbon polymers containing polar groups that retain considerable high amount of water over a wide range of temperature are known to be particularly attractive and relatively cheaper to synthesise than their perfluorinated counterparts (Zonqwu et al., 2006).

Exploring copolymers, especially with aromatic ring, has therefore, received much attention in recent times for proton exchange membranes because of their inherent combined characteristics that enhance membrane properties suitable for fuel cell application. Based on a general belief that no single material possesses all the excellent properties required for membranes, polymer materials are, therefore, required to be subjected to some modifications to improve their performance for specific application such as fuel cell (Huange et al 2001). Preparations of Polystyrene sulphonate (PSS) membranes from sulphonated copolymer of styrene-ethylene-butylene have been carried out recently. This was achieved with the aromatic rings being sulphonated. This promotes the flexibility of the membrane against brittleness, necessary to make good contact with the electrodes (Cheng et al., 2004).

Numerous studies have been carried out on the hydrogenated form of sulphonated polystyrene-butadiene salts in terms of morphology, chemical and physical properties

(Mokrini and Acosta, 2001; Weiss et al; 1991a & b). In this research, the focus is on the chemical modification of a copolymer rubber, polystyrene-butadiene rubber by sulphonation for fuel cell application. Polystyrene butadiene rubber is cheap and it possesses attractive mechanical properties and high chemical stability. Tailoring the degree of sulphonation is vital in order to balance hydrophilic-hydrophobic performance of the membrane and to reduce excessive swelling in aqueous environment.

2.3 SULPHONATION OF POLYMERIC MATERIALS FOR PEM

In recent times polymeric materials have found a very promising area of application as ion-conductive membranes for batteries (Samuleson et al; 1998) or as proton exchange membrane for fuel cells (PEMFC) (Yeager and Steak, 1981; Scherer and Bunsenges, 1990; and Savadogo and Mater, 1998). Sulphonation of complex molecules is a technique widely used in chemical processes (Larminie and Dicks, 2000). Early sulphonation treatments were geared towards hydrophilicity of membrane improvement, because hydrophilic membrane offer and retain relatively higher water flux based on the enhanced antifouling capacity and favourable hydrodynamic environment of the membranes (Huang et al., 2001). Currently, sulphonation is being geared towards performance enhancement of pervaporation and gas separation membranes (Ihm and Ihm, 1995; Kruczek and Matsuura, 2000). Sulphonation being a powerful and versatile process is simultaneously used to render polymers proton conductive and hydrophilic in nature, which can be achieved either in the form of free acid ($-\text{SO}_3\text{H}$), a salt (e.g. $-\text{SO}_3^-\text{Na}^+$) or an ester ($-\text{SO}_3\text{R}$) (Smitha et al., 2003).

There are, therefore, two methods of preparing sulphonated hydrocarbon polymers. These are direct polymerization of sulphonated monomers (Rikukawa and Sanui, 2000) and post-sulphonation of prepared polymers using different sulphonating agents such as concentrated

sulphuric acid, fuming sulphuric acid, trimethylsilyl chlorosulphonate, sulphur trioxide-triethyl phosphate complex and chlorosulphuric acid (Zonqwu et al., 2006). The post-sulphonation reactions involve aromatic electrophilic substitution of the sulphonic group, and in the case of aromatic ether polymer the substitution is usually restricted to the active ortho position of the aromatic ether bond. This can affect the chemical stability of the polymer because of cleavage of the ether linkage (Zonqwu et al., 2006). In another study, Akovali and Özkan 1986 found that only the para position of the phenyl ring was sulphonated on the kinetics study of polystyrene sulphonation (Akovali and Özkan, 1986). With post-sulphonation strategy, difficulty is associated with controlling the degree of sulphonation as high degree of sulphonation often leads to solubility of the functionalised polymer in water. Moreover, the attached sulphonic groups are relatively easily removed by desulphonation and the membrane can experience partial degradation especially when strong sulphonating agent is used (Zonqwu et al., 2006).

However, fuel cells membranes made from this post-sulphonation type have no history of failure under fuel cell operation when the degree of sulphonation is well controlled. On direct polymerization which is expected to attach the sulphonic acid groups to the deactivated positions and provide chemical stability with enhanced acidity of the resulting polymer structure and more facile proton transport (Hickner et al., 2004) has been found to fail generally under fuel cell operation, which might be attributed to either or combination of hydrolytic and oxidative degradation (Zonqwu et al., 2006)

Sulphonation of polymers for PEMs requires high degree of control because high degree of sulphonation leads to high swelling and dissolution of the membrane in water whereas low degree of sulphonation leads to low conductivity of the membrane. Therefore, it is important

to optimise the degree of sulphonation to obtain membrane with good performance (Wonbong et al., 2005).

The introduction of SO_3H by sulphonation into the polymer matrix is such that it is ionically bonded and can not be leached out. As the SO_3^- molecules are fixed to the polymer the protons (H^+) on the acid groups migrate through the membrane when fully hydrated (Larminie and Dicks, 2000; Xianguo, 2006). Thus there exist on the membrane two nanophased domains known as the hydrophobic and the hydrophilic domains. The hydrophobic backbone domain provides the film with morphological stability in the presence of water and preventing the film from over-swelling while the hydrophilic sulphonic acid group domain provides channels for hydrated protons transport (Kreuer, 2001; Kerres, 2001). As a result of this it is expected that the membrane should be fully hydrated to obtain adequate ion conductivity and the fuel cell to be operated under such condition that the product water does not evaporate faster than its production as well as keeping reactant gases, hydrogen and oxygen humidified (Xianguo, 2006). Water and thermal management, therefore, remain a critical issue for efficient PEM fuel cell performance as well as maintaining operating temperature of PEM fuel cell to about 80-100°C (Xianguo, 2006).

The sterling disadvantages associated with the state-of-the-art membrane together with excessive swelling in the presence of methanol fuel and methanol crossover to the cathode in the fuel cell, result in output crippling mixed potential as a result of chemical oxidization (Wasmus and Kuver, 1999; McNicol et al., 1999). The problem of very high cost and monopoly of the market have necessitated intensified research towards finding an alternative by chemical modification of polymeric materials for PEM fuel cell through sulphonation process.

Sulphonated sodium salt of butyl rubber has been reported to be stronger than the unsulphonated (Canter, 1969; Farrel and Serniuk, 1974). So also the sulphonation of polystyrene has been carried out (Akovali and Özkan, 1986). The sulphonation of a single polymer in solution gives rise to a material with excellent proton conductivity but lower thermal stability as a result of recognised thermal instability of the sulphonated group, whereas heterogeneous sulphonation of blend polymer produces membranes of high conductivity and excellent dimensional and thermal stability (Bashir, et al., 2001). An ion-exchange resin/polystyrene sulfonate membrane has been attempted but was found to require further refinement to possess the quality for PEM (Sheng-Li et al., 2004). Sulphonation of styrene(ethylene-block-butylene)-styrene as PEM by Ehrenberg et al. (1997) and Ehreberg et al. (1995) with SO₃ have been claimed to have proton conductivity in the range of 10⁵S/cm in its fully protonated state but was found to absorb 50% of its weight in water (Sangeetha, 2005). Several other ionomers that are relatively lower in cost have also been studied because of their morphologies arising from their structural combination of both hydrocarbon block and ionomer block (Gauthier and Eisenberg, 1987; Zhou et al., 1994; Desjardins and Eisenberg, 1991; Weiss et al., 1990). Intensive efforts have now been devoted to stable aromatic polymers such as poly(ether-ether ketone) (Wang et al., 1998), polyethersulfone (Ueda et al., 1993; Wang et al., 2002), polyamide (Genies et al., 2001) and poly(phenylene sulphide) (Allam et al., 1999) along side with polybenzimidazole (Jones and Rozière, 2001; Staiti et al., 2001), polyphosphazene (Wycisk and Pintauro, 1996), polyether-sulphone with cardo (Blanco et al., 2001), polyphenoxybenzoil-phenylene (Kobayashi et al., 1998), and composite membranes (Honma et al., 2001; Staiti et al., 2001).

Going by the great effort of getting a possible alternative PEM, the sulphonation of a glassy poly-ether ether ketone at 80°C that was carried out in 96 % H₂SO₄ was found that both the

ion exchange capacity and the degree of sulphonation can be influenced by the reaction time during sulphonation. Although a calculated specific conductivity of about 1.7×10^{-2} S/cm was achieved but the membrane was found to achieve only 14 % water uptake and this is an important property for the proton transport through dense membrane during fuel cell operation (Basile et al., 2006). Sulphonated polystyrene-poly(ethylene-butylene)-polystyrene triblock polymer that was prepared from a low cost material by sulphonating the styrene blocks of the polymer using chlorosulphonic acid was found to achieve proton conductivity of 10^{-1} S/cm, however, the thermal analysis of the membrane using differential calorimetric analysis (DSC) and thermogravimetric analysis (TGA) showed that the thermal stability of the polymer decreases due to sulphonation. An extensive study of solvent adsorption on the membrane showed that the uptake of water molecules per sulphonic acid group is higher than the uptake of methanol molecules per sulphonic acid group in the ionomer molecule, but, the membrane was found to have a challenge of high rate of water desorption. A situation that will require proper humidification of the membrane in fuel cell assembly in order to maintain the water content and subsequently the conductivity, especially at temperature higher than just 60°C (Sangeetha, 2005). Sulphonated poly(phthalazinones) with different degrees of sulphonation ranging from 1 – 1.37 were prepared from poly(phthalazinones) using dilute fuming sulphuric acid as both the solvent and the sulphonating agent. Although the membranes were able to achieve conductivity in the order of 10^{-2} S/cm but the thermal analysis showed that the membranes were losing sulphonic acid groups in two steps followed by degradation of the polymer main chain. Water uptake study of the membrane also showed that the membrane thin film absorbs water and swollen with degree of sulphonation and temperature, and were soluble at around degree of sulphonation of 1.2 at 80°C water (Gao et al., 2003).

In the same vein, sulphonated polystyrene by Smitha and co-workers (2003), showed that the resulting membrane exhibited a steep fall in glass transition temperature to a level which does not comply with requisite operating conditions in PEM fuel cells. However this drawback was said to have been overcome by crosslinking or copolymerization with other suitable polymers (Smitha, 2003). A comparative study of sulphonation and product characterization of both commercial Victrex[®] and Gatone[®] poly(ether-ether ether ketone) (PEEK) was conducted (Peixiang et al., 2004) and both PEEKs were found to have similar molecular weights and identical chain structure according to NMR spectroscopy study. It was confirmed that higher temperature sulphonation (55°C) did not induce any apparent chain degradation of PEEK as TGA test for both Victrex[®] and Gatone[®] showed a high first thermal degradation temperature (~250°C). However, films cast from dimethylacetate (DMAc) showed higher proton conductivity than those cast from dimethylformamide (DMF) and the effect of the solvents on the proton conductivity of the sulphonated PEEK was attributed to strong complexes formation between the decomposed product of the solvent and the sulphonic acid group (Robertson et al., 2003).

A new kind of composite proton exchange membranes comprising of polystyrene sulphonate (PSS) and 50 % polystyrene ion exchange resin has also been reported (Sheng-Li et al 2004). It was found that the resin/PSS composite membranes had much higher ion exchange capacity than the PSS membranes, but the ion conductivity was similar to that of PSS. The water swelling of the composite membranes was, however, lower than that of the PSS. The PSS structure was found to be attacked by the free radicals, so that the PSS degraded during fuel cell operation. It was recorded that the impregnation of Nafion layers between the PSS and the electrodes did not prevent the membrane from being degraded during the fuel cell operation, an indication that degradation reaction occurred throughout the membrane.

However, the resin/PSS composite membranes were found to degrade much slowly than PSS membranes suggesting that the very large molecular weight and small channel for diffusion of the free radicals inhibited the rate of the degradation (Sheng-Li et al 2004). As the search for a better alternative proton exchange membrane continues, the synthesis and characterisation of sulphonated polyimide was also carried out and the result showed that the presence of hexafluoroisopropylidene groups in the polymer chain induced more easily molecular degradation of the sulphonated polymer (Jian-Li, 2005).

The first proton exchange membrane employed in the Gemini program was a crosslinked polystyrene sulphonic acid (Liebhafsky and Cairns, 1968; Okada and Yokoyama, 2001). The one kilowatt (1 kW) fuel cell stack was used as both an auxiliary power source and also a source of water for the astronauts (William, 2002). However, the monomer polystyrene sulphonic acid membrane was not durable enough under actual PEM fuel cell operating conditions.

Styrene-butadiene rubber is one of the most versatile copolymer rubber compounds in the world today with high molecular weight, and due to its excellent abrasion resistance it is widely used in automobile and lorry (truck) tyres, cable insulation, footwear, belting, flooring, wire and for paper coating. Poly (styrene-butadiene) block copolymer (Figure 2.5) is known to possess two-phase macrostructure consisting of polystyrene domains dispersed in a rubbery (butadiene) continuous phase (Mokrini and Acosta, 2001).

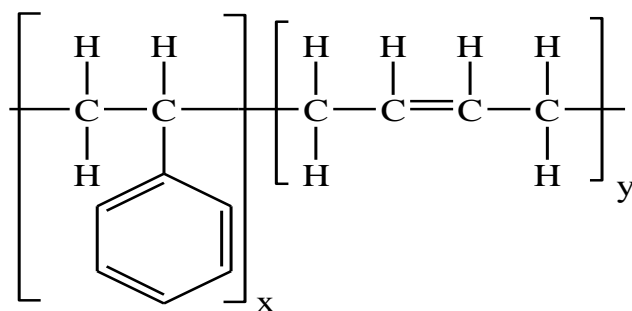


Figure 2.5: Poly (styrene-butadiene) rubber repeat unit structure

The presence of the butadiene makes the polymer flexible, which is necessary for good electrode contact (Sheng-Li et al., 2004) and thus enhanced proton conductivity. Therefore, this work attempts to synthesise sulphonated membrane using polystyrene-butadiene rubber by creating hydrophilic regions within the hydrophobic polymer matrix for proton conductivity. The resulting sulphonated polymer is expected to manifest itself with qualities suited for fuel cell such as mechanical properties, thermal transitional behaviour, morphology and ion exchange capacity. The very high cost of membrane which remains the biggest challenge to be overcome in membrane synthesis can be achieved by choosing low cost polymer that is readily available locally, and polystyrene-butadiene rubber is such a candidate.

2.4 ION EXCHANGE CAPACITY AND PROTON CONDUCTIVITY

Ion exchange capacity of a membrane depends on the membrane's acid concentration. The acid concentration of the membrane is seen to be closely related to the amount of ionic groups in the membrane. Hence it is referred to as the measure of the degree of sulphonation which is an indirect and reliable approximation of the proton conductivity (Sangeetha, 2005). The ion exchange capacity is conventionally characterised by two important properties which

are: the equivalent weight, EW (or ion – exchange capacity) and the level of hydration of the functional sulfonic acid groups (Zonquo, 2006). Equivalent weight is thus defined as.

$$EW = \frac{\text{Dry polymer mass in g}}{\text{Mole of ion-exchange sites (i.e., fixed } SO_3^-)} = \frac{1000}{\text{Ion-exchange capacity}} \quad (2.4)$$

There is a significant impact of the equivalent weight on the proton conductivity of the membrane, the amount of water uptake by the membrane and the membrane thermal properties, such that the higher the equivalent weight, the more stable the membrane becomes and the lower the equivalent weight the higher the proton conductivity and the water uptake. If the equivalent weight is sufficiently low the membrane eventually becomes aqueous (Zonquo, 2006). However, for a membrane to be proton conductive it must be fully hydrated rather than in the dry state (insulator). It has been found that the Nafion polymer is conductive in a humid atmosphere, absorbing approximately what is considered to be membrane hydration of 6 H_2O/SO_3^- (Yeo and Yeager, 1985). The Proton conductivity of a membrane is largely determined by the product of the density and mobility of the charge carrier (proton) (Zonquo, 2006). The proton density in the membrane with an equivalent weight of 1100 is reported to be equivalent to that in 1 M aqueous sulphuric acid solution, and the proton mobility in a fully hydrated membrane is about one order of magnitude lower than that of the aqueous solution (Gottesfield and Zawodzinski, 1997). As a result, conductivity of a fully hydrated membrane is at least three to four orders of magnitude higher

than what is realised when a solvent-free ionically conducting polymer is used out at the same temperature (Gottesfield and Zawodzinski, 1997).

In the context of fuel cell operating requirements, high levels of sulphonation typically lead to realization of higher conductivity of the resulting membrane. But at the same time, it has a drastic undesirable effect to increase the swelling of membrane in a humid environment (Brandon et al., 2003).

The present commercially used perfluorinated ionomer Nafion membranes ensure high proton conductivity, $\sigma \geq 10^{-2} \text{ S cm}^{-1}$ (Gao et al., 2003) in a fully hydrated state and under fuel cell operating conditions.

Succinctly put, in sulphonic acid membrane, the proton conductivity is known to depend on the number of available acid groups and their dissociation capability in water such that when the membrane is in hydrated form, water molecules dissociate the acid functionality and thus facilitate proton transport. Therefore the conductivity and ionic exchange capacity are vital factors in PEM technology (Mokrini et al., 2006).

CHAPTER THREE

3.0 EXPERIMENTAL

3.1 Materials and Method

The chemicals used in this study are all of analytical grade of between 98 to 99.5% purity. The following chemicals were obtained from MERCK (RSA): 1, 2 dichloroethane, chlorosulphuric acid, dichloromethane, trichloromethane, methyl alcohol, ethanol, deuterated chloroform and petroleum ether, sulphuric acid, fuming sulphuric acid, acetic anhydride. Dimethyl formamide and dimethyl acetamide, hydrochloric acid were obtained from FLUKA (RSA), while polystyrene-butadiene rubber was kindly donated by KARBOCHEM (RSA). Nafion 112 was used for performance testing, while Nafion 117 and 112 were used for mechanical properties comparison, respectively.

3.2 Solubility Determination

Polymers are solvent selective in nature and because the base material which is polystyrene-butadiene rubber (PSBR) is in solid form, and the sulphonation reaction is carried out in liquid medium, there was the need to check for the right solvent that could dissolve it. Hence, prior to the commencement of the sulphonation process, solubility determination of PSBR was carried out. Here, an array of polar aprotic solvents such as dimethylformamide (DMF), dimethylacetamide (DMAc), dimethylsulphoxide (DMSO) and chlorinated solvents such as 1, 2 dichloroethane ($C_2H_4Cl_2$) dichloromethane (CH_2Cl_2), trichloromethane ($CHCl_3$) as well as petroleum ether (PE) and chloroform ($CDCl_3$) were tested. The solubility result is presented in the result section.

3.3 Sulphonation of Polystyrene-butadiene Rubber (PSBR)

A number of experiments were carried out to determine the optimum conditions of sulphonation of PSBR, by varying weight of polymer, concentration of sulphonating agent, reaction time, stirring speed of reaction in revolution per minute (rpm) and temperature. Initially, equal concentration of different sulphonating agents (fuming sulphuric acid, sulphuric acid, fuming sulphuric/sulphuric acid, acetyl sulphate and dichlorosulphonic acid) was used to investigate the sulphonation of known weight of PSBR at selected time. The reactivity of the polymer with these sulphonating agents was thus evaluated where chlorosulphonic acid became the choice of sulphonating agent in this study (shown in result section). 10 g of polystyrene-butadiene rubber (PSBR) was dissolved in 250 ml 1, 2 dichloroethane. The experimental set up can be seen in Figure 3.1. This was followed by the gradual addition of 0.2 M of dichlorosulphonic acid that was initially chilled in an iced bath to eliminate content heat into vigorously stirred solution of PSBR equipped with a magnetic stirrer in a four-neck round bottom flask reactor under argon atmosphere at room temperature.



Figure 3.1: Experimental set up of chlorosulphonation of polystyrene-butadiene rubber

The sulphonation reaction was allowed to proceed for 2, 4, 6, 8 and 10 hours. The reaction was terminated by adding ethanol and the precipitated sulphonated polymer was recovered, washed with deionised water until the pH reached values of 6 – 7. The product was then dried in an oven at 80°C for 2-3 hours. The Sulphonated Polystyrene Butadiene Rubber (SPSBR) was characterized to determine the thermal properties, percentage sulphur, and degree of sulphonation, ion exchange capacity and viscosity. Fourier Transform Infra-red (FTIR) and Proton Nuclear Magnetic Resonance (¹H NMR) were used to verify sulphonation and identify the site available for proton conduction in the SPSBR. Process scale up was carried out after evaluating preliminary results by optimizing the process parameters.

3.4 Fourier Transform (FT) Infra-red (IR) Studies of Polymer

The FT IR spectra of unsulphonated and sulphonated PSBR were scanned using a Vector 0-model FTIR spectrometer to confirm sulphonation of PSBR. This was achieved by dissolving 10 mg of both unsulphonated and sulphonated PSBR in 1, 2 dichloroethane to form a film. The film was introduced onto a sodium chloride plate, where the infrared spectra were recorded in the range of 400 – 4000cm⁻¹.

3.5 Proton Nuclear Magnetic Resonance (¹H NMR) Studies of Polymer

The ¹H NMR spectra of unsulphonated and sulphonated PSBR were scanned using Bruker 400 Spectrometers to detect the occurrence of sulphonation. This was carried out by dissolving 10 mg of both unsulphonated and sulphonated PSBR in deuterated chloroform (CDCl₃).

3.6 Viscosity Measurement of Unsulphonated and Sulphonated PSBR

0.5 g of samples (both sulphonated and unsulphonated PSBR) were dissolved in 100 ml of 1, 2 dichloroethane over night. Inherent viscosities were determined using a Cannon – Fense Capillary viscometer with 1, 2 dichloroethane solutions of polymer at a concentration of 0.5 gdl⁻¹ at 30°C.

3.7 Thermal Analysis of Polymer

The Differential Scanning Calorimetric (DSC) analysis of sulphonated and unsulphonated PSBR were carried out using an 822E DSC analyzer. Measurements were performed over the range of 30°C to 400°C at a heating rate of 5°C/minute under nitrogen atmosphere (flushed at 75 ml/minute). The thermal stability of sulphonated and unsulphonated PSBR were conducted using a Perker Elmer Pyris 1 TGA/DTA analyzer. The sample was heated to 800°C at 10°C/minute in nitrogen (flushed at 150 ml/minute) to determine the decomposition temperature of both the sulphonated and unsulphonated PSBR.

3.8 Determination of Ion Exchange Capacity (IEC) and Degree of Sulphonation (DS)

The Ion Exchange Capacity (IEC) and Degree of Sulphonation (DS) of Sulphonated Polystyrene Butadiene (SPSBR) were determined by measuring the percentage of sulphur in the dry sample of SPSBR using an elemental analysis method. The IEC was then calculated using Equation 3.1 (Bebin et al, 2005):

$$IEC = \frac{1000 S_c}{MW_s} \quad (3.1)$$

where S_c is the sulphur content (percentage weight rate), MW_s is the molecular weight of sulphur and 1000 is the multiplication factor to obtain IEC value in mmol/g. The value of IEC calculated from Equation 3.1 was used to determine the degree of sulphonation of SPSBR using the relationship shown in Equation 3. 2 (Paturzo et al, 2005):

$$DS = \frac{IEC \times M_{PSBR}}{1 - (IEC \times MW_{SO_3H})} \quad (3.2)$$

where: M_{PSBR} is the molecular weight of the polystyrene butadiene (g/mol) and MW_{SO_3H} is the molecular weight of SO_3H (g/mol)

3.9 Quantification of HCl in Aqueous Solution of the Copolymer

The aromatic sulphonation of PSBR with chlorosulphonic acid is expected to produce HCl acid as a by-product according to the balance chemical equation shown in Figure 3.2.

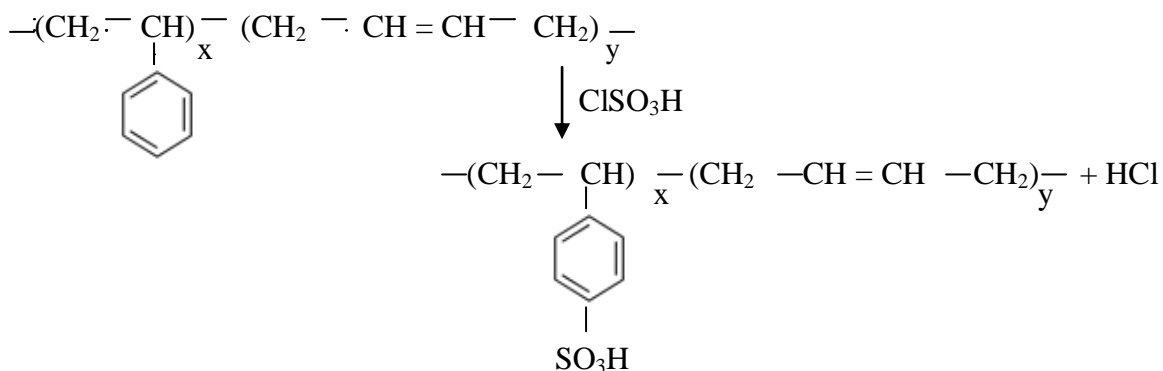


Figure 3.2: Sulphonation reaction of PSBR in chlorosulphonic acid

The need to quantify the concentration of HCl produced is important as to judge its effect on the rate of PSBR sulphonation. A scenario of two acids (ClSO_3H and HCl) in the aqueous

solution would be a problem in determining the actual concentration of HCl. As a result, acid-salt precipitation reaction was immediately carried out to yield a precipitating product of BaSO₃ from the ClSO₃H acid. Here, after sulphonation reaction was terminated, solution mixture was filtered and the precipitated PSBR was recovered. A required volume of 1.8 x 10⁻³ M BaCl₂ (in excess of acid) solution was added into 150 cm³ of the filtered solution mixture in a 500 ml beaker, containing 40 ml of 0.2 M sodium acetate buffer (pH 6.7). This was accompanied with stirring for about two minutes. A clean, dry cover slide was placed over it and properly sealed with a paraffin material. The experiment was left to stand for about 5 hours to allow white precipitate of BaSO₃ to settle. The solution mixture was again filtered to obtain a clear supernatant. A total solution volume of 100 cm³ was thereafter used in the acid-base reaction. This involves placing (100 cm³) an aqueous solution of the precipitated filtered copolymer in a 500 ml beaker and titrated against 25 ml NaOH of a predetermined concentration (3.9 x 10⁻⁵ mol L⁻¹) using methyl red as an indicator. The change in colour from red to yellow confirmed acid-base reaction. The end point of each neutralisation reaction was determined from different volumes of the base consumed. Each experiment was repeated at least twice, starting with blank titration.

3.10 Casting of Membrane into a Thin Film

10 g of SPSBR was dissolved in 200 ml of 1, 2 dichloroethane at elevated temperature to form a casting solution of about 15-30 % wt, and cast onto a clean polymer paper support using a laboratory doctor blade casting machine as shown in Figure 3.3. Prior to the casting, the doctor blade was set to a known thickness with the aid of feeler gauges of the appropriate thickness. The casting was done by drawing the casting head of the blade along the length of the substrate, and cured for 4 days by exposing it to air and then peeled off from the support. The cast membrane was dried further in an oven at 75°C for 4-5 hours and was finally

vacuum dried for 4 hours to remove the residual solvent. The membrane was analysed to determine water absorption, water desorption and swelling ratio.

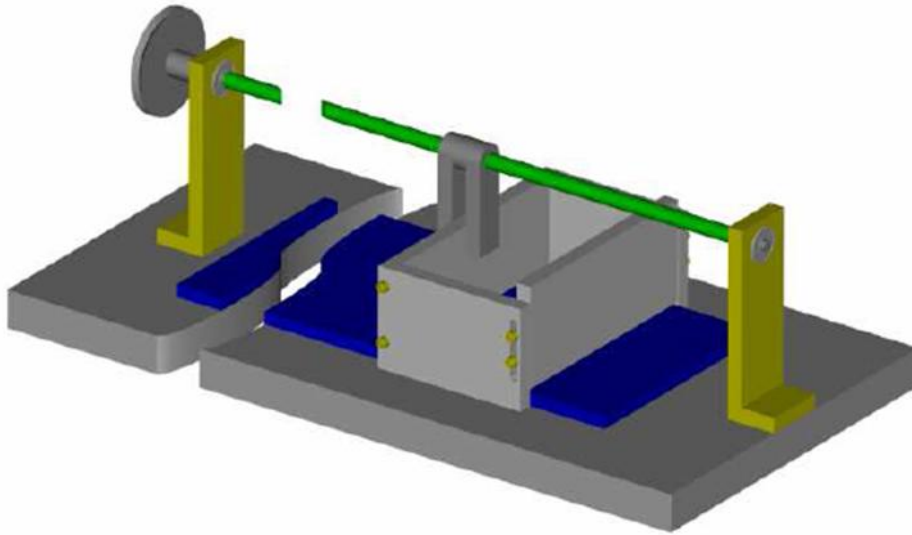


Figure 3.3: Laboratory scale tape caster (Lavisage, 2004)

3.11 Water Uptake Capacity of the Fabricated Membrane

The water absorption capacity of the membrane was determined by immersing a known weight and dimensions of membrane in distilled water for a number of days until the membrane was saturated with water. The water uptake was determined from the weight difference between the wet and dry membrane as shown in Equation 3.3 (Gao et al, 2003):

$$\text{Water uptake (absorption) \%} = \frac{W_{wet} - W_{dry}}{W_{dry}} \times 100 \quad (3.3)$$

where W_{wet} and W_{dry} are the weights of the wet membranes (g) and dry membranes, respectively.

To measure the water desorption rate of the membrane, the sample membrane was immersed in distilled water for 24 hours. It was then removed from the water and exposed to air at different temperatures and the weight of the membrane was measured at intervals of one hour. Equation 3.4 is then used to calculate the percentage of water desorbed.

$$\text{Water desorption (\%)} = \frac{W_{wet} - W_{dry(t)}}{W_{wet} - W_{dry}} \times 100 \quad (3.4)$$

where w_{wet} is weight of wet membranes and $w_{dry(t)}$ is the weight of the dry membranes at time (t) in grams.

The membrane swelling ratio was evaluated by:

$$\frac{T_{wet} - T_{dry}}{T_{dry}} \times 100 \quad (3.5)$$

where T_{wet} is the thickness of wet membranes and T_{dry} is the thickness of dry membranes.

3.12 Scanning Electron Microscopy Studies of PSBR

About 1 g of sample (unsulphonated and sulphonated PSBR) was mounted on aluminium stubs using colloidal graphite as a mounting medium. Thereafter samples were first coated with carbon using an Edwards Coating Unit. This was followed by a deposition of a thin layer of gold palladium onto the samples to make it conductive. These were finally examined under the Jeol 840 Scanning electron microscope for morphological determination.

3.13 Total Solvent Uptake Determination and Porosity of the Synthesised Membrane

Solvent uptake of the synthesised membranes was carried out gravimetrically. Prior to the analysis, membranes of different degree of sulphonation and thickness were dried at 80°C overnight to expel the residual solvent and weighed for their dry weight (W_{dry}). The dried membranes were then immersed in methanol of various concentrations in M/l (0, 0.5, 1, 2, 4, 6, 8, 10, 12 and 100% concentration) until equilibrium was reached. The saturated membranes were blotted to absorb all the surface solvent and weighed (W_{wet}). The wet membrane porosity (ε) to methanol, and water/methanol uptake were calculated using equations 3.6 and 3.7, respectively (Sangeetha et al., 2005):

$$\varepsilon = \frac{\text{Fluid uptake volume}}{\text{Total volume}} = \frac{(W_{wet} - W_{dry})\rho_{dry}}{(W_{wet} - W_{dry})\rho_{dry} + (W_{wet}\rho_{sol})} \quad (3.6)$$

where: ρ_{dry} is the density of dry membrane = 0.93g/cm³

ρ_{sol} is the density of the methanol solution (g/cm³)

W_{wet} is the weight of the wet membrane (g)

W_{dry} is the weight of dried membrane (g)

ε = porosity of the wet membrane

The overall uptake of solvent molecules per sulphonic acid group in the membrane (λ_{total}) was calculated using equation 3.7

$$\lambda_{total} = \frac{W_{wet} - W_{dry}}{W_{dry}} \cdot \frac{EW}{18x_{water} + 32.04(1 - x_{water})} \quad (3.7)$$

where: x_{water} is the molar fraction of water in the solution

EW (mol/g) is the equivalent weight of the membranes, can be calculated from equation 3.8 (Shang et al., 2005):

$$EW = \frac{1}{IEC} \quad (3.8)$$

The uptake of water molecules per sulphonic acid group (λ_{water}) and uptake of methanol molecules per sulphonic acid group ($\lambda_{methanol}$) were calculated using equation 3.9 and 3.10, respectively.

$$\lambda_{water} = \lambda_{total} X_{water} \quad (3.9)$$

$$\lambda_{methanol} = \lambda_{total} (1 - x_{water}) \quad (3.10)$$

3.14 Measurement of the Proton Conductivity of the Synthesised Membrane

The proton conductivity of the membrane was measured by alternating current impedance over a frequency range of 1-10⁶Hz, using a 1M H₂SO₄ as electrolyte. The value at the intersection (Appendix 14) of the high frequency impedance curve was taken as the membrane resistance and the proton conductivity was calculated using:

$$\sigma = \frac{T}{RS} \quad (3.11)$$

where σ is the proton conductivity (S/cm), T (cm) the thickness and S (cm²) the surface area of the membrane and R is the resistance determined from the impedance plane.

3.15 Methanol Permeability Measurement

Methanol crossover through the synthesised membranes at different degrees of sulphonation and membrane thickness was measured in two identical chamber containers. A schematic of

the chamber container is shown in Figure 3.4. Here, Membrane of known degree of sulphonation and thickness with surface area of 7.069cm^2 was placed between identical chambers of volume 70 cm^3 . One of the chambers contains concentrated methanol while the second chamber contains water. The contents in the two chambers were well stirred with a magnetic stirrer to obtain a homogenous solution. A small amount of the solution was drawn from the second chamber at different times to determine the concentration of methanol that crossed over. The methanol concentration in the water chamber was measured with UV spectroscopy of 4802 UV/VIS model.

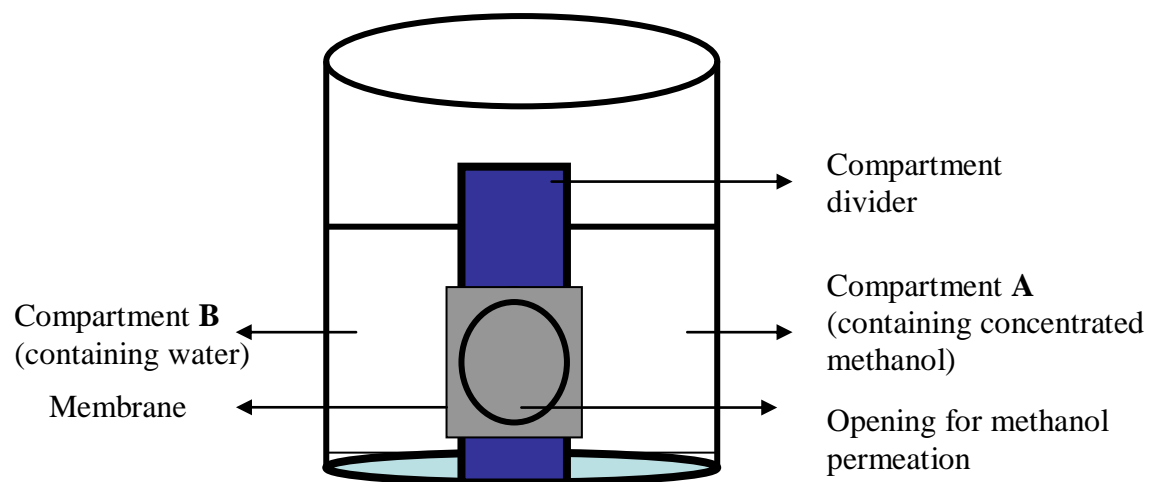


Figure 3.4: Schematic of two identical chamber containers for solvent permeability determination

CHAPTER FOUR

4.0 SULPHONATION OF PLYSTYRENE-BUTADIENE RUBBER

4.1 The Choice of Polystyrene-butadiene Rubber

The idea of synthesising a membrane of high degree of sulphonation to encourage good ionic conductivity for fuel cell application has been seen to be balanced with moderate water uptake, vis-a-vis maintaining thermal stability. Searching for an alternative proton exchange membrane for PEM fuel cell application from available literature has shown that the base polymers explored so far are either in their powder or crystal form with low viscosity and high solubility in common organic solvents (Smitha et al., 2003; Kim et al., 2003; Gao et al., 2003; Xing et al., 2004; Chen et al., 2004; Blackwell and Maurtiz, 2004; Jelcic et al., 2005; Mokrini and Acosta, 2001; del Rio et al., 2005; Sangeetha, 2005). The foregoing situation often presents the resulting membranes as vulnerable to mechanical failure. In this research, a careful selection of polystyrene-butadiene rubber for the synthesis of proton exchange membrane is not only due to its availability in South Africa and excellent mechanical properties, but because of its versatility, arising from its high viscosity, compared to the powder/crystal polymers. However, this is a situation that makes the sulphonation process difficult to control. Therefore, there is the need to conduct preliminary investigation on this rubber to ascertain the possibility of processing it and using it as an alternative polymer for proton exchange membrane synthesis. This section presents the results and discussion on the sulphonation conducted on PSBR for the membrane synthesis.

4.2 Preliminary Investigation

The process of sulphonation is an important technique that can be used to render polymers that are generally insulators to be proton conductive as well as to make them hydrophilic. In

this study, the sulphonation of Polystyrene-butadiene rubber (PSBR) was conducted, first, by using different sulphonating agents in order to arrive at the best suitable sulphonating agent. This was important considering the fact that polymer affinity and compatibility for the right sulphonating acid is expected to enhance good result (ion exchange capacity and conductivity), especially when the base polymer in this study contains a hydrocarbon aromatic ring. Among the sulphonating agents investigated were sulphuric acid, fuming sulphuric acid, a mixture of fuming sulphuric acid and sulphuric acid, acetylsulphate and chlorosulphonic acid. But before the commencement of sulphonation, the solubility determination of the polymer in different solvents was investigated since polymers are solvent selective. Also investigated, were the effects of the weight of the polymer, stirring speed, sulphonation time and temperature on the degree of sulphonation. Results obtained for various analyses on the sulphonated rubber are, therefore, presented.

4.2.1 Identification of a Suitable Solvent for PSBR and SPSBR

Polymers are solvent selective in nature with respect to solubility due to several factors, which include the type of polymer, structure and, to some degree, the nature of the starting monomer. As a result, modification and workability of any polymer requires its solubility in solvents. The solubility of PSBR and SPSBR in different solvents such as; dimethylformamide, dimethylacetate, dimethylsulphoxide, trichloroethane, dichloroethene, 1, 2 dichloroethane, petroleum ether and deuterated chloroform, was determined and the results obtained are presented in Table 4.1. Results show that the solubility of the polymer is different before and after sulphonation. PSBR and SPSBR are found to be insoluble in polar aprotic solvents such as dimethylformamide, dimethylacetate and dimethylsulphoxide.

Table 4.1: Solubility determination of PSBR and SPSBR

Polymer	DMF	DMAc	DMSO	CHCl ₃	CH ₂ Cl ₂	C ₂ H ₄ Cl ₂	PE	CDCl ₃
PSBR	-	-	-	±	±	+	-	±
SPSBR	-	-	±	±	+Δ	+	-	+

Soluble (+); insoluble (-); soluble at high temperature (+Δ); swelling or partially soluble (±); DMF (dimethylformamide); DMAc (dimethylacetate); DMSO (dimethylsulphoxide); CHCl₃ (trichloromethane); CH₂Cl₂ (dichloroethene); C₂H₄Cl₂ (1, 2 dichloroethane); PE (petroleum ether); CDCl₃ (deuterated chloroform)

Among the chlorinated solvents investigated, PSBR is only found to be soluble in C₂H₄Cl₂ and shows partial solubility at high temperature (< 120 °C) to others of the same group. SPSBR also shows solubility with C₂H₄Cl₂ and CDCl₃, and at high temperature (< 120 °C), it is found to be soluble in CH₂Cl₂. The solubility differences between the PSBR and SPSBR are due to the sulphonic acid group introduced into the polymer matrix, which caused changes in the polarity of the polymers and intermolecular forces relating to hydrogen bond (Gao et al., 2003). C₂H₄Cl₂ is therefore selected as the right solvent to dissolve PSBR and SPSBR in the entire course of this study.

4.2.2 Choice of Sulphonating Agent

As mentioned in literature, different sulphonating agents such as concentrated sulphuric acid, fuming sulphuric acid, trimethylsilyl chlorosulphonate, sulphur trioxide-triethyl phosphate complex, chlorosulphonic acid (Zonqwu et al., 2006) and acetylsulphate (Smitha et al., 2003) are used to carry out sulphonation reaction on polymer materials. The selection of a sulphonating agent depends strongly on the compatibility of such agent with the polymer, the film forming properties and the mechanical strength of resulting sulphonated polymer (Smitha et al., 2003). Across the array of these agents, concentrated sulphuric acid, chlorosulphuric acid and acetylsulphate have been employed, especially, for polymers with

aryl backbones where the SO₃H group is attached to the aromatic ring (Smitha et al., 2003; Zonqwo, et al., 2006). Akovali and Özkan (1986) used concentrated sulphuric acid to sulphonate polystyrene and found out that sulphonation was limited to the para position of the phenyl ring.

Table 4.2 shows the preliminary results of different sulphonating agents on PSBR sulphonation with respect to their percentage sulphur, degree of sulphonation and ion exchange capacity. The results show that PSBR has affinity for the entire sulphonating agents investigated (as confirmed with IR and ¹H NMR analysis in section 4.2.3 and 4.2.4) though with varying degrees of sulphonation, ion exchange capacity and sulphur content. In an equimolar concentration (1.4 M/ml) of acids used for the sulphonation of PSBR and at a constant stirring speed of 1000 rpm, mixture of sulphuric acid and fuming sulphuric acid in ratio 60/40 and 40/60 (%) showed the lowest sulphur content (< 0.3 %), DS (< 6 %) and IEC (< 0.39 mmol/g). This is followed by sulphuric acid which also showed low sulphur content, degree of sulphonation and ion exchange capacity both at short and prolonged times of sulphonation. This is probably due to a hydrolytic desulphonation effect normally associated with sulphuric acid (Nobuhiru and Rogers, 1992; Daoust et al., 2001). However, the use of acetylsulphate and fuming sulphuric acid at prolonged time of sulphonation demonstrated relatively high values of DS (11.02 and 12.64 %) with IEC of 0.6875 and 0.7875 mmol/g, respectively. Overall, the use of chlorosulphonic acid gave sulphonated PSBR with the highest values of sulphur content and consequently DS and IEC (0.80 %, 16.12 % and 1 mmol/g) which, therefore, promote chlorosulphonic acid over other sulphonating agents, since the conductivity of ionic membranes is a function of the degree of sulphonation.

Table 4.2: Results of investigated sulphonating agents

Sulphonating Agents									
Time (hrs)	ClSO₃H		H₂SO₄		F-HSO₄H		H/F (60/40) (%)		
	4	12	4	12	4	12	4	12	
Sc (%)	0.37	0.80	0.17	0.31	0.33	0.63	0.04	0.19	
DS (%)	7.65	16.12	3.37	6.17	6.57	12.64	0.79	3.77	
IEC(mmol/g)	0.4625	1	0.2125	0.3375	0.4125	0.7875	0.05	0.2375	

where *ClSO₃H* = chlorosulphonic acid; *H₂SO₄* = sulphuric acid; *F-H₂SO₄H* = fuming sulphuric acid; *H/F* = mixture of sulphuric acid and fuming sulphuric acid; *Sc* = Sulphur content; *DS* = degree of sulphonation and *IEC* = ion exchange capacity.

Table 4.2 continues

Sulphonating Agents				
Time (hrs)	H/F (40/60) (%)		AcSO₄H	
	4	12	4	12
Sc (%)	0.10	0.27	0.18	0.55
DS (%)	1.98	5.37	3.57	11.02
IEC (mmol/g)	0.125	0.388	0.225	0.6875

where *H/F* = mixture of sulphuric acid and fuming sulphuric acid; *AcSO₄H* = acetylsulphate; *Sc* = Sulphur content *DS* = degree of sulphonation and *IEC* = ion exchange capacity.

When concentrated sulphuric acid and fuming sulphuric acid were used, it was found that fuming sulphuric acid was less controllable in the sulphonation of PSBR compared to concentrated sulphuric acid. However, the use of concentrated sulphuric acid for the sulphonation leads to partial precipitation of the resulting polymer. Together with the formation of the by-product water is known to retard sulphonation and induce desulphonation (Nobuhiro and Roger, 1992; Huang et al., 2001). Cowdrey and Davies, (1949) in Nobuhiro and Roger (1994) has asserted that due to isomerisation induced with the use of sulphuric

acid in aryl sulphonation, it is, therefore, considered as a case of complication for aryl sulphonation.

Furthermore, report on the use of concentrated sulphuric acid on some aryl backbone polymer was found to cause the resulting polymer obtained to dissolve in water despite its use in small quantities, and when used in excess, it led to the degradation of the polymer, which made it undesirable (Smitha et al., 2003). These characteristics are also associated with the use of fuming sulphuric acid.

Acetyl sulphate used as a sulphonating agent is freshly prepared by introducing a known amount of acetic anhydride into 1, 2 dichloroethane, and after a period of cooling, sulphuric acid was added into the solution in such a way that the acetic anhydride is slightly in excess of the sulphuric acid (60/40 % v/v) in order for the sulphuric acid to be completely converted to acetyl sulphate (Carratta et al., 2000). The use of acetyl sulphate has been reported to give a homogeneous distribution of sulphonic acid groups in the resulting polymer obtained with Polystyrene (Kibler and Lappin, 1973). But with polystyrene-butadiene rubber on investigation, it could not surmount the result obtained using chlorosulphonic acid as shown earlier in Table 4.2.

Chlorosulphonic acid is a very strong acid compared to other acids used because of the weak Cl-S bond (Huang et al., 2001), a situation that could lead to a less controllable sulphonation reaction. But on investigation, it was observed that the use of chlorosulphonic acid was not only compatible with polystyrene-butadiene rubber in solution, but also with a reasonable degree of control in spite of the high viscosity of PSBR. Sulphonation of aromatic compounds has been found to be easy with chlorosulphonic acid and, hence, reported to be

advantageous in the sulphonation of even sensitive aromatic compounds (Behre et al., 1989). The triblock of polystyrene(ethylene-butylene)polystyrene polymer has been sulphonated successfully with chlorosulphonic acid (Sangeetha, 2005). Report has shown that chlorosulphonation of aryl compounds is satisfactory, even though some degradation (poly aryl - ether - ether – ketone) occurred (Bailly et al., 1987).

4.2.3 IR Analysis of Sulphonated PSBR with Different Sulphonating Agents

To support the results presented in Table 4.2, an IR study of the sulphonated PSBR was carried out. Figure 4.1 presents the IR spectra of the different sulphonating agents on PSBR in view of finding the right choice of sulphonating agent. All the spectra show that the array of sulphonating agents investigated are able to sulphonate PSBR. The weak peak inside the square box on each of the spectra represents the O-H vibration from sulphonic acid group upon sulphonation. The changes in the combination vibrations around $1800 - 1650 \text{ cm}^{-1}$ (finger band) characterise the phenyl group (Mokrini and Acosta, 2001). The peak identified in the spectra between 1350 cm^{-1} and 1360 cm^{-1} corresponds to the asymmetric stretching of S=O. The vibrations of phenyl ring substituted with a sulphonate group and sulphonate anion attached to phenyl ring results in the absorbance between 950 and 1126 cm^{-1} respectively, in all the sulphonated spectra.

4.2.4 ^1H NMR Analysis of Sulphonated PSBR with Different Sulphonating Agents

Figure 4.2 shows the ^1H NMR spectra of the PSBR and SPSBR using different sulphonating agents. All the spectra indicate that the array of sulphonating agents investigated showed affinity for PSBR. The hump appearing between 4 and 5 ppm indicates the presence of sulphonic acid linkage on the aromatic phenyl ring which is lacking in the unsulphonated sample. The characteristic sharp peaks of the sulphonated over the unsulphonated are as a

result of the influence of the acid group grafted on the polymer matrix. The strong deshielding effect of the phenyl ring serves to shift the protons bonded to it to a very low field in the region between 7 – 7.5 ppm. The deshielding effect of carbon-carbon double bond can be observed at 2 ppm, while C = C proton at 1.70 ppm. As a result of negligible neighbouring centre, the end chain methyl proton peaks appear at a position of high field (0.23 - 0.88 ppm), which exhibit four-bands of reduced intensity as against three – proton bands possibly either due to effect of the acid (Biemark et al., 1963) or proton's resonance effect. Peaks at 2.30 ppm are attributed to the C₆H₅ protons while peaks between 1.30 -1.80 ppm are that of CH₂ protons, and the distinct shift in peaks can be associated with the different chemical environment. But the peaks between 5 – 6 ppm should be deshielding values of some typical terminal methylene groups of proton (Biemark et al., 1963). The presence of the sulphonic acid linkage on the aromatic phenyl ring results in a new peak between 4 – 5 ppm which is lacking in the unsulphonated sample and, thus, confirms the successful attachment of the acid group on the polymer.

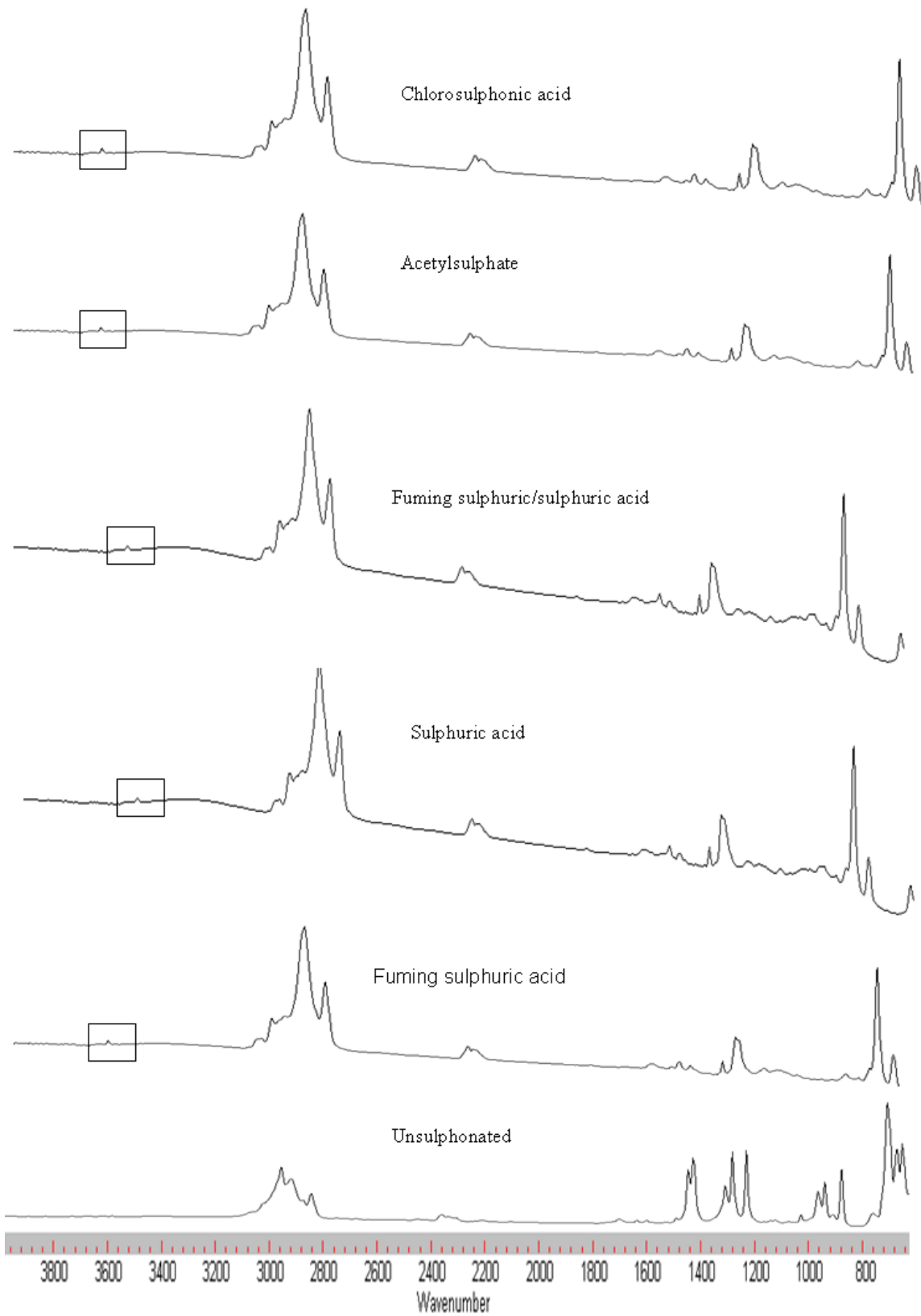


Figure 4.1: IR of different sulphonating agents

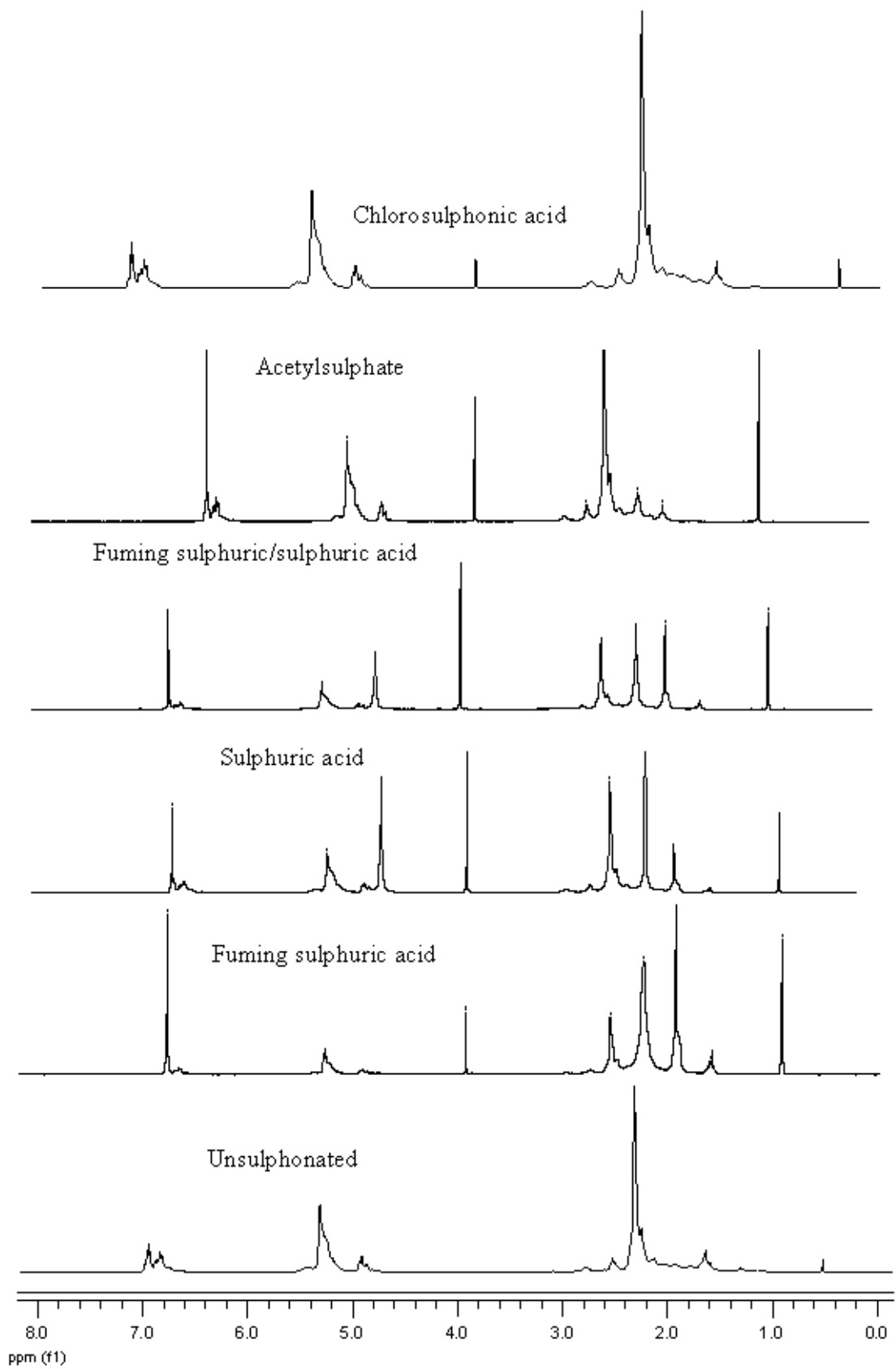


Figure 4.2: ¹H NMR of different sulphonating agents

Comparatively, although all the sulphonating agents show affinity for PSBR, chlorosulphonic acid gives a more promising result with higher degree of sulphonation, ion-exchange capacity, thus having better tendency to promote conductivity of the resulting membrane intended for fuel cell application, especially when processing parameters are scaled up. High level of ion exchange capacity and degree of sulphonation are very essential for proton conductivity of PEM in fuel cell application (Zonqwu, 2006; Larminie and Dicks, 2000). These make chlorosulphonic acid the sulphonating agent of choice.

4.3 Sulphonation of PSBR with Chlorosulphonic Acid

The initial study of the sulphonation of PSBR involved a series of experiment that were carried out in order to optimise the conditions of sulphonation by varying the weight (5, 10, 15, 20, 25 and 30 g) of the polymer and sulphonation time at constant concentration (0.2 M) of chlorosulphonic acid. Results show how various reaction conditions affect the IEC, DS and viscosity of the resulting polymer as well as its thermal properties.

4.3.1 Effects of the weight of polymer and sulphonation time

The sulphur contents of the SPSBR at various weights of the polymer and sulphonation time at constant concentration of sulphonating agent were investigated using elemental analyser. The results obtained revealed the presence of sulphur in the SPSBR, which also confirmed that the polymer was sulphonated by the sulphonating agent used. The low percentage of sulphur obtained in the samples can be attributed to the low concentration of acid used for sulphonation. The percentage of sulphur content in the SPSBR was used to evaluate the ion exchange capacity and degree of sulphonation of the polymer using previous equations 3.1 and 3.2, respectively.

For a quick recall, ion exchange capacity is the number of milli-equivalent of ions in 1g of the dry polymer. It is also used to calculate the degree of sulphonation of the polymer. The ion exchange capacity of the SPSBR is calculated from the sulphur content (equation 3.1) obtained by elemental analysis. Table 4.3 shows how the sulphonation time and weight of the polymer used at constant concentration of chlorosulphonic acid (0.2 M/ml) affect the ion exchange capacity of the sulphonated polymer.

Table 4.3: Effect of weight of polymer rubber and sulphonation time on the ion exchange capacity of the sulphonated rubber at constant stirring speed of 1000 rpm

Ion Exchange Capacity (IEC) (mmol/g) of Dry Membrane						
T (h)	5 g	10 g	15 g	20 g	25 g	30 g
2	0.15	0.24	0.23	0.21	0.17	0.15
4	0.18	0.30	0.26	0.23	0.20	0.20
6	0.19	0.36	0.33	0.28	0.26	0.24
8	0.21	0.50	0.39	0.36	0.31	0.27
10	0.23	0.63	0.46	0.43	0.38	0.34

As sulphonation time increases the IEC character of the SPSBR also increases, as sulphonation time of 10 hrs gives the highest IEC of 0.63 mmol/g. Decreasing the weight of the polymer from 30 to 10 g also increases the IEC of the SPSBR from 0.34 to 0.63 mmol/g. It is interesting to note that at < 10 g of PSBR investigated (5 g) at a maximum time (10 hrs) of sulphonation, the results of the degree of sulphonation (%), ion exchange capacity (mmol/g) and viscosity (η) obtained were of lower values (3.7 %, 0.23 mmol/g and 0.29 η) to 10 g that gives the optimum result. This is probably due to higher acid ratio over the rubber

concentration, thereby, leading to the consumption of the aromatic active site of sulphonic linkage. Although the preliminary result obtained reveals low values of ion exchange capacity for the SPSBR, it is an indication of the presence of acid group in the polymer matrix. The acid group changes the property of polymer from insulator to conductor, and thus gives the polymer the ability to conduct protons. The low ion exchange capacity is also necessary to keep the quality of the membrane, i.e. reduce swelling of the membrane, which occur in a more stable membrane, and also as the basis for assessing the quality of the membrane along scale-up parameters during synthesis.

The DS, which indicates the average number of sulphonic groups present in the sulphonated polymers was also investigated using the results of ion exchange capacity calculated. Results in Table 4.4 show a corresponding low DS due to low concentration of the acid used. Low concentration of acid prevents polymer from being soluble in water and as such, extensive sulphonation can lead to high solubility in water soluble membrane which is not good for fuel cell applications (Xu, 2005; Sangeetha, 2005). Results obtained also show that the ratio of weight of polymer to acid (w/v) and sulphonation time affect the DS. As time of sulphonation increases it in turn increases the DS and as weight of polymer increases the degree of sulphonation decreases. As such, the maximum DS (10.48 %) was achieved with 10 g PSBR in 10 hours of sulphonation and at a constant stirring speed of 1000 rpm. The percentage increase of DS between 10 and 30 g of polymer considered is of appreciable value of approximately 53 %. The results in Table 4.4 further reveal that an increase in the degree of sulphonation, with time, increases viscosity of the sulphonated rubber.

Table 4.4: Effect of sulphonation time and weight of polymer rubber on the degree of sulphonation (DS) and viscosity (η) of the sulphonated rubber carried out at a constant stirring speed of 1000 rpm

Degree of Sulphonation (DS) (%) and Inherent Viscosity												
	5g		10 g		15 g		20 g		25 g		30 g	
T	DS	η	DS	η	DS	η	DS	η	DS	η	DS	η
2	2.39	0.36	3.86	0.41	3.70	0.41	3.37	0.39	2.72	0.37	2.39	0.36
4	2.88	0.37	4.85	0.49	4.19	0.42	3.70	0.41	3.21	0.38	3.21	0.38
6	3.04	0.37	5.85	0.53	5.35	0.51	4.52	0.43	4.19	0.42	3.86	0.41
8	3.37	0.39	8.23	0.61	6.36	0.57	5.85	0.55	5.02	0.46	4.36	0.44
10	3.70	0.41	10.48	0.66	7.54	0.63	7.03	0.62	6.19	0.50	5.52	0.46

where T = time in hrs; DS = degree of sulphonation in % and η = inherent viscosity in $dl\ g^{-1}$

The inherent viscosities of the polymers were also seen to be affected by the introduction of the sulphonic acid group. $C_2H_4Cl_2$ was the solvent of choice for determining the inherent viscosities (η) of SPSBR. The inherent viscosities of the sulphonated polymer at different sulphonation time, different weight of the polymer at constant concentration of the acid were determined. The inherent viscosity of the SPBR varies between 0.36 – 0.66 dlg^{-1} (Table 4.4). The viscosity of the starting polymer (PSBR) in $C_2H_4Cl_2$ at 30°C is 0.28 $dl\ g^{-1}$. The results show that the inherent viscosities of the SPSBR are higher than that of PSBR in $C_2H_4Cl_2$ in all the samples. The higher viscosity value of SPSBR is as a result of increase in hydrogen–bonding interactions associated with the sulphonic acid group.

4.3.2 FT – IR and ¹H NMR Studies

The IR spectra (Figure 4.3) on the effect of sulphonation time showed a weak broad band at 3573 cm⁻¹ on the sulphonated polystyrene butadiene rubber (SPSBR) spectra, which represents the O-H vibration from sulphonic acid group upon sulphonation. The effect of time causes the band to increase as DS increases, although not sharply. The peak identified in the spectra at 1346 cm⁻¹ is due to the asymmetric stretching of S=O band, which leads to drastic reduction in peaks around 1000 cm⁻¹. The presence of the acid causes a shift in peak originally (PSBR) close to 700 cm⁻¹ to 800 cm⁻¹. The symmetric vibration of this bond affects the characteristic splint at 1309 – 1235 cm⁻¹ which also confirms the attachment of the sulphonic group. The peaks identified at 2846, 2919 and 3027 cm⁻¹ for both the PSBR and SPSBR are the bands for C-H, C-C and C=C, while the aromatic C=C and C-C were identified at 1649 and 1494 cm⁻¹, respectively (Biemark et al., 1963; Silverstein et al 1991). No significant change was observed at 700 and 759 cm⁻¹ within the region of the -C-H, which is out of plane deformation that indicates reaction substitution type, probably due to low concentration of acid. It suffices to note that the sharp band at 1450 cm⁻¹ which is unique to PSBR became reduced to broad peak after sulphonation. This reduction increases with DS. This is attributed to the interaction of the introduced sulphonic group by reducing the C-H bending vibration intensity of the polymer chain, thereby promoting the appearance of a new peak at 1403 cm⁻¹. Thus the results of the FT-IR analysis clearly show the occurrence of sulphonation through the presence of the sulphonate group on the SPSBR.

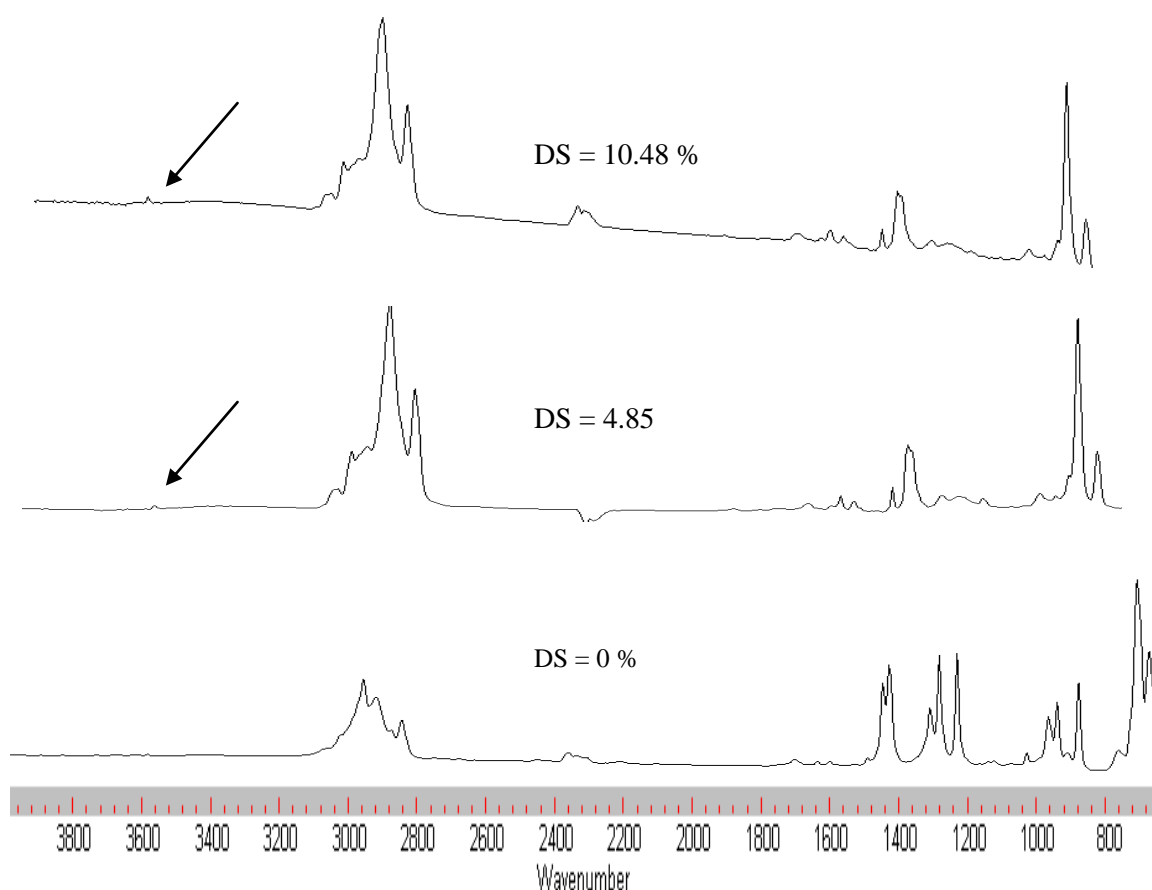


Figure 4.3: FT-IR spectra on effect of weight and time at constant acid concentration;
 unsulphonated PSBR and sulphonated PSBR

The ^1H NMR spectra showed in Figure 4.4 indicates that there is no significant change in the signals at 7.3 and 7.6 ppm for the SPSBRs (having DS = 4.85 and = 10.48 %). The only hump appearing between 4 and 5 ppm indicates the presence of sulphonic acid linkage on the benzene ring, confirming substitution to be limited to the para-position of the phenyl ring (Nobuhiro and Roger, 1994). The increase in chemical shift (7.16 to 7.24) in the aromatic protons range is observed in the case of the SPSBRs. This is as a result of the stronger electron attracting force of the sulphonic acid group.

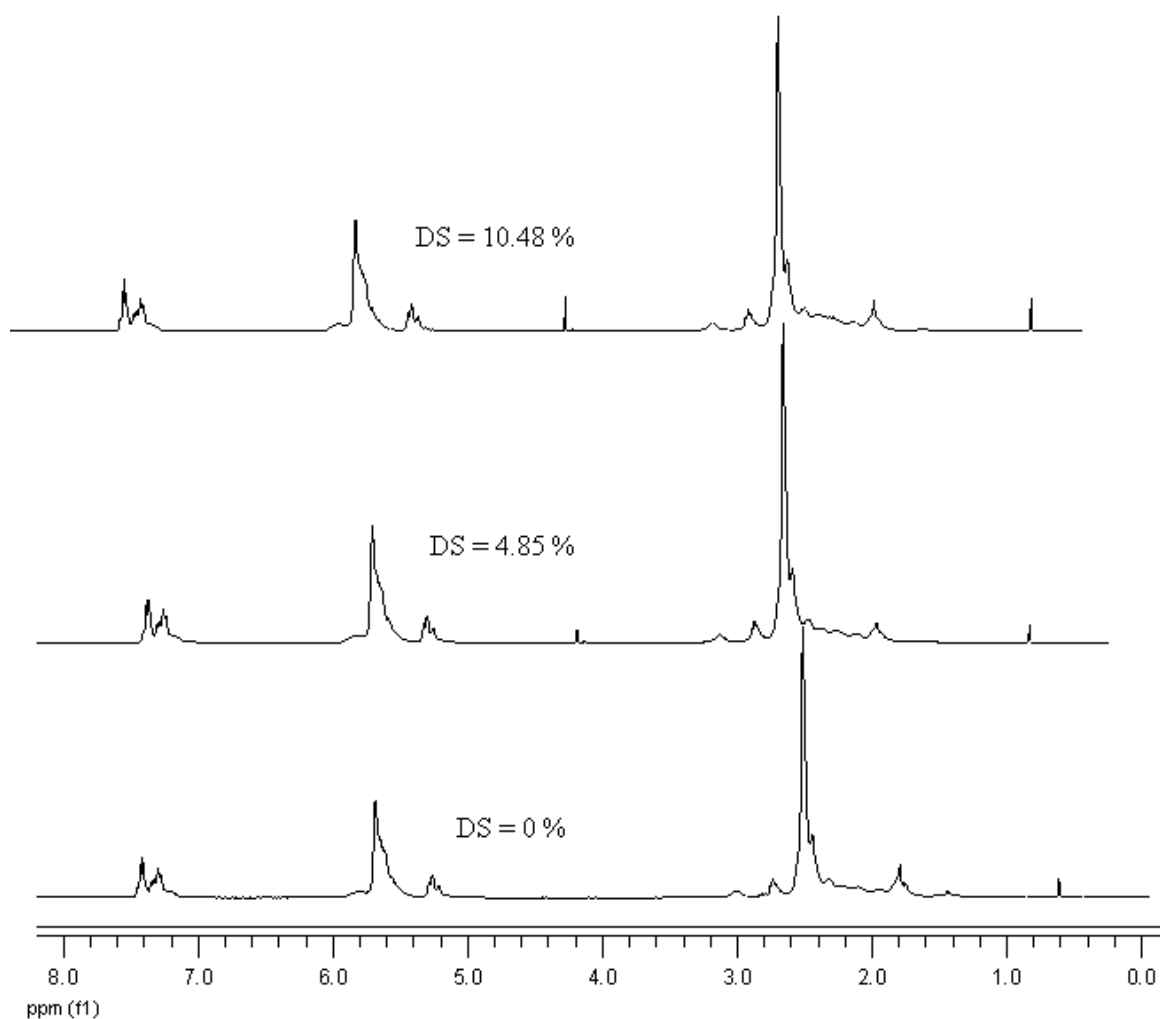


Figure 4.4: ^1H NMR spectra on effect of weight and time at constant acid concentration; unsulphonated PSBR and sulphonated PSBR

4.3.3 Effect of concentration of acid on the sulphonation of PSBR

About 0.4 – 2.0 M/ml of chlorosulphonic acid were investigated and the effect on DS and IEC at constant sulphonation time of 10 hours, weight of PSBR of 10 g and stirring speed of 1000 rpm were determined. It is noteworthy to state here that several attempts to go beyond 2.0 M/ml were impossible as they resulted in complete burning of the rubber and forming a large lump (Figure 4.5) and thereby bringing stirring to zero rpm.



Figure 4.5: Lump formation as a result of acid over (2 M/ml) concentration

The results of Sulphur content analysis (%), ion exchange capacity and degree of sulphonation at varying concentrations of chlorosulphuric acid are presented in Table 4.5. The results show that S_c , IEC and DS increase with increase in acid concentration until 1.6 M/ml before the polymer experienced reduction (S_c , IEC and DS) at 1.8 and 2.0 M, respectively. The reduction is as a result of over concentration (> 1.6 M/ml) of the acid on the polymer, which leads to scission and chemical degradation (Figure 4.6) of the polymer chain with the resulting consequence of limited site for SO_3H attachment. A situation that presents the polymer to suffer decrease in S_c , IEC and DS. The behavioural effect of the acid concentration on the degree of sulphonation and ion exchange capacity is illustrated in Figure 4.7. Also, the relationship between the optimum IEC and DS together with viscosity is illustrated in Figure 4.8

Table 4.5: Results of Sulphur content analysis (%), ion exchange capacity and degree of sulphonation at varying concentration of chlorosulphuric acid

Conc.	0.4	0.6	0.8	1.0	1.2	1.4	1.6	1.8	2.0
S_c	1.32	1.76	2.27	2.35	2.49	2.88	3.68	3.39	3.13
IEC	0.412	0.552	0.711	0.735	0.779	0.903	1.150	1.062	0.977
DS	6.73	9.13	11.92	12.34	13.13	15.39	20.04	18.35	16.76

where Conc. = Concentration (mol); S_c = Sulphur content (%); IEC = Ion exchange capacity (mmol/g); DS = Degree of sulphonation (%)

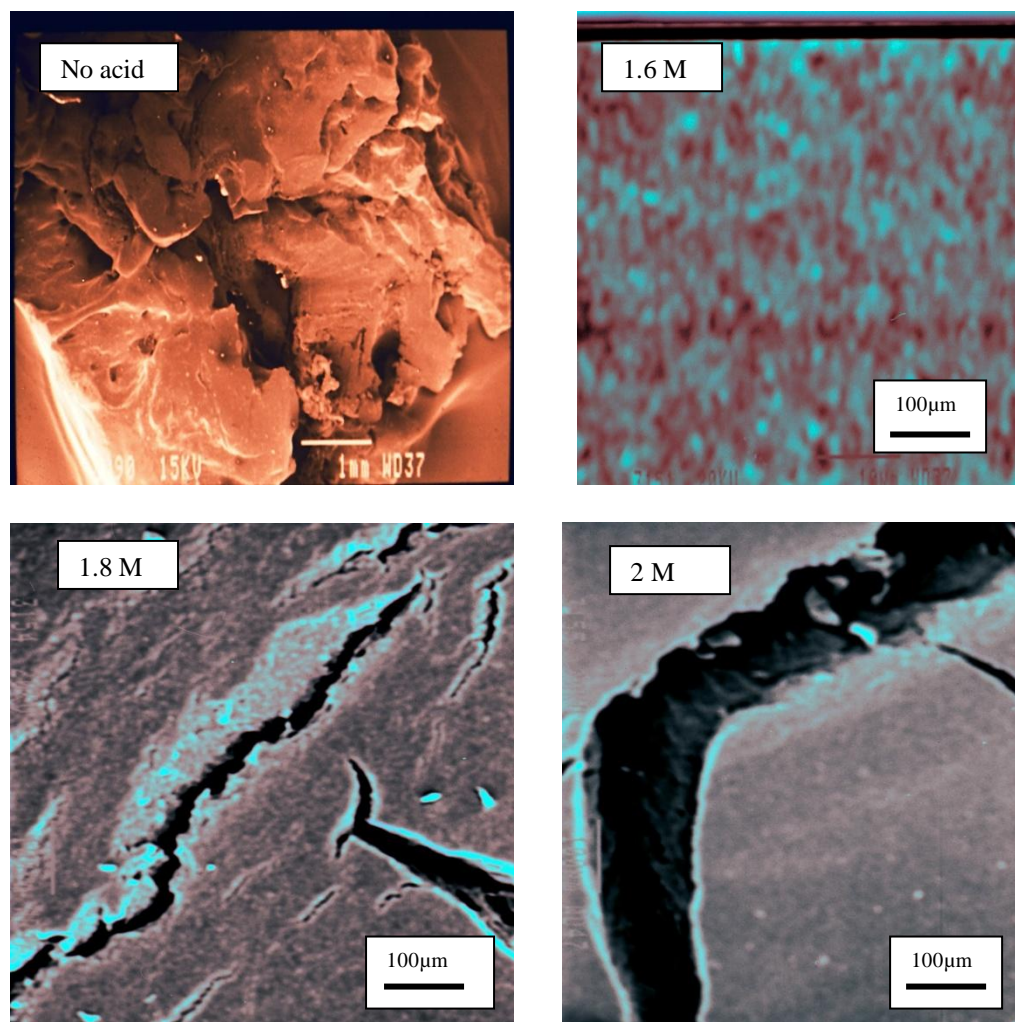


Figure 4.6: SEM images of different concentration of chlorosulphuric acid

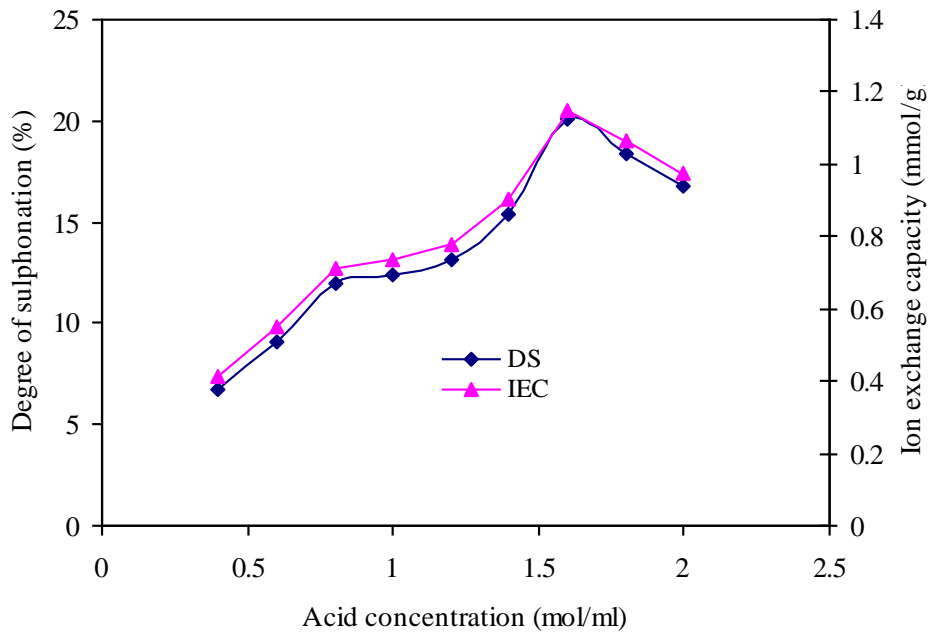


Figure 4.7: Effect of increasing acid concentration on sulphonation of PSBR

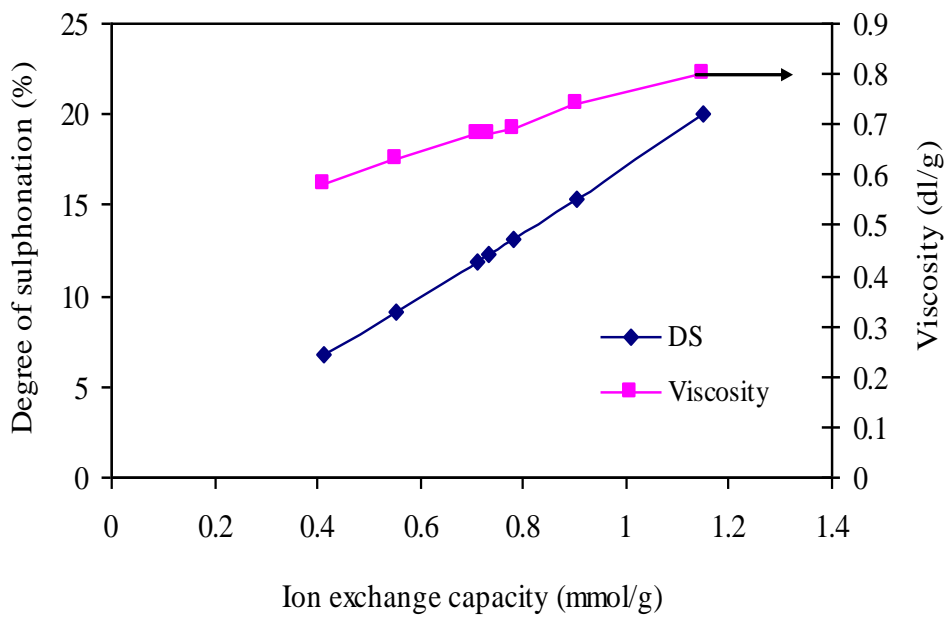


Figure 4.8: Relationship between ion exchange capacity, degree of sulphonation and viscosity

From Figure 4.8, the degree of sulphonation indicates that the content of the acid groups present in the polymer matrix is proportional to the ion exchange capacity which in turn is proportional to the inherent viscosity of the resulting SPSBR. As IEC increases from 0.412 – 1.15 mmol/g the DS correspondingly increases from 6.73 – 20.04 %. Since IEC is dependent on acid concentration (Table 4.6) (Zonquo, 2006), it is expected that as the ion exchange capacity increases more of the SO_3H group attached to the polymer matrix, which serves to increase the polymer hydrophilicity and thus promotes proton mobility and conductivity of the resulting membrane (Zongwu et al., 2006; Smitha et al., 2003). It can be seen that the IEC value (1.15 mmol/g) for the SPBR at DS of 20.04 % is highest for the acid concentration of 1.6 M/ml, exhibiting the highest viscosity of 0.8 dl g^{-1} . There is also IEC of 0.412 mmol/g for DS of 6.73 % is the lowest, exhibiting the lowest viscosity of 0.58 dl g^{-1} .

4.3.4 Effect of stirring speed

Stirring is an important factor in any chemical process that cannot be ignored as it affects reaction performance and product yield. Therefore, the effect of stirring speed on the sulphonation of PSBR was investigated using the Heidolph MR3002 dual plate machine (ordered from Germany) to see the mass transfer behaviour of the sulphonic group on the aromatic ring. This was carried out under sulphonation time of 10 hrs and acid concentration of 1.6 M/ml. The dual plate is calibrated from 100 – 1500 rpm. Figure 4.9 shows the effects of stirring speed on the degree of sulphonation and ion exchange capacity of the SPSBR.

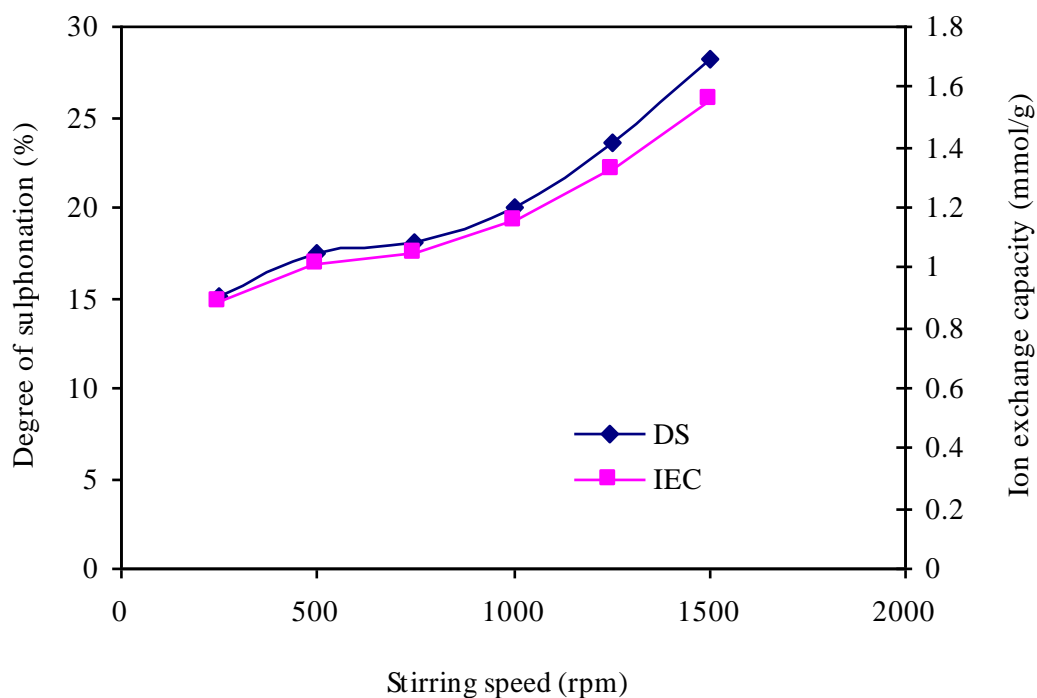


Figure 4.9: Effect of stirring speed on sulphonation of PSBR using 1.6 M of acid and 10 g of PSBR

The result shows that stirring speed is a significant factor in the sulphonation of PSBR as both the degree of sulphonation and ion exchange capacity increase with increase in stirring speed. The graph (Figure 4.9) shows almost a linear increase of degree of sulphonation and ion exchange capacity as stirring speed increases from 250 rpm rise to 1500 rpm. But between 1000 rpm to 1500 rpm, the result turns towards almost vertical, which indicates that high stirring speed favours the sulphonation reaction of PSBR. The increase in DS and IEC as stirring speed increases could be due to increase in the rate of SO_3H distribution to the phenyl ring which encourages sulphonation reaction of PSBR to proceed in a desired direction by maintaining uniform distribution of SO_3H group.

4.3.5 Effect of time on sulphonation of PSBR

The effect of time on the sulphonation of 10 g of PSBR at constant acid concentration (1.6 M/ml) was investigated under a predetermined stirring speed of 1500 rpm to see how it affects the IEC or DS as well as the viscosity of the resulting polymeric material. Since the conductivity of sulphonic acid based membranes is largely dependent on the number of available acid groups (DS) and their dissociation capability in water (Mokrini et al., 2006), it is of vital importance to explore process parameters in achieving the best result in terms of IEC or DS and viscosity relative to the SO₃H group. The SO₃H group creates the hydrophilic domain in the membrane which confers on the membrane the ability to absorb water as a result of affinity for water molecules. This, therefore, changes the acid functionality and facilitates proton transport (Larminie and Dicks, 2000; Mokrini et al., 2006). On the hand, the viscosity measurement of the membrane can suggest if the sulphonating polymer is undergoing chemical degradation or not, in which the former can impair the mechanical performance of the fuel cell drastically. It therefore means that the ion exchange capacity and viscosity measurement are integral parameters in PEM synthesis (Mokrini et al., 2006) because it defines both the membrane conductivity and its mechanical properties.

Figure 4.10 shows the result of degree of sulphonation, ion exchange capacity and the viscosity of the sulphonated PSBR as a function of optimum time of sulphonation. The behaviour of sulphonation of PSBR from 2 - 48 hrs clearly shows that optimum time of sulphonation is required for the sulphonation of PSBR to achieve its optimum ion exchange capacity, degree of sulphonation and viscosity. The figure reveals an initial increase of degree of sulphonation (13.22 %), ion exchange capacity (0.784 mmol/g) and viscosity (0.69 dl/g) with increasing sulphonation time, where an optimum yield of degree of sulphonation of 39.38 %, ion exchange capacity of 2.074 mmol/g and viscosity of 0.84 dl/g at 24 hrs were

achieved, respectively. Above 24 hrs (36 and 48 hrs) there is a steep decrease in the degree of sulphonation, ion exchange capacity and the viscosity values but progress slowly after 36 hrs.

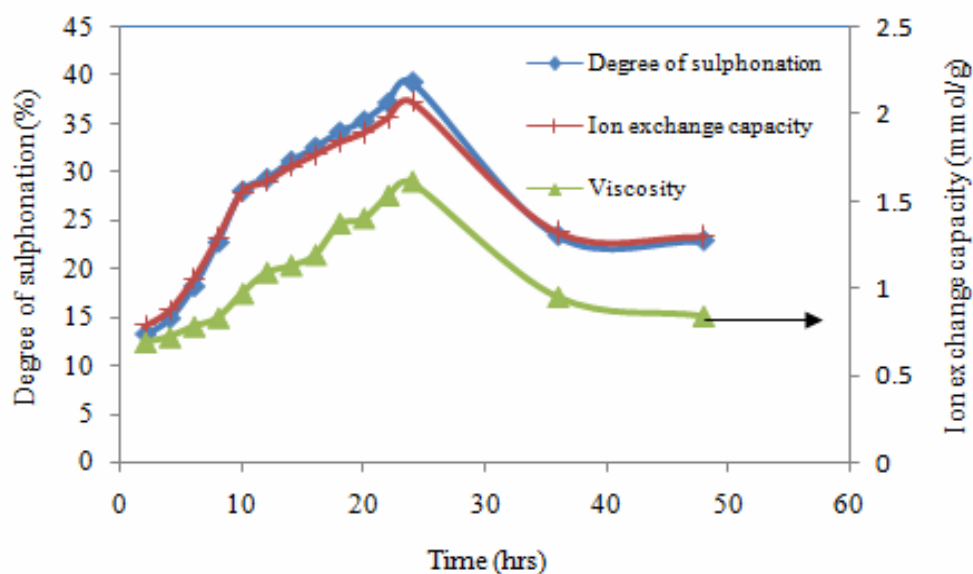


Figure 4.10: Degree of sulphonation, ion exchange capacity and viscosity as a function of optimum reaction time using 1.6 M of acid at room temperature and 1500 rpm.

This is an indication that prolonged time of sulphonation (> 24 hrs) is unfavourable to PSBR which leads to possible breakdown of the polymer chain with reduction of available site of attachment (for $-\text{SO}_3\text{H}$ group) and hence a reduction in the degree of sulphonation, ion exchange capacity and viscosity of the SPSBR. With this, a maximum reaction time of 24 hrs is chosen as a result of compromise arising from two phenomena that occurred during the process of sulphonation as described by Jia and co-workers (1996).

The first phenomenon involves the increase in interaction among the polar $-\text{SO}_3\text{H}$ groups that facilitate increase in the polymer viscosity. The second phenomenon is the degradation of the polymer chain which leads to reduction in molar mass that causes decrease in viscosity

(Basile et al., 2006), ion exchange capacity and consequently degree of sulphonation. This is seen to affect the film forming properties of the sulphonated polymer as membrane cast from this resulted in brittleness, indicating partial degradation and loss of molar mass of the polymer and as such not suitable for fuel cell application because of poor mechanical stability. The higher inherent viscosity values obtained as against 0.28 dl/g of the starting material with high degree of sulphonation is not due to increase in molecular weight but increase in the ion content of the polymer solution as shown in Figure 4.11, where increase in ion exchange capacity increases the viscosity of the sulphonated polymer along degree of sulphonation.

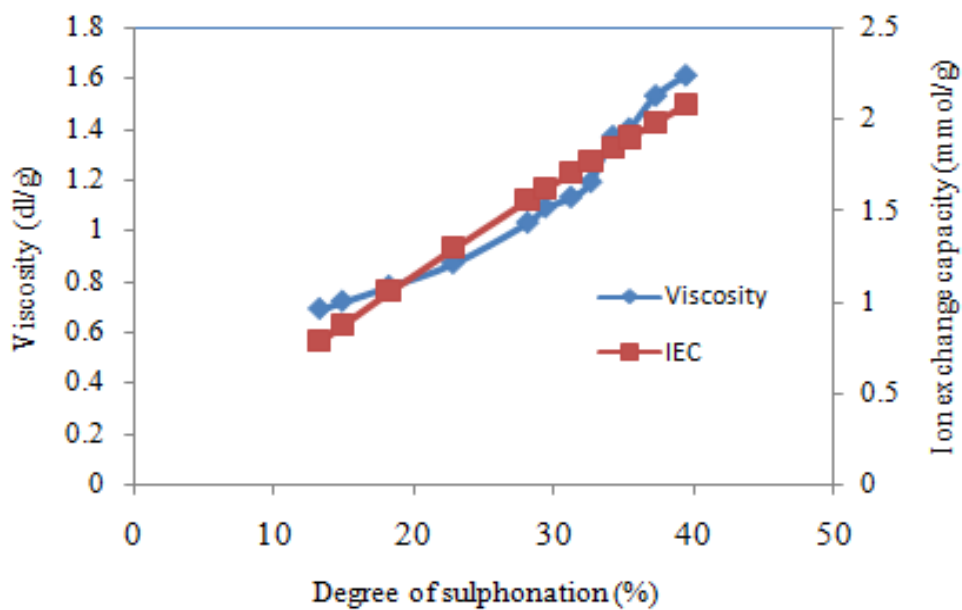


Figure 4.11: A graph of viscosity against degree of sulphonation and ion exchange capacity; where IEC = ion exchange capacity (using 1.6 M of acid, room temperature and 1500 rpm)

This concept has also been reported by Nazan, (2001) on the synthesis and characterisation of polyimides and it was found out that increase in viscosity is due to increase in ion content of the polymer solution and not molar mass increase. This implies that the high inherent

viscosity with high ion exchange capacity is an indication that the polymer chain aggregates as a result of electrostatic interactions between pendants ionic $-\text{SO}_3\text{H}$ groups in the polymer solution (Rusanov and Bulycheva, 1991; Nazan, 2001).

4.3.6 FT- IR analysis of effect of time on SPSBR

Figure 4.12 shows the FT-IR spectroscopy spectra on the effect of DS as a function of sulphonation time (8 – 24 hrs) on PSBR. The weak broad bands at 3573 cm^{-1} indicated by arrows represent the O-H vibration from sulphonic acid group upon sulphonation which grows out very slowly with increasing sulphonation time and DS. The peak identified in the spectra at 1360 cm^{-1} corresponds to the asymmetric stretching of S=O band with gradual increase in intensity with time. The symmetric vibration of this bond affects the characteristic splint at $1309 - 1200\text{ cm}^{-1}$. As the DS increases with time the symmetric and asymmetric stretching vibration resulting from the S=O group between $1500 - 900\text{ cm}^{-1}$ increases significantly, which simultaneously increases the intensity of the aromatic C=C and C-C at 1649 and 1494 cm^{-1} and that of the non-aromatic at 2846 and 2919 cm^{-1} , respectively. The single strong peak on SPSBR at 920 cm^{-1} can be attributed to the first type electrophilic substitution of an H atom with the $-\text{SO}_3\text{H}$ group in the aromatic ring. The sharp band at 1500 cm^{-1} on PSBR reduces to broad peak after sulphonation. This reduction increases with DS as a result of increased interaction of the introduced sulphonic group as sulphonation time increases.

Further analysis of the effect of time on sulphonation is shown in Figure 4.13. The $^1\text{HNMR}$ spectra indicate a hump appearing between 3 and 4 ppm which represents the presence of sulphonic acid linkage on the benzene ring. The increase in peak intensity between 3 and 4 ppm is observed in the case of the SPSBR, which increases as the degree of sulphonation

increases with time as a result of the effect of the sulphonic acid group attached to the aromatic ring. This indicates that electrophilic substitution is limited to only the para position of the aromatic ring (Nobuhiro and Roger, 1994). Therefore, increase in the degree of sulphonation continues to increase the strength of the peak.

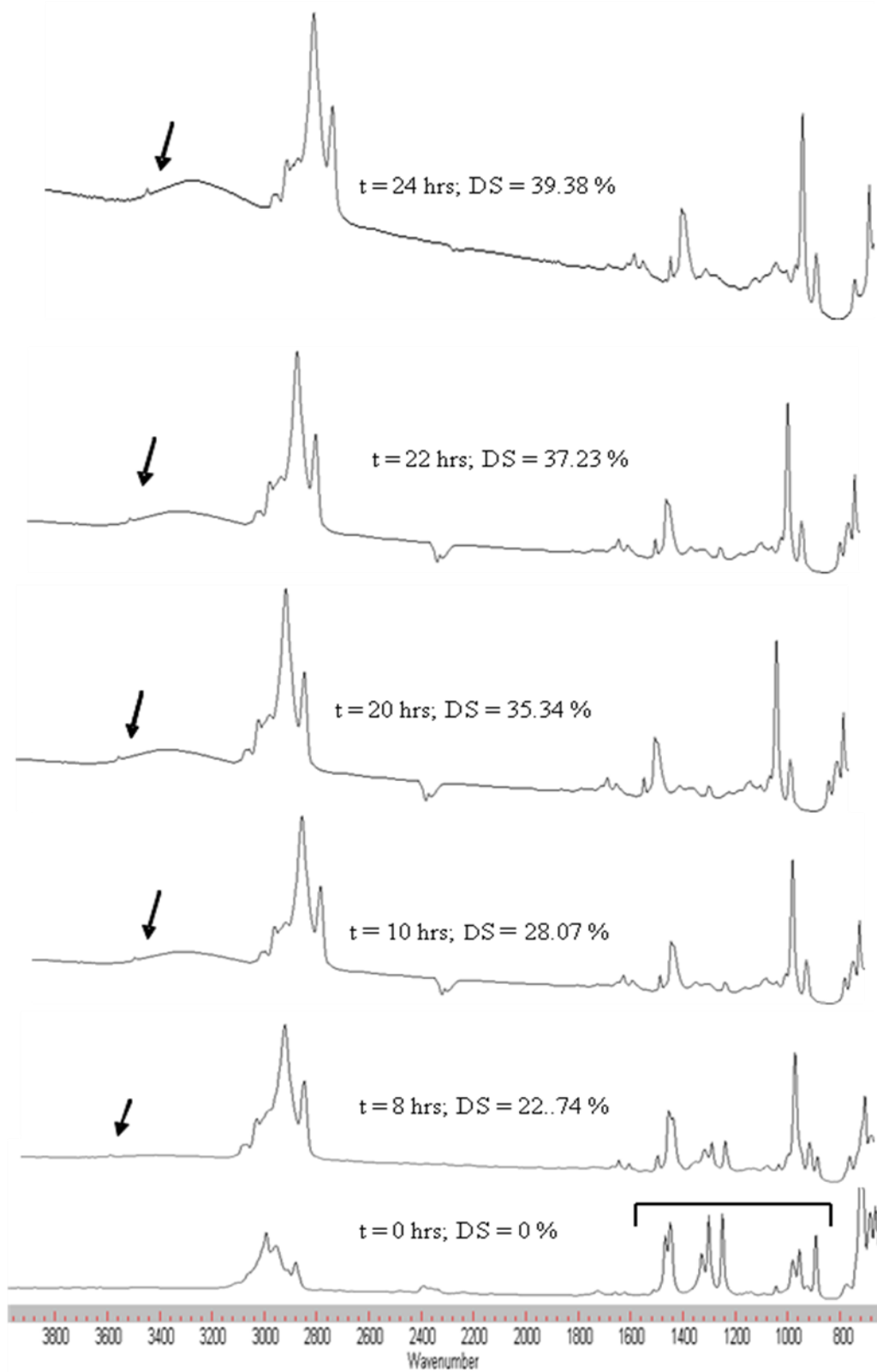


Figure 4.12: IR spectra of SPSBR on the effect of sulphonation time.

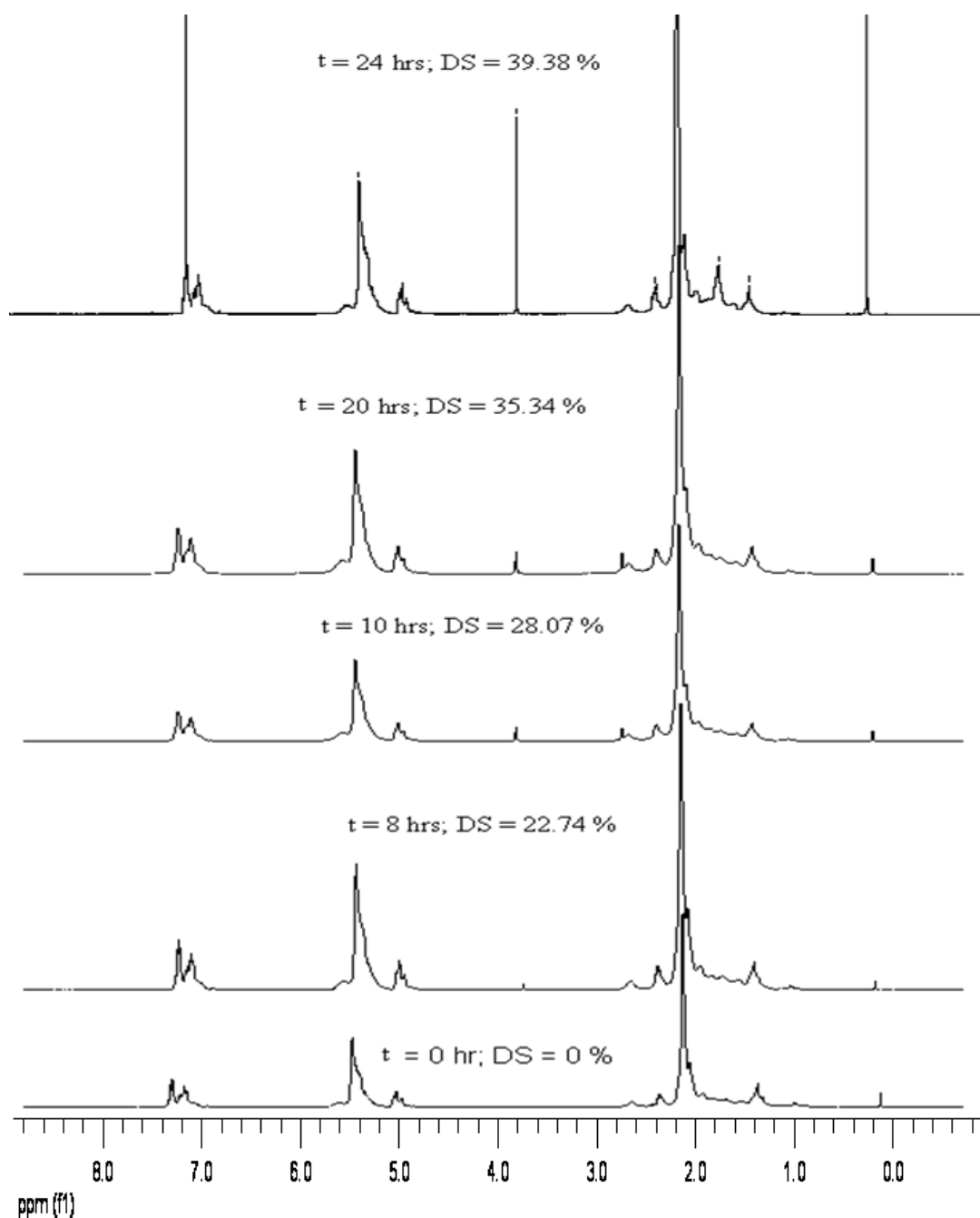


Figure 4.13: ¹H NMR spectra of SPSBR on the effect of sulphonation time

4.3.7 Effect of temperature on ion exchange capacity and degree of sulphonation

The effect of temperature on the sulphonation of PSBR was similarly investigated between 22 – 75°C. Several attempts to go beyond 75°C the solution turned into a solid. Results in

Figure 4.14 and 4.15 show that an increase in temperature significantly increases the ion exchange capacity and the degree of sulphonation of the resulting polymer. This indicates that elevating the temperature of the sulphonation process the thermal energy of the system is raised which therefore facilitates the rate of electrophilic substitution on the aromatic ring.

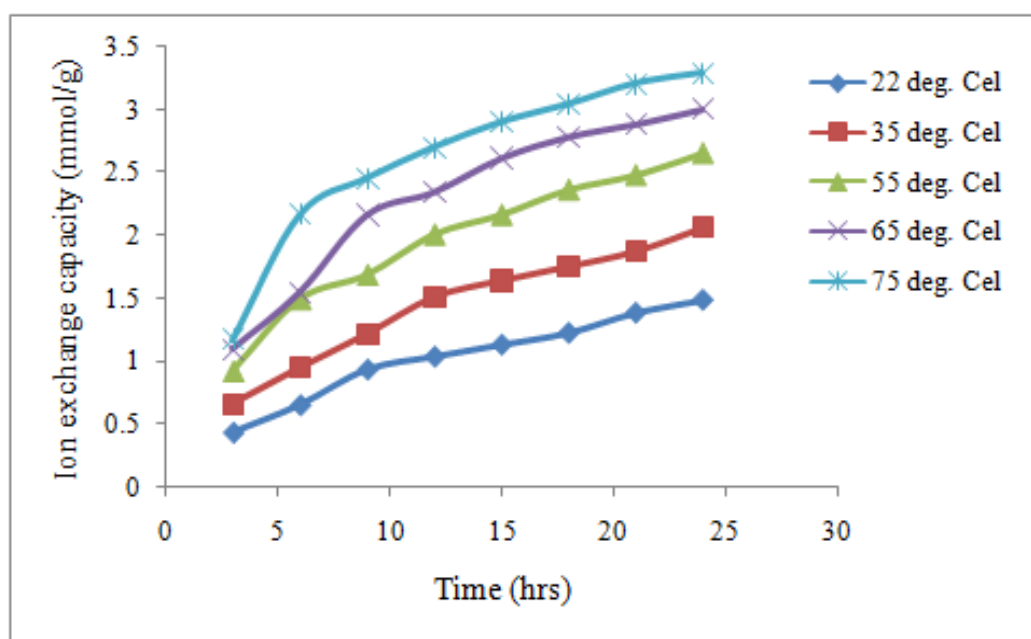


Figure 4.14: Effect of temperature on the ion exchange capacity of PSBR using 1.6 M of acid and a stirring speed of 1500 rpm

As the rate of electrophilic substitution increases, increase on the ion exchange capacity of the polymer is therefore encouraged. This directly increases the degree of the PSBR sulphonation. The above graph (Figure 4.14) clearly shows an optimum ion exchange capacity of 3.29 mmol/g at 75°C as against 1.35 mmol/g at 22°C, and a degree of sulphonation (Figure 4.15) of 70.26 % at 75°C as against 23.8 % at 22°C. Over 2 folds increase in ion exchange capacity and degree of sulphonation was achievable on the effect of temperature on the sulphonation of PSBR within the above stated temperature. However the poorest ion

exchange capacity and degree of sulphonation was achieved at a very short time of sulphonation both at 22°C and 75°C, respectively.

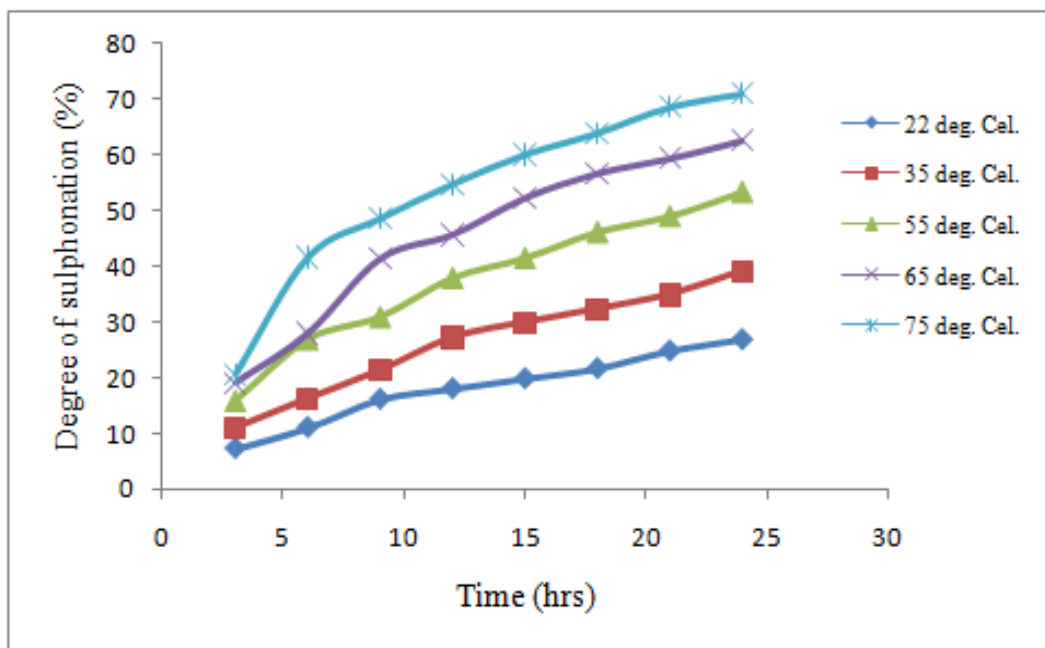


Figure 4:15: Effect of temperature on the degree of sulphonation using 1.6 M of acid and a stirring speed of 1500 rpm

CHAPTER FIVE

5.0 KINETIC STUDY OF THE SULPHONATION OF POLYSTYRENE-BUTADIENE RUBBER

5.1 Kinetic Study of Aromatic Sulphonation of PSBR with Chlorosulphonic Acid

The kinetic study of the aromatic sulphonation of PSBR with chlorosulphonic acid was carried out in order to establish the rate of the PSBR sulphonation reaction with chlorosulphonic acid, the activation energy of the process and also to be able to understand the reaction mechanism involved. This is important because the manner in which materials behave within reactors, both chemically and physically, is significant in the design of any chemical process (Fogler, 1992).

The kinetics of aromatic sulphonation are useful for commercial production and, according to Nobuhiro and Roger (1994), it has been under study since 1908. However, very few aromatic compounds especially in sulphuric acid have been successfully studied kinetically in the past due to challenges involved. Akovali and Özkan reported the kinetics of atactic polystyrene (PS) with concentrated sulphuric acid where the phenyl ring of each repeat unit of the polymer was treated as the substrate for the kinetics (Akovali and Özkan, 1986).

Sulphonation is an electrophilic substitution reaction (Huang et al., 2001; Bailly et al., 1987) and its application depends on the substituents present on the ring (Bailly et al., 1986). Aromatic sulphonation is widely used in chemical synthesis and fuel refinery (Nobuhiro and Roger, 1994). The corresponding arylsulphonic acid is achieved with various aromatic structures upon sulphonation. Thus, property modification of aromatic polymers is possible

as a result of the sulphuric group that is strongly acidic (Akovali and Özkan, 1986 and Bailly et al., 1987).

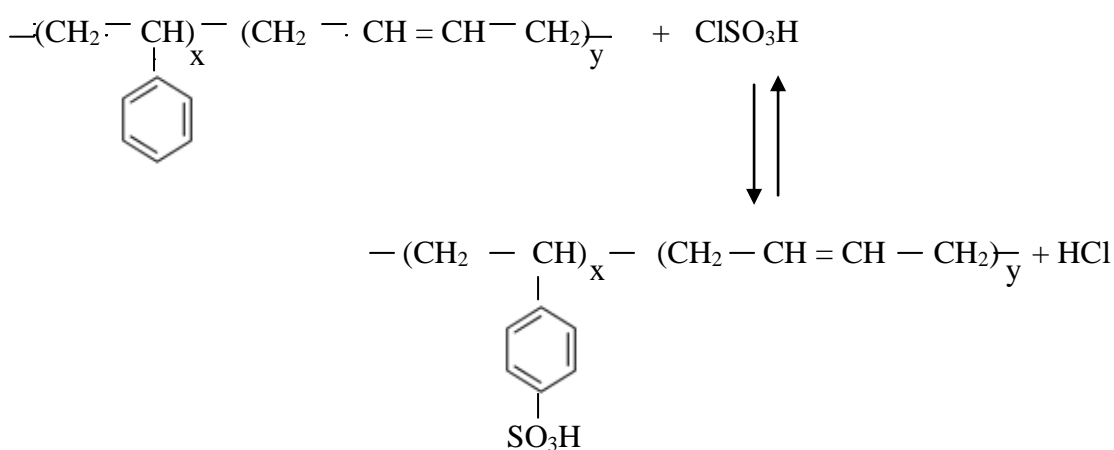
Sulphonation of polyether-ether-keton (PEEK) in the mixture of sulphuric acid and methanesulphonic acid has been treated kinetically, where only the phenyl ring flanked by two ether groups in the repeat unit, having only one of the four protons being substituted by sulphuric acid group was considered as the substrate (Bishop et al., 1985). This is expected as the introduction of the strong electron-withdrawing group deactivates the bonding phenyl ring to further sulphonation (Bishop et al., 1985). Hence, only one of the phenyl rings in each repeat unit is sulphonated at a time. Also, Daoust et al. (2001), has carried out the arylsulphonation of PEEK in concentrated sulphuric acid at room temperature where the small aromatic molecule, being the phenyl ring, was used for the kinetic treatment in terms of degree of sulphonation of the aromatic ring concentration (Daoust et al., 2001). However, Bailly et al. (1987) studied the kinetics of PEEK sulphonated in the mixture of methanesulphonic acid (MSA) and sulphuric acid and found out that the sulphonation degree was a function of the fourth power of the sulphuric acid concentration (Bailly et al., 1987).

The rate of aromatic compound sulphonation was reported to be first-order with respect to the phenyl ring (substrate) concentration (Cerfontain, 1968, Nobuhiro and Roger, 1994; Daoust et al., 2001).

5.2 Reaction Mechanism of Polystyrene-butadiene Rubber with Chlorosulphonic acid

Scheme 5.1 presents the reaction between polystyrene-butadiene rubber and chlorosulphonic acid. Chlorosulphonation of PSBR is essentially an electrophilic substitution reaction and in an equimolar amount, chlorosulphonic acid reacts with aromatic hydrocarbons to yield its

arylsulphonic product (Cremlyn, 2002; Adams, 1946). However, the reversibility of the process can not be ignored because of the tendency of the HCl produced causing desulphonation.



Scheme 5.1: Sulphonation reaction of polystyrene-butadiene rubber with chlorosulphonic acid

Figure 5.1 is the reaction mechanism of polystyrene-butadiene rubber in chlorosulphonic acid as proposed in this study. The first step of the reaction mechanism involves the electron rich aromatic ring attacking the electrophile (SO₃H), which leads to the formation of a positively charged cyclohexadienyl cation (carbonium ion). The carbocation is always unstable due to the positive charge on the molecule as well as the temporal loss of aromaticity. But the cyclohexadienyl cation will gain partial stability by resonance, which will then allow the positive charge to be distributed over three carbon atoms (Nick an David, 2001; Bigi et al., 1985).

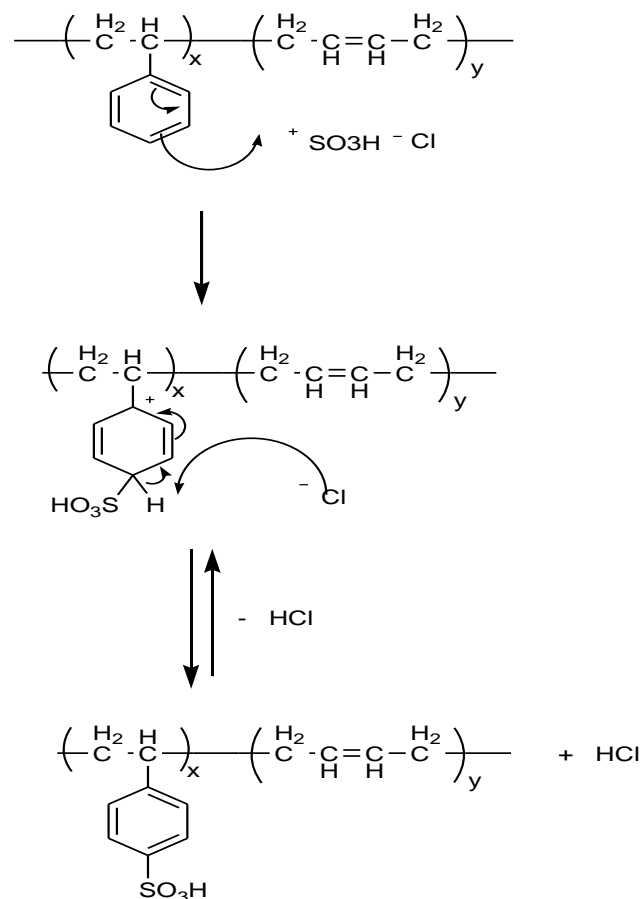


Figure 5.1: Reaction mechanism of polystyrene-butadiene rubber in chlorosulphonic acid

The second stage of the reaction involves a kind of a lone-pair Lewis base (Cl^-) reacting with the hydrogen atom at the point of electrophilic attack, and the electrons shared by the hydrogen return to the p_i system, thereby restoring the aromaticity of the styrene ring. Electrophilic substituents will usually withdraw electrons from the aromatic ring and consequently deactivate it from further reaction.

The extra electron density delivered into the ring by the substituent usually concentrates on the ortho and para positions of the aromatic ring. The highest electron density for benzene ring is seen to be located on both ortho positions, though increased reactivity might be offset by steric hindrance (Bigi et al., 1985; Nick and David, 2001). However, a thorough sulphonation study carried out on polystyrene showed that the substituent (SO_3H) attached on

the first para position (Akovali and Özkan, 1986). This could be due to steric effect hindrance on the ortho position since the first para position on the aromatic ring is already occupied.

As mentioned previously, sulphonation is an electrophilic substitution reaction and the active site for substitution is determined mainly by the electron density of the site (Huang et al., 2001). Generally the substitution can preferably take place in one of the five vacant positions of the aromatic ring of the repeat unit of PSBR. From scheme 5.1, only the vacant para-position is the farthest from the electron attracting effect of the carbonyl group compared to the meta and ortho positions. It will, therefore, possess higher electron density and thus be a point for aromatic substitution. It can be assumed that only one $-\text{SO}_3\text{H}$ group can be attached to each of the repeat units. Taking this into consideration, the assumptions below can be made.

1. Only the phenyl ring of each repeat unit of PSBR is sulphonated at a time
2. The electrophilic substitution reaction involves only the vacant para proton on the aromatic ring
3. Probable volume change in the course of reaction is ignored
4. HCl produced alongside sulphonation may and may not have effect on the reaction.

As a result two reaction mechanisms are proposed:

A. Sulphonation of PSBR with chlorosulphonic acid, HCl has no effect and thus no desulphonation

B. Sulphonation of PSBR with chlorosulphonic acid, HCl has effect and thus desulphonation

5.3 IR and ^1H NMR Studies of Sulphonated Rubber

The IR of the sulphonated PSBR was analysed before and after termination time (15 mins) of sulphonation to check for differences in their spectra. Both IR spectra (before and after termination) are found to be identical with the ones previously discussed (Figure 4. 3). However, degree of sulphonation (0.33 %) was found to be negligible, which revealed an insignificant asymmetric stretching effect of the $\text{S} = \text{O}$ group around $800 - 1600 \text{ cm}^{-1}$ (Figure 5.2).

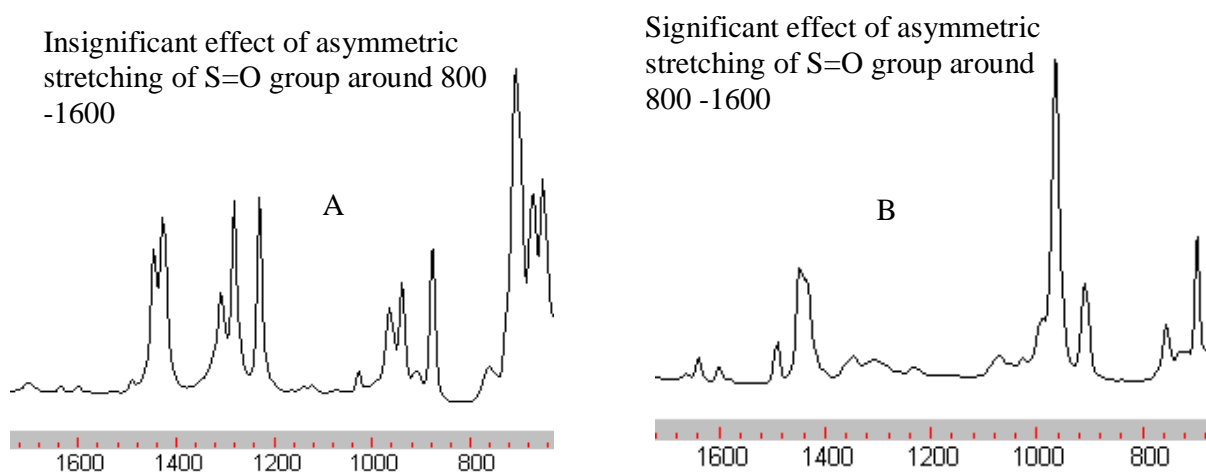


Figure 5.2: IR of short time (A) and at sulphonation $> 1\text{hr}$

The degree of sulphonation before termination was found to be higher than that of after termination (0.02 %), reason being that reaction had taken place before the sample was mounted on the IR for analysis, in spite of the short time involved. The ^1H NMR analysis of the before and after termination of PSBR are similar to that of the sulphonated rubber (Figure 4.4) with a single peak appearing at about 3 – 4 ppm. The peak represents the sulphonic acid linkage on the aromatic phenyl ring. This points to the fact that sulphonation of PSBR is an electrophilic substitution reaction involving only the aromatic ring.

5.4 Rate of Sulphonation of PSBR

The rate of aromatic sulphonation is considered to be first-order in respect of the substrate concentration which is the phenyl ring (Cerfontain, 1968; Akovali and Özkan, 1986; Daoust et al., 2001). In this study, the repeat unit is regarded as a small aromatic molecule for the kinetic treatment since it is the active site for sulphonation, and X is thus considered as the reaction conversion of the aromatic molecules sulphonated.

5.4.1. The kinetic treatment of case (A) mechanism

First-order rate law is proposed;

Mass balance of the sulphonation of polystyrene-butadiene rubber in the absence of desulphonation



Mass balance assuming first-order reaction with respect to $PSBR$ repeat unit concentration (C) in a batch reactor system; non effect of HCl on the reaction

$$-\frac{dC}{dt} = k_1 C \quad (5.2)$$

where t and k_1 represent the reaction time and the rate constant, respectively. This equation is integrated from the beginning of the reaction ($C = C_0$ at $t = 0$) to a concentration (C at $t = t$) to give:

$$-\int_{C_0}^C \frac{dC}{C} = k_1 \int_0^t dt \quad (5.3)$$

$$-\ln \frac{C}{C_0} = k_1 t \quad (5.4)$$

Equation (5.5) describes the substrate concentration:

$$\frac{c_0 - c}{c_0} = X \quad (5.5)$$

where X is equal to reaction conversion

Substituting equation (5.5) into equation (5.4) gives;

$$-\ln(1 - X) = k_1 t \quad (5.6)$$

If the reaction is first-order without HCl effect on the reaction then a plot of $-\ln(1-X)$ against t should give a straight line unless otherwise HCl produced has effect on the reaction. Therefore, mechanism (B) may be considered. Figure 5.3 is the kinetic of PSBR sulphonation in different initial concentrations of chlorosulphonic acid to obtain representative kinetic curves.

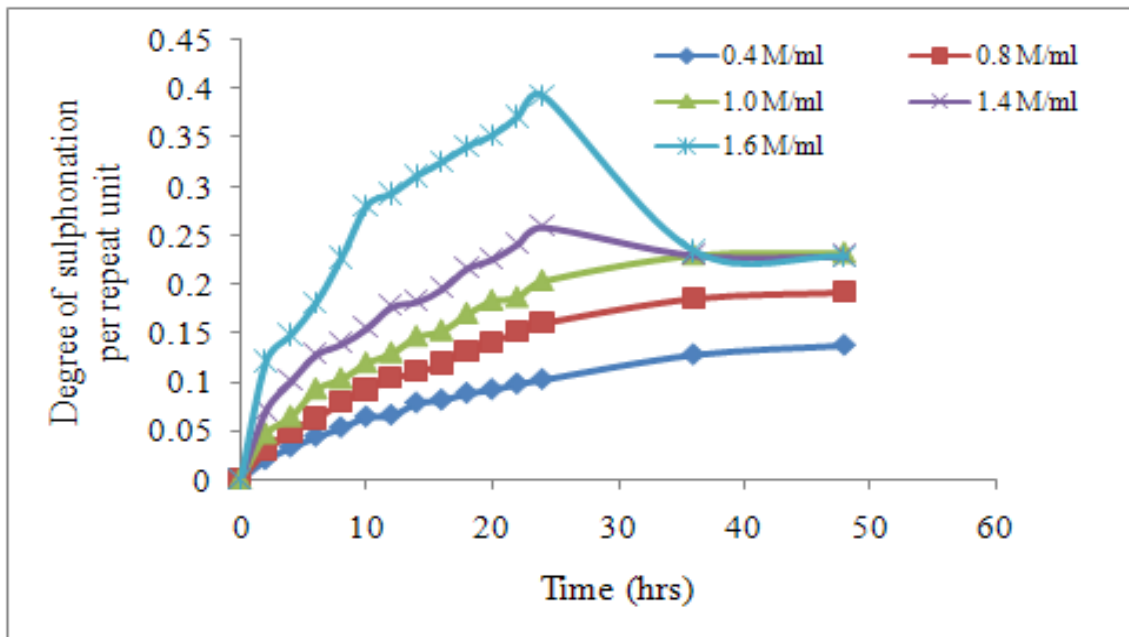


Figure 5:3: Kinetics of PSBR sulphonation in chlorosulphonic acid in different initial concentration of chlorosulphonic acid

From the shape of the curves in Figure 5.3, it appears that the rate of sulphonation gradually decreases with reaction time. However, a drastic drop in degree of sulphonation can be seen with sulphonation involving 1.4 and 1.6 M/ml after 24 hrs where all the reactions have started attaining completion. This can be due to molar mass breakdown and degradation of the PSBR (Basile et al., 2006). The use of different chlorosulphonic acid concentrations emphasizes the influence of the acid strength on the sulphonation rate

Figure 5.4 shows the plot of $-\ln(1-X)$ vs time which could not fit a straight line as expected (all R^2 values are < 0.9) as the experimental data show curvature indicating that the reaction has HCl effect.

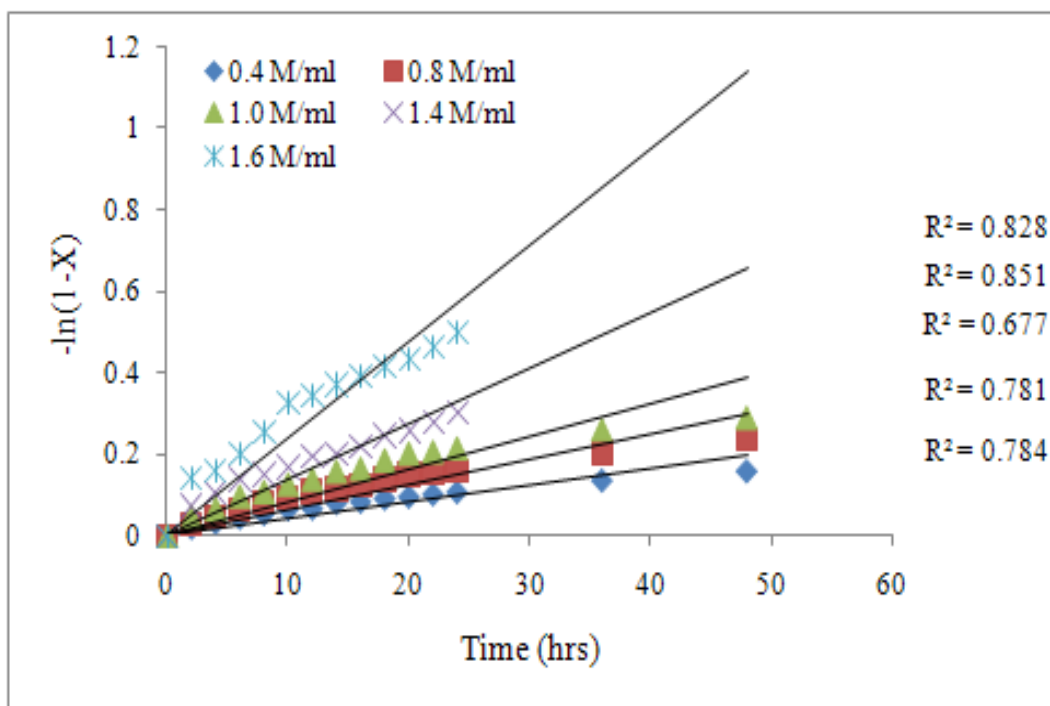
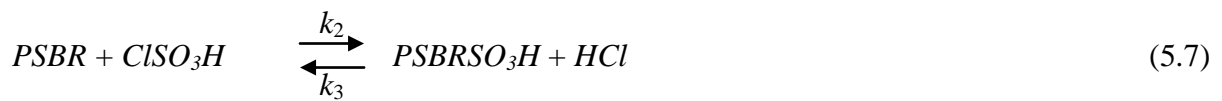


Figure 5.4: Kinetics of PSBR sulphonation in chlorosulphonic acid: the first-order rate treatment in respect to non effect of HCl on the substrate concentration

Data from Figure 5.4 simulate a linear function only at the early stage of the reaction and the rate subsequently becomes slow, showing a sign of inhibition, with the difference between the data and the straight line gradually increasing as the reaction progresses. As a result of this phenomenon mechanism B is thus considered.

5.4.2. Rate of reaction in case (B) mechanism

The possible effect of HCl desulphonation on the reaction system



where k_2 and k_3 are the rate constants for both forward and backward reactions, respectively.

Mass balance assuming first-order reaction with respect to *PSBR* repeat unit concentration (*C*) in a batch reactor system; effect of HCl on the reaction

$$-\frac{dC}{dt} = \frac{k_2 C}{k_3 (C_0 - C)} \quad (5.8)$$

Integrating equation (5.8) from C_0 to C gives equation (5.9)

$$-\int_{C_0}^C \frac{C_0 - C}{C} dC = \frac{k_2}{k_3} \int_0^t dt \quad (5.9)$$

$$-\int_{C_0}^C \frac{C_0 dC}{C} + \int_{C_0}^C \frac{C}{C} dC = \left[\frac{k_2}{k_3} t \right]_0^t \quad (5.10)$$

$$-C_0 [\ln C]_{C_0}^C + [C]_{C_0}^C = \left[\frac{k_2}{k_3} t \right]_0^t \quad (5.11)$$

$$-C_0 (\ln C - \ln C_0) + (C - C_0) = \frac{k_2}{k_3} t \quad (5.12)$$

$$-C_0 (\ln \frac{C}{C_0}) + (C - C_0) = \frac{k_2}{k_3} t \quad (5.13)$$

$$-C_0 \ln \frac{C}{C_0} + C - C_0 = \frac{k_2}{k_3} t \quad (5.14)$$

But substrate concentration is given in equation (5.5) and substituting into equation (5.14) gives:

$$-C_0 \ln \frac{C_0(1-X)}{C_0} + C_0 - C_0X - C_0 = \frac{k_2}{k_3} t \quad (5.15)$$

$$-C_0 \ln (1 - X) - C_0X = \frac{k_2}{k_3} t \quad (5.16)$$

$$-C_0 \{ \ln (1 - X) + X \} = \frac{k_2}{k_3} t \quad (5.17)$$

But $\frac{k_2}{k_3} = K_c = K$ (*equilibrium constant*)

Then equation (5.17) becomes

$$C_0 \{ 1 - \ln(1 - X) - X \} = Kt \quad (5.18)$$

Equation (5.18) can as well be expressed as:

$$C_0 \{ -X - \ln(1 - X) \} = Kt \quad (5.19)$$

A plot of $C_0 \{ -X - \ln(1 - X) \}$ against t (time) gives a straight line as shown in Figure 5.5

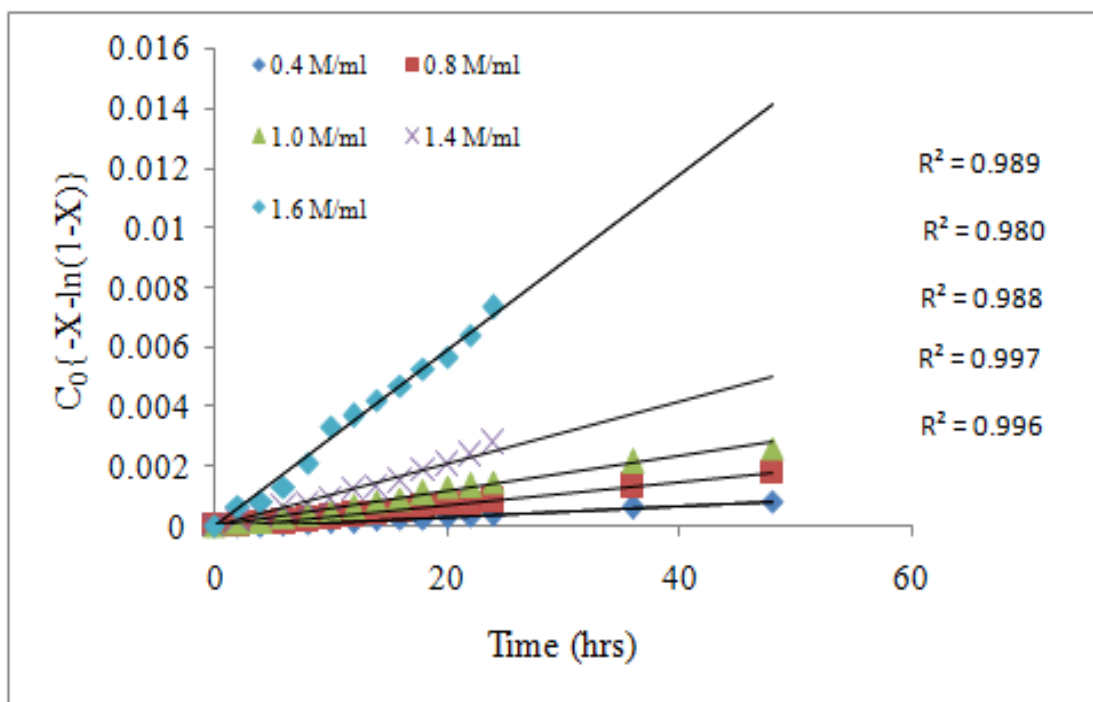


Figure 5.5: First-order effect of HCl on PSBR sulphonation in chlorosulphonic acid.

The plot of Figure 5.5 fits a straight line for all these experiments (0.4 – 1.6 M/ml). Each of the least square fits of the plots does intersect (0,0), indicating that HCl produced has effect on the sulphonation of PSBR in chlorosulphonic acid causing desulphonation and thus inducing reversibility of the process. Table 5.1 shows the concentration of HCl produced alongside the sulphonation of PSBR. The result shows that the concentration of HCl produced increases gradually with time of sulphonation before attaining a constant value at 24 hrs. This is affirming the cause of the inhibition experienced during the sulphonation of PSBR in chlorosulphonic acid that is inducing the reversibility of the process. However, for concentration of 1.4 and 1.6 M/ml of ClSO_3H considered, the amount of HCl produced is higher and decreases after 24 hrs of reaction completion.

Table 5.1: Amount of HCl produced alongside sulphonation of PSBR

Concentration of ClSO_3H (mol L^{-1})	HCl Concentration (mol L^{-1})			
	3 hrs	12 hrs	24 hrs	48 hrs
0.4	8.34×10^{-6}	8.38×10^{-6}	8.43×10^{-6}	8.43×10^{-6}
0.8	8.35×10^{-6}	8.40×10^{-6}	8.45×10^{-6}	8.46×10^{-6}
1.0	8.36×10^{-6}	8.42×10^{-6}	8.47×10^{-6}	8.47×10^{-6}
1.4	2.13×10^{-5}	2.19×10^{-5}	2.25×10^{-5}	2.20×10^{-5}
1.6	2.68×10^{-5}	2.83×10^{-5}	2.9×10^{-5}	2.78×10^{-5}

This suggests that the drastic reduction in degree of sulphonation experienced after 24 hrs of reaction completion when 1.4 and 1.6 M/ml (Figure 5.3) of ClSO_3H acid are considered could be associated with the reduction of HCl concentration experienced after the 24 hrs of reaction. The consumption of high HCl concentration at that point might have contributed to the polymer molar mass breakdown (Jia et al., 1996; Basile et al., 2006) which reduces the degree of sulphonation drastically. However, in all the concentrations of ClSO_3H considered for the sulphonation of PSBR, 1.6 M/ml gives the optimum degree of sulphonation (Figure 5.3). Previous result in this study (section 4.3.3) on the effect of ClSO_3H concentration on PSBR sulphonation shows that concentration above 1.6 M/ml could not achieve the optimum degree of sulphonation but also destroyed the rubber (Figure 4.6). Thus, 1.6 M/ml becomes the optimum concentration for the sulphonation of PSBR in chlorosulphonic acid. Besides, at other concentrations lower than 1.6 M/ml considered, the corresponding degrees of sulphonation obtained appear to be too low to achieve the ionic conductivity for proton exchange membrane fuel cell application, which is the major objective of this study.

The model equation used to predict the degree of sulphonation of polystyrene-butadiene rubber at any initial concentration of chlorosulphonic acid is given in equation (5.20).

$$DS = 1 - e^{-\left(\frac{1}{2-C_0}\right)t^{0.55}} \quad (5.20)$$

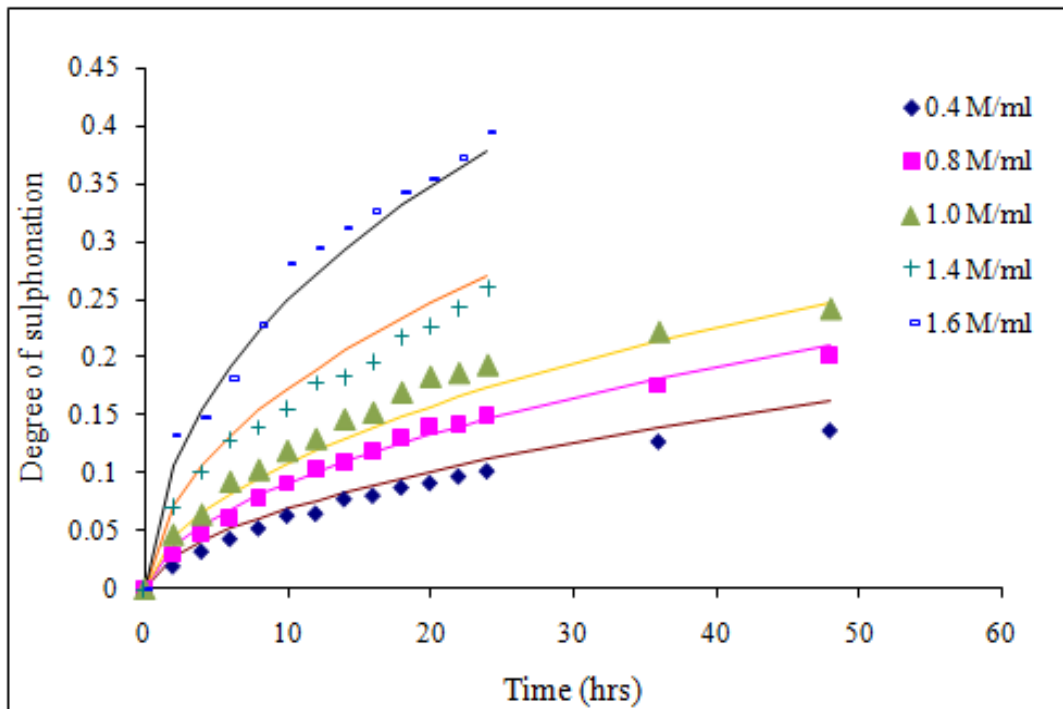


Figure 5.6: A plot of degree of sulphonation against time: smooth lines represent model while marked lines represent experiment.

Figure 5.6 is able to show that the model predicts the experiment quite well with correlation coefficients of 0.996, 0.995, 0.991, 0.997 and 0.994 for initial acid concentrations of 0.4, 0.8, 1.0, 1.4 and 1.6 M/ml, respectively. At different initial concentrations it is important to note that before now no literature has been able to report a predictive model for the degree of sulphonation of polymers which could be due to the kinetic complexity of polymer sulphonation, especially aromatic sulphonation (Daoust et al., 2001; cerfontain, 1968).

The sulphonation kinetics of PSBR in 1.6 M/ml of ClSO_3H was measured at five constant temperatures ranging from 295 to 348 K, where the origin of time scale was set at an approximate time of complete dissolution of PSBR.

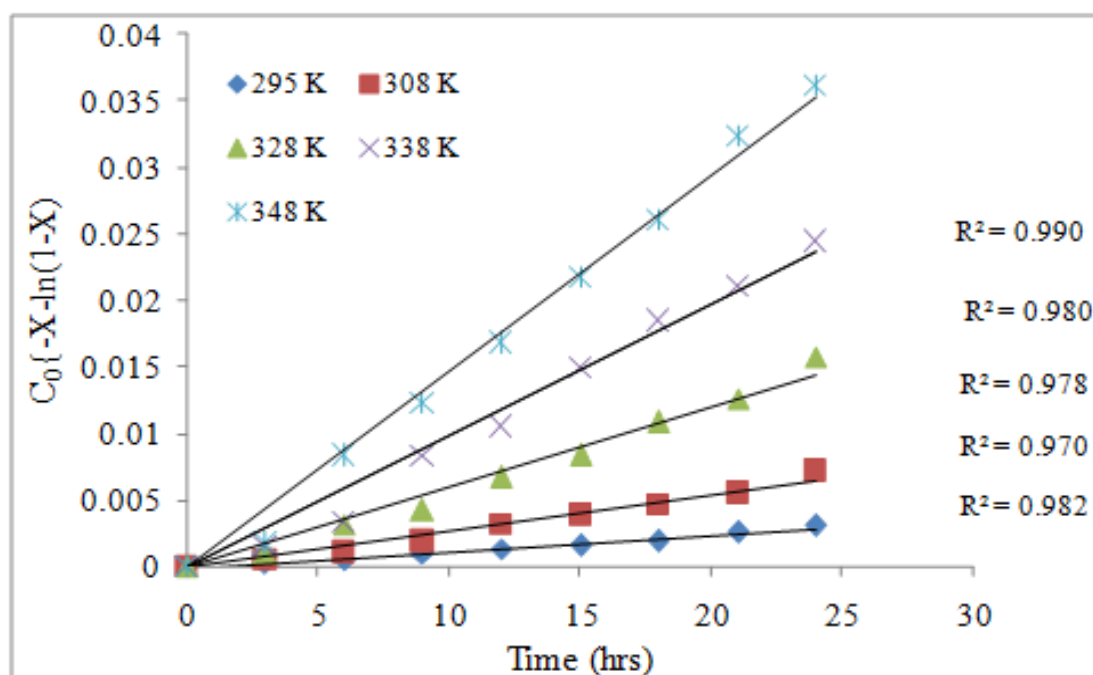


Figure 5:7: Kinetics of PSBR sulphonation in chlorosulphonic acid: the effect of temperature using 1.6 M/ml of acid and a stirring speed of 1500 rpm

The result (Figure 5.7) shows that temperature significantly increases the rate of sulphonation, as about 40 % increment of conversion is achieved. Evaluating reaction progress, data simulate a linear function thereby obeying first-order reversible process under the effect of temperature. The different values of K at different temperatures are shown in Table 5.2. Result shows that K value increases with temperature. The activation energy (E_a) of the process is thus obtained from the logarithm of equilibrium constants versus the reciprocal temperatures. An E_a of the reaction is calculated to be 41.56 kJ/mol of PSBR repeat unit

Table 5.2: *K* values at different sulphonation temperatures

Temperature	295 K	308 K	328 K	338 K	348 K
<i>K</i> values	0.0001	0.0003	0.0006	0.001	0.0015

5.5 Thermodynamic Study of PSBR Sulphonation

The thermodynamic study of the PSBR sulphonation is hereby considered in order to understand further the properties of the sulphonation reaction in terms of enthalpy, entropy and the Gibbs free energy of the system.

Since

$$\Delta G^\circ = \Delta H^\circ - T\Delta S^\circ \quad (5.21)$$

And

$$\Delta G^\circ = -RT \ln K \quad (5.22)$$

It implies that

$$\ln K = -\frac{\Delta H^\circ}{RT} + \frac{\Delta S^\circ}{R} \quad (5.23)$$

where: *K* is the equilibrium constant; ΔH° and ΔS° are the standard enthalpy and standard entropy change, respectively and *R* is the gas constant. A plot of the natural logarithm of the equilibrium constant versus the reciprocal temperature gives a straight line as shown in Figure 5.8. The slope and the intercept are used to get the ΔH° and ΔS° , respectively.

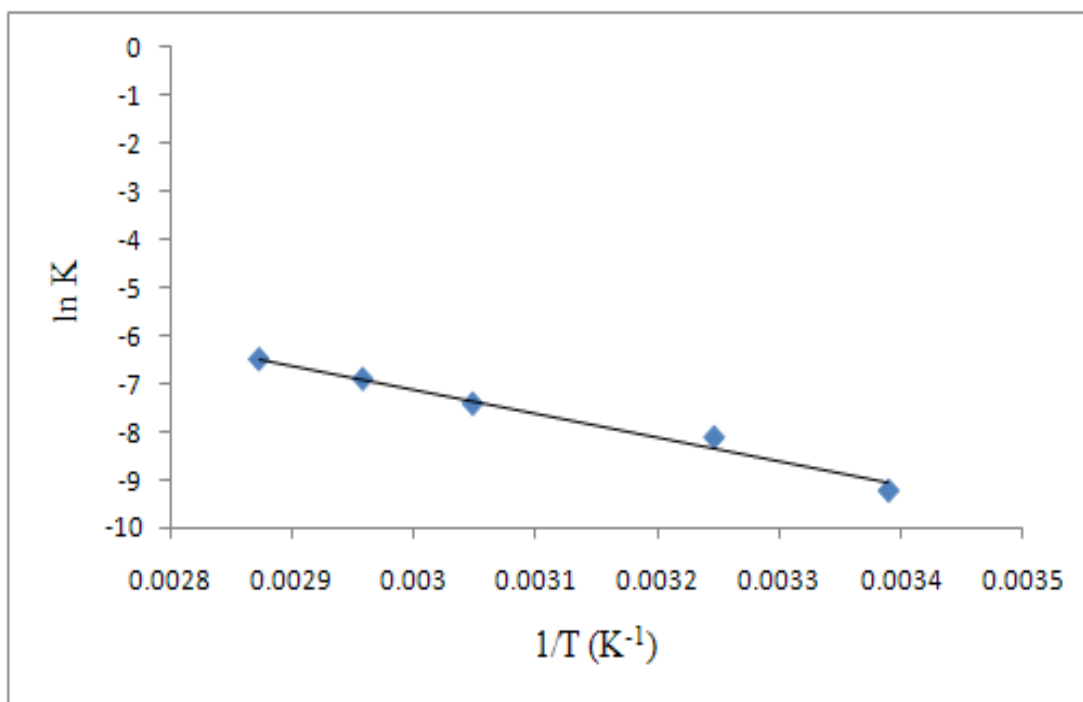
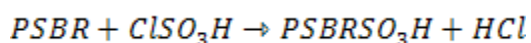


Figure 5.8: Logarithm of equilibrium constant versus the reciprocal temperature

From the analysis, ΔH° and ΔS° give 40.708 kJ and 64.22 J K⁻¹, respectively, while ΔG° gives 22.916 kJ. This implies that the positive value of ΔG° indicates that the reaction is not thermodynamically favourable and thus products are less favoured compared to reactants. This follows that the reaction is non-spontaneous and thus requires energy; hence the ΔH° value is high. This should be expected since the material under consideration is a polymeric rubber with high molecular weight (106,100 g/mol MW) and viscosity, having a repeat unit weight of 158 g/mol. The low ΔS° value shows that the system is relatively less disordered and the implication of the positive ΔS° is that the product has more tendency to be disordered than the reactant. However, temperature dependence of entropy of reaction may warrant us to ascertain product stability with temperature. Recalling equation 5.1 therefore;



The heats of reaction of the different reactants and products are obtained as;

$$H_B = M \times C_p(T) \quad (5.24)$$

where H_B , M , C_p and T represent heat for ClSO_3H , mass, specific heat capacity and temperature, respectively.

But C_p is a function of temperature = $1.204 + 1.402 \times 10^{-4} T - 2.887 \times 10^{-6} T^2$ ($\text{J k}^{-1} \text{g}^{-1}$)
(Kapias and Griffiths, 2001)

$$H_D = M \times C_p \times T \quad (5.25)$$

where H_D represents heat for HCl

But $C_p = 4.186$ ($\text{J k}^{-1} \text{g}^{-1}$) (C_p of HCl is constant in the range of temperature between 295-348 K)

H_A and H_C (being heat for PSBR and PSBR SO_3H) were obtained calorimetrically using the Differential Calorimetry Curve (DSC) Machine. Table 5.3 shows the heat of the different reactants and products at different temperatures.

Table 5.3: Heats of reaction of the different reactants and products at different temperatures

Temp (K)	H_A (J)	H_B (J)	H_C (J)	H_D (J)
295	-17.33	44976.99	-9759.47	44960.06
308	-1888.36	47262.49	-5303.77	46941.35
318	-4046.85	49046.18	-3218.16	48465.42
328	-6178.19	50852.91	-1205.85	49989.49
338	-8306.95	52683.34	99.20	51513.56
348	-10426	54538.15	43.10	53037.63

The sensible heat change of each of the reactant is obtained as shown below;

$$\Delta H_B = M \int_{298}^{348} C_p dT \quad (5.26)$$

$$\Delta H_D = H_D^T - H_D^0 \quad (5.27)$$

$$\Delta H_A = H_A^T - H_A^0 \quad (5.28)$$

$$\Delta H_C = H_C^T - H_C^0 \quad (5.29)$$

Table 5.4 shows the heat change of the different reactants and products at different temperatures, where the heat is found to increase as temperature increases.

Table 5.4: The heat change of different reactants at different temperatures

Temp (K)	ΔH_A	ΔH_B	ΔH_C	ΔH_D
298-295	71.36	-524.14	-2268.96	-457.22
298-308	-1799.67	1761.34	2186.75	1524.07
298-318	-3958.16	3545.04	4272.36	3048.14
298-328	-6089.5	5351.77	6284.66	4572.21
298-338	-8218.26	7182.20	7589.72	6096.28
298-348	-10337.3	9037	7533.52	7620.35

The enthalpy change, entropy change and the free Gibbs energy of the reaction at different temperatures are finally obtained from the following relation;

$$\Delta H_R^T = \Delta H_R^0 + \Delta H_{products}^T - \Delta H_{reactants}^T \quad (5.31)$$

$$\Delta S_R^T = -\frac{\Delta G_R^T - \Delta H_R^T}{T} \quad (5.31)$$

$$\Delta G_R^T = RT \ln K_T \quad (5.32)$$

Table 5.5 shows the ΔG_R^T , ΔH_R^T and ΔS_R^T and at different temperatures. Result shows that as ΔH_R^T , and ΔS_R^T increase as temperature increases, ΔG_R^T decreases with temperature which indicate that the reaction is becoming more feasible as temperature increases, and thus product formation or rather forward reaction is favoured. The increase of ΔS_R^T with temperature will increase the level of disorderness of the reaction. The nature of the entropy of the reaction as temperature changes can be seen in Figure 5.9.

Table 5.5: ΔG_R , ΔH_R , and ΔS_R at different temperatures

Temp (K)	ΔG_R	ΔH_R	ΔS_R
295	22589.56	38434.61	53.71
308	20771.8	44457.14	76.90
328	20230.41	52302.61	97.78
338	19411.70	55430.05	106.56
348	18812.89	57162.13	110.20

The reaction involving PSBR and chlorosulphonic acid is non-spontaneous, the particles of the system is expected to exhibit relatively low degree of randomness. This is shown in the low value of ΔS^o obtained. But as the solution gets warm with temperature, the particles start to move, generating some disorderness, as a result of increase in the entropy of the system (Figure 5.9) with temperature and as such, the average kinetic energy of the particles increases.

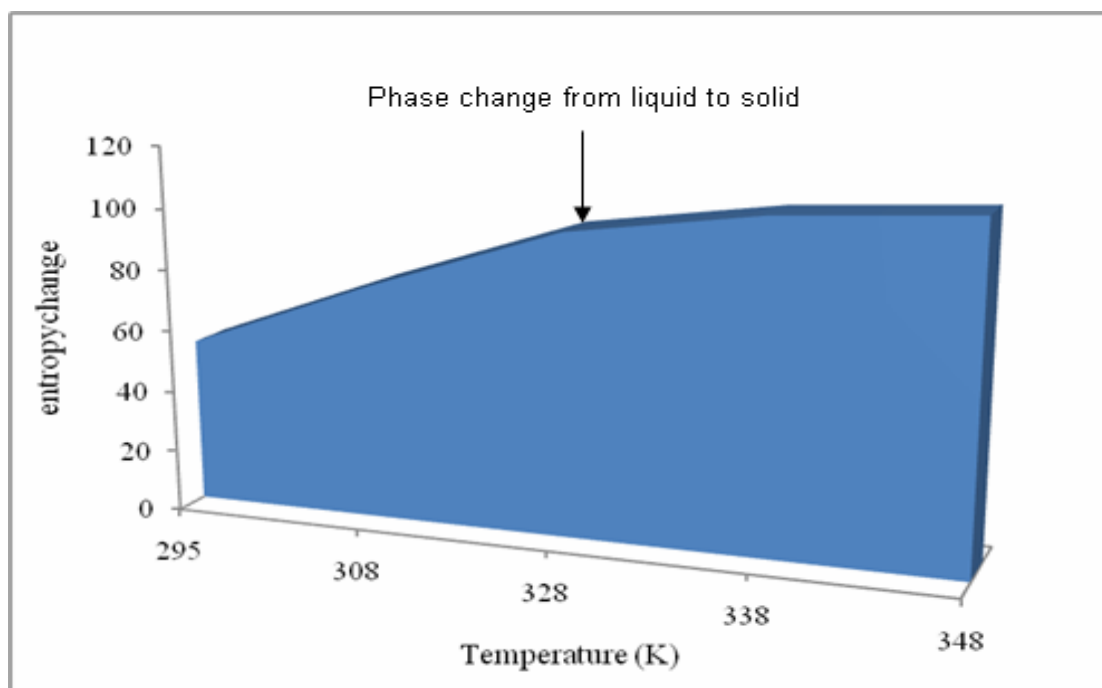


Figure 5.9: Entropy plot against temperature

However, at above 328 K the degree of disorderness of the system can be seen to be reducing gradually and which will thus decrease the randomness of the system. This is the point where the solutions is becoming a solid and hence decrease in the average kinetic energy of the particles. This phenomenon is actually encountered during the experiment as reaction carried out above 328 K, the viscosity of the solution gets so high and resulting into a solid with time. Therefore, this indicates that the optimum temperature to carry out sulphonation of PSBR in chlorosulphonic acid should be within 328 K.

CHAPTER SIX

6.0 MEMBRANE CASTING AND CHARACTERISATION

6.1 Membrane Casting

10 g of SPSBR that was dissolved in 200 ml of 1, 2 dichloroethane at elevated temperature to form a casting solution of about 15-30 % wt, was cast onto a clean polymer paper support using a laboratory doctor blade casting machine. The membrane was then analysed to determine its thermal stability, morphology, proton conductivity, water absorption, water desorption, swelling ratio, porosity and methanol crossover in line with fuel cell application.

6.2 Thermal Stability of Synthesised Membranes

Apart from the high cost of Nafion[®], another major factor hindering its use in hydrogen fuel cell applications is the loss of properties at high temperature in the ranges of 120-150°C. Since hydration of the Nafion[®] must be high enough to give the membrane sufficient conductivity, this factor therefore limits the operating temperature of fuel cell to 80°C in order to prevent the membrane from drying out and to retain ionic mobility. The difference between the ambient and operating temperature, therefore, makes it difficult to utilize the heat generated by the electrochemical reaction in hydrogen fuel cell (Ogaji et al., 2006). The possibility of raising the operating temperature of hydrogen fuel cells should be able to resolve the problems associated with heat generation/utilization on the current system. At present the current technology in membrane development for hydrogen fuel cells application is aimed at synthesising a mechanically stable membrane that can withstand high temperature at low cost. In this study, differential scanning calorimeter (DSC), thermo gravimetric analysis (TGA) and differential thermal analysis (DTA) were used to analyse the thermal stability of the unsulphonated and sulphonated polystyrene butadiene rubber. Also analysed

were the effects of concentrations of sulphonating agent, sulphonation time and degree of sulphonation on the thermal stability of the sulphonated rubber. The theoretical values of the degree of sulphonation was calculated from the TGA curves, on the assumption that the difference between the decomposition temperature ranges for the unsulphonated and sulphonated rubber is as a result of the sulphonic group that is attached to the styrene group.

Figure 6.1 and 6.2 represent the DSC curves of the unsulphonated and sulphonated PSBR at different sulphonation time and degree of sulphonation. As a result of the need for high aqueous proton conductivity obtainable at elevated temperature, and the fact that Nafion[®] has relatively low glass transition temperature (T_g) ($< 120^\circ\text{C}$) when it is hydrated, difficulty in operating fuel cells at high temperature as elucidated earlier becomes imminent. It is therefore important for the synthesised membrane to have a higher glass transition temperature. The curves shown in Figures 6.1 and 6.2 show that polystyrene-butadiene rubber is a highly thermo stable polymer with a glass T_g of about 198°C compared to Nafion 117 and 112 with $T_g < 120^\circ\text{C}$. Recalling, T_g is the temperature at which polymer becomes brittle on cooling and soft on heating which is taken as the point of inflexion on the slope change of DSC curve. Relating this to SPSBR, this means that the styrene group where the SO_3H attached after sulphonation becomes weak and consequently results in the degradation of the group from the main chain (Gu et al., 2006). This is a situation that can lead to poor output of fuel cell performance under operation due to membrane failure

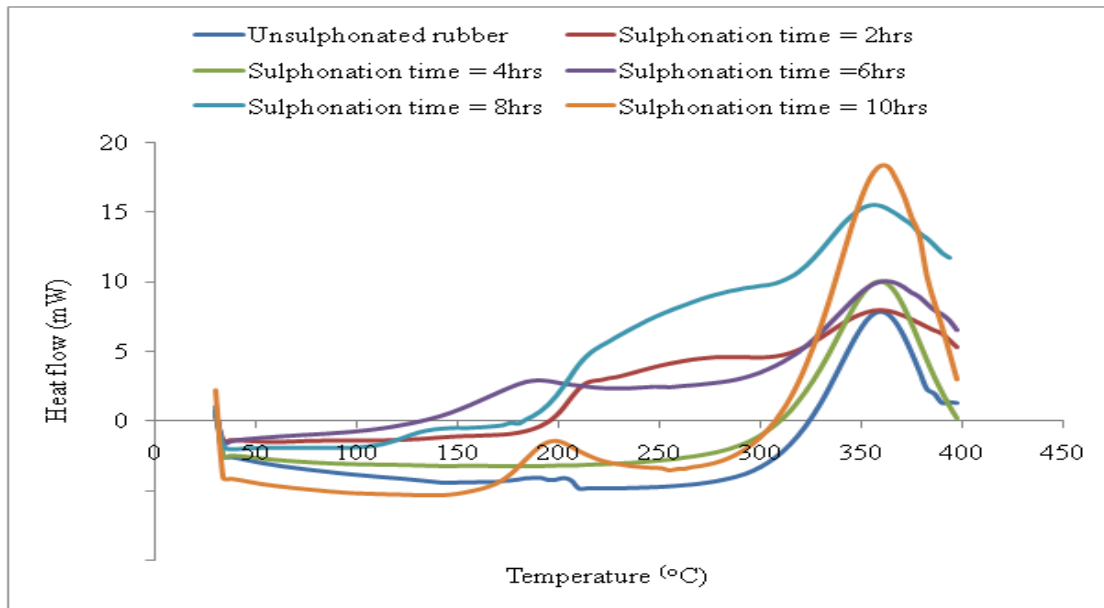


Figure 6.1: DSC curves of the unsulphonated and sulphonated rubber at different sulphonation time.

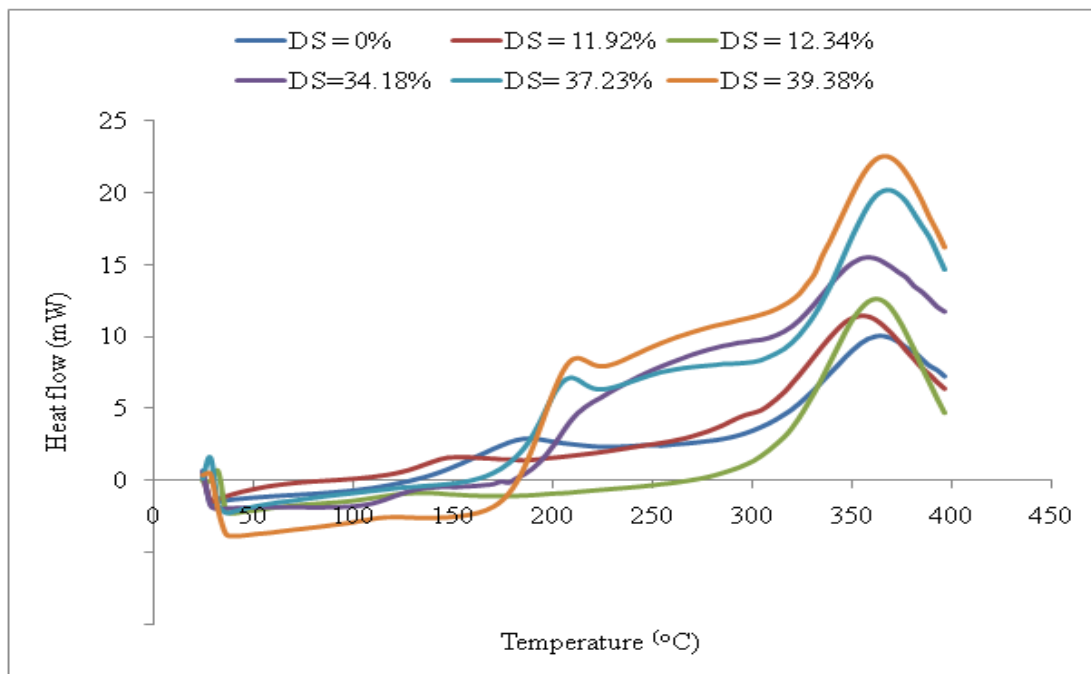


Figure 6.2: DSC curves of the unsulphonated and sulphonated rubber at different degrees of sulphonation.

Analysing the thermal properties of the membrane further for thermal stability assurance, thermo gravimetric analysis (TGA) was conducted using unsulphonated and sulphonated rubber. TGA is used to determine change in weight relative to temperature. Figure 6.3 illustrates the TGA curve of the unsulphonated and sulphonated rubber at different degrees of sulphonation. Three loss in weight, in three ranges of temperature, can be observed in the TGA curves for both the unsulphonated and sulphonated rubber. It is important to note that during the pre-treatment of the samples in the presence of air that the sulphonated rubber did not undergo oxidation as the weight remained constant. For the unsulphonated rubber, the first weight loss can be observed in the range of 23°C-219°C as shown in Figures 6.3 and 6.4. This is attributed to the presence of moisture and some other additives used in the production of polystyrene-butadiene rubber.

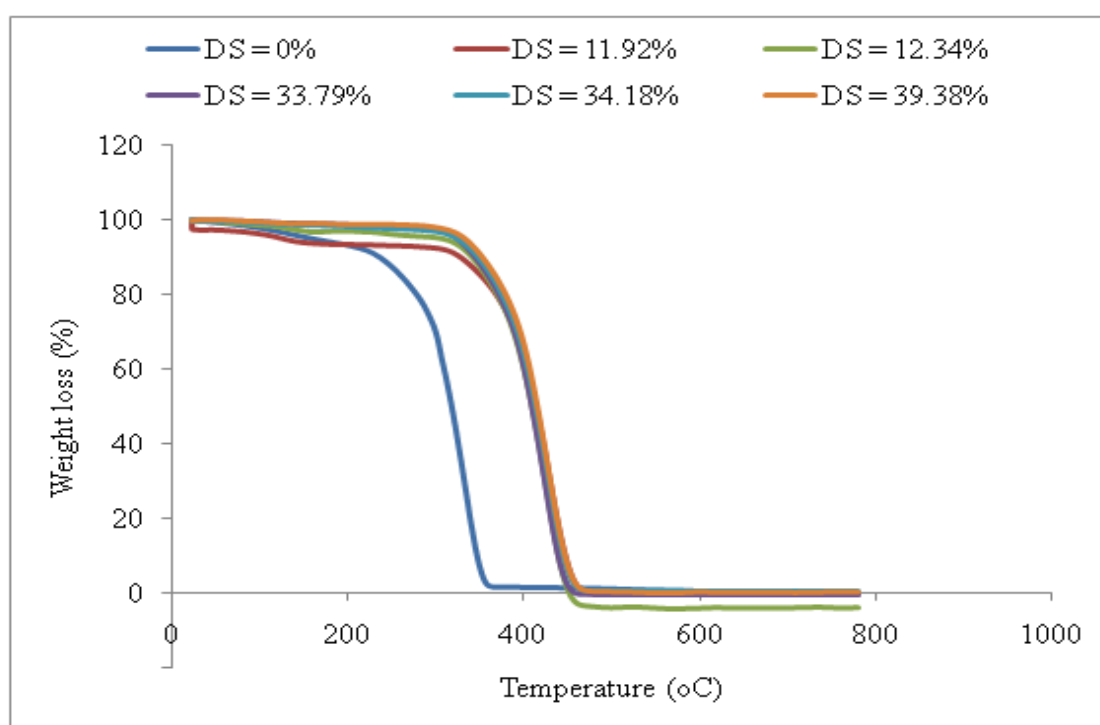


Figure 6.3: TGA curve of the unsulphonated and sulphonated rubber at different degrees of sulphonation.

The second loss in weight can be observed in the range of 219°C-302°C. This range represents the thermal degradation of the styrene group attached to the butadiene which is the backbone of the polymer chain. In the case of the sulphonated rubber the second weight loss can be observed around 306.9°C-412°C depending on the degree of sulphonation and is mainly associated with the loss of styrene-sulphonic group. It can be observed from the TGA curves that drop in weight at these temperatures reduces as the degree of sulphonation increases and this is an indication that the attached SO₃H group improved the strength of the rubber. The final loss in weight is the third transition in the range of 402°C- 475°C which represents the decomposition of the main chain. It can be observed also from Figures 6.3 and 6.4 that the scission temperature of styrene-sulphonic acid increases along with increase in degree of sulphonation and it is higher than that of the unsulphonated rubber.

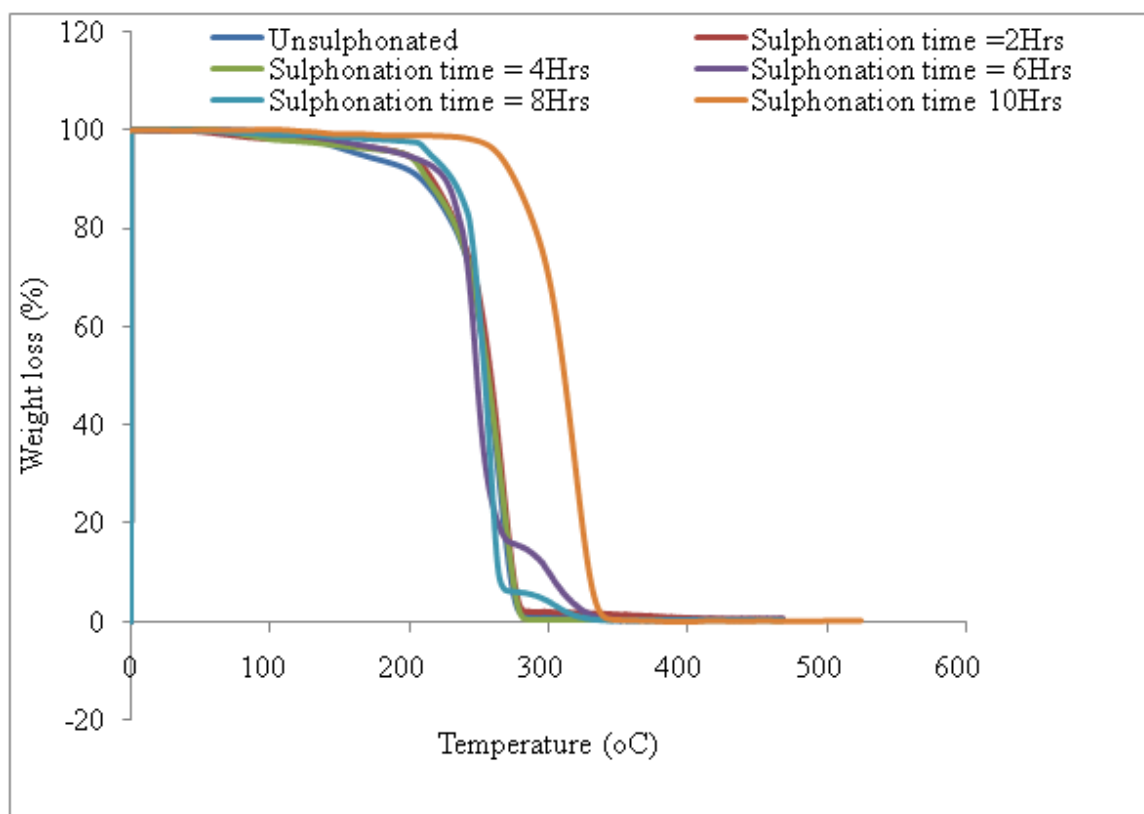


Figure 6.4: TGA curve of the unsulphonated and sulphonated rubber at different sulphonation time.

The attached SO_3 group on the aromatic group has, in a way, reinforced the strength of the sulphonated rubber. This result is found to contradict the results reported by Gao and co-worker (2003), such that in their case the sulphonic acid degradation temperatures reduces with increase in degree of sulphonation. The difference can be associated with the fact that the base polymer used in this work is composed of two monomer i.e. styrene (25%) and butadiene (75%) (Karbochem report). The SO_3H group is directly attached to the aromatic styrene group after sulphonation as shown in scheme 6.1, thereby contributing to the bond strength between the styrene and butadiene. The higher degree of sulphonation therefore means higher number of sulphonic groups attached to the styrene and consequently improving the strength of the resulting polymer.

Scheme 6.1: Sulphonated PSBR

Results on the thermal stability of the rubber from the TGA curves also show that as the sulphonation time increases (with increasing degree of sulphonation), the sulphonated rubber loses weight faster in the range of 306°C - 410°C depending on degree of sulphonation. This situation can be associated with the elimination of residual SO_3H group (Gao et al., 2003).

Results obtained on the theoretical values of degree of sulphonation at various concentration of acid are presented in Figure 6.5. This is the degree of sulphonation values calculated from the TGA otherwise known to be theoretical values at various concentrations of acid. An observation of the result reveals a little variation between the experimental and theoretical values with the correlation coefficient of 0.9975 and standard deviation of 2.7094.

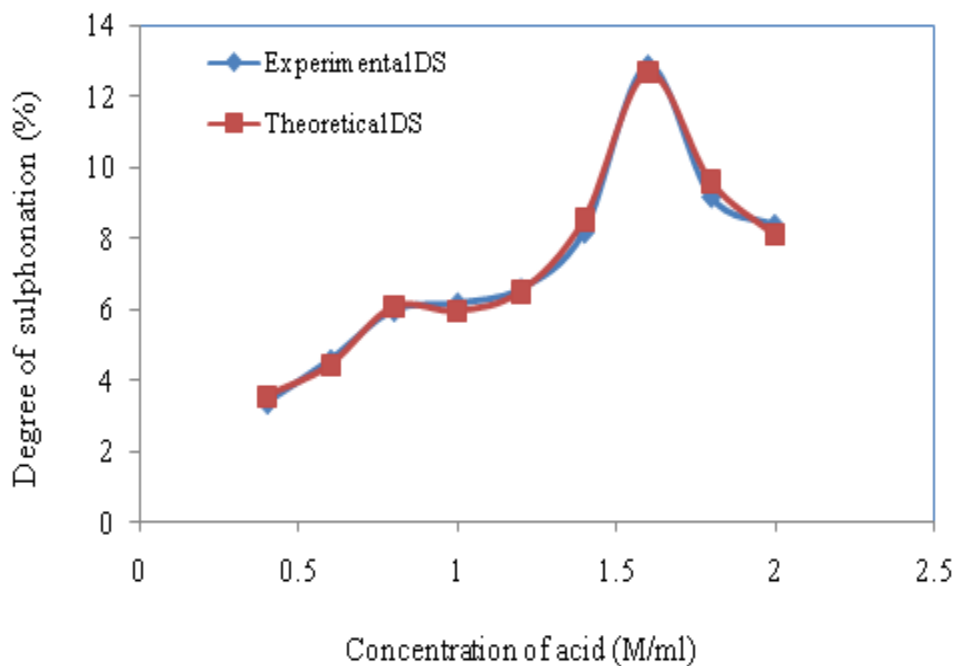


Figure 6.5: Experimental and theoretical degree of sulphonation at different concentration of acid

These variations can be attributed to the fact that not all SO_3H group attached to the styrene degraded from the main chain (Gao et al., 2003). The difference in variations can also be linked to the fact that TGA test is carried out under non equilibrium conditions, and the possibility of low degree of chain scission at the sulphonated styrene-butadiene linkage only got involved in the first step degradation (Xing et al., 2004). From all these analysis it can be deduced that the sulphonated membrane has an adequate thermal property for PEM fuel cell applications, since the thermal decomposition is found to be $>120^\circ\text{C}$, being the maximum

operating temperature for polymer exchange membrane fuel cell. Finally, DTA curves shown in Figure 6.6, also affirm the results of the thermal stability of the synthesised membrane.

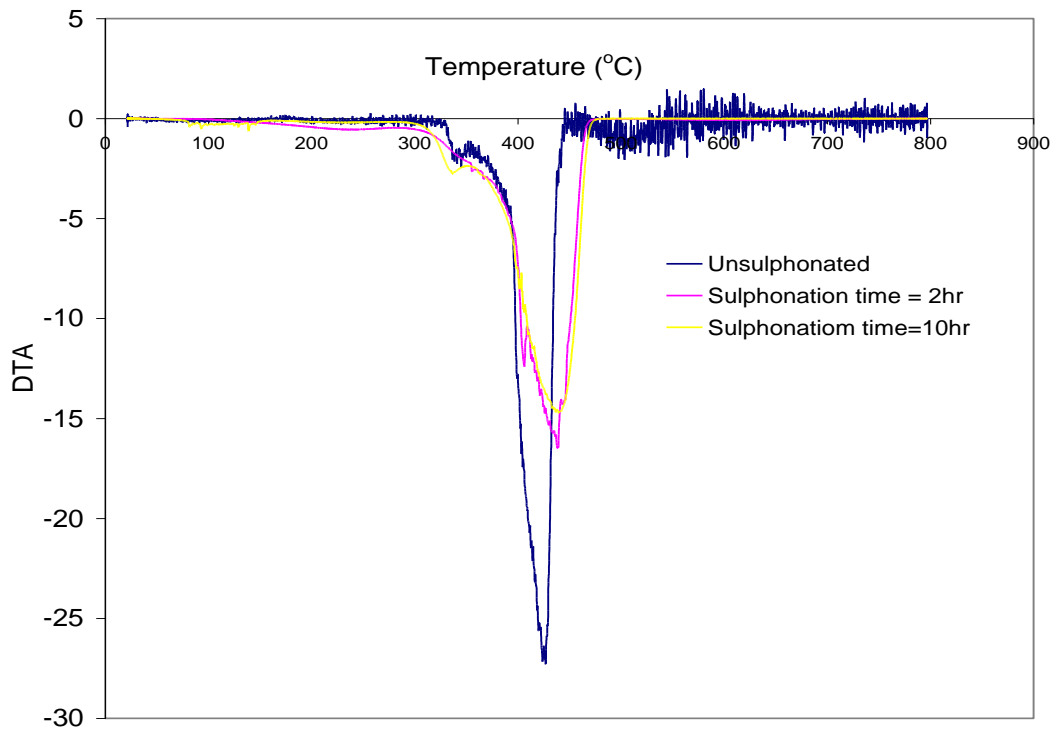


Figure 6.6: Differential thermal curve of sulphonated and unsulphonated polystyrene butadiene-rubber at different sulphonation time.

6.3 Morphology of Unsulphonated and Sulphonated PSBR

A scanning electron microscopy (SEM) was used to study the morphology of the PSBR. It can be observed from the unsulphonated rubber shown in Figure 6.7a that the polystyrene-butadiene rubber used in this work has a morphology that is very porous and coarse with irregular and large size domain but found to improve significantly with sulphonation (Figure 6.7b-d).

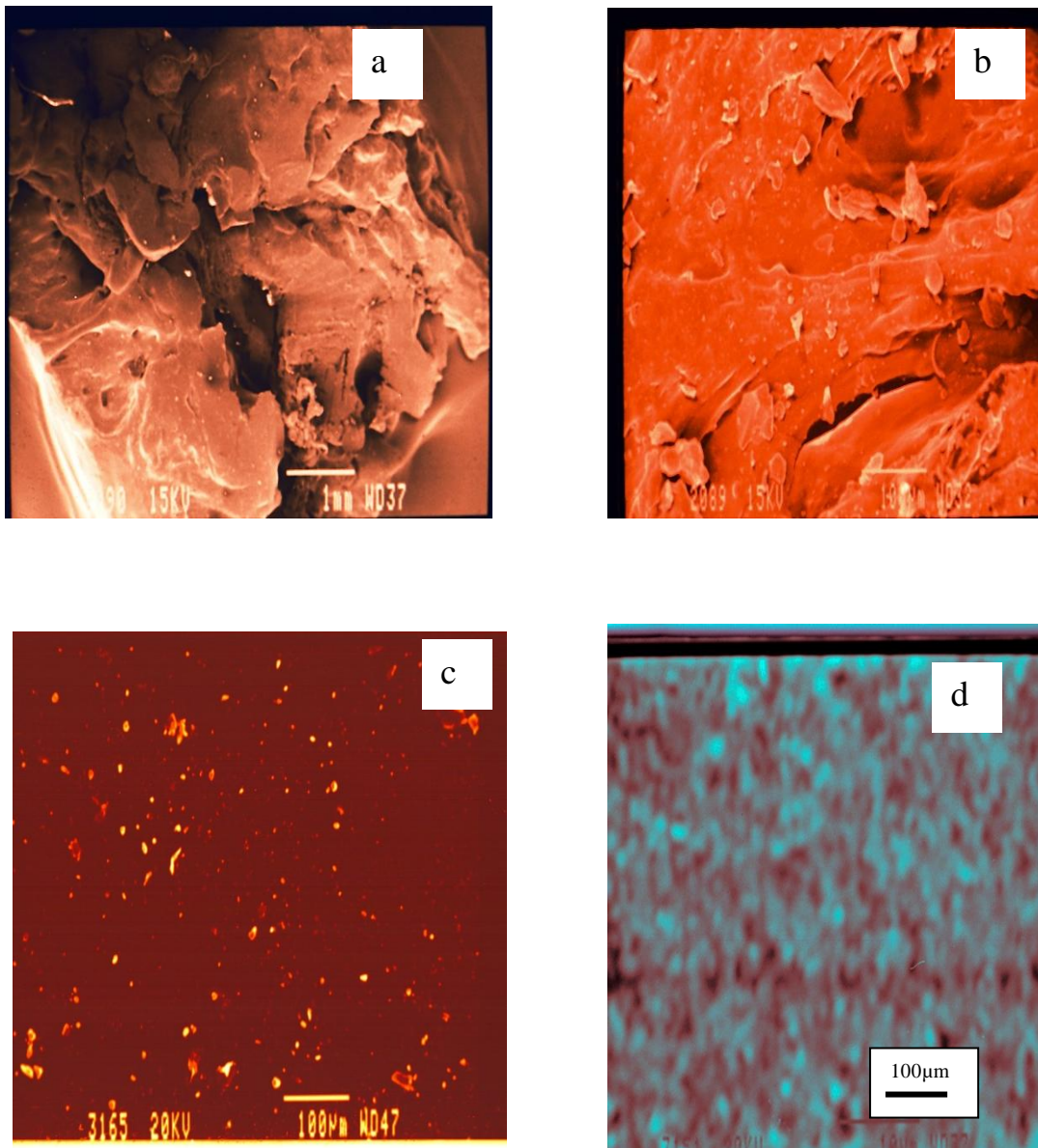


Figure 6.7: SEM images of (a) unsulphonated and (b-d) sulphonated rubber at DS = 2.31 %, 7.54 % and > 10 % respectively.

It can be observed from the figure that the morphology of PSBR changes as the degree of sulphonation increases from a porous base material to a dense material. The enhancement in the size of pores after sulphonation is revealed, and at high degree of sulphonation, pores become more adequate and appear to have a uniform distribution throughout the membrane (as shown in Figure 6.7d). This is a situation that will cause the synthesised membrane to

exhibit desirable and efficient ionic conductivity (Smitha et al., 2003). The large number of pores per sq.cm for sulphonated PSBR, is an indication of large interfacial area between the hydrophobic and hydrophilic interface (Krueuer, 2001) suitable for fuel cell application.

6.4 Proton Conductivity of Synthesised Membranes

The measurements of the proton conductivity of the synthesised membranes were carried out at different temperature and membrane thickness. This was done by soaking the membrane samples in distilled-water for hydration since a well hydrated membrane is expected to achieve a better level of conductivity especially for a membrane that depends on sulphonic acid to conduct protons (Sangeetha, 2005). Figure 6.8 shows the hydration dependence of proton conductivity of the SPBR at different degrees of sulphonation. Results show that the membrane will conduct better when it is fully hydrated than when it is partially hydrated. For instance the proton conductivity of the partially hydrated membrane (10 hours hydration period) and fully hydrated at room temperature and degree of sulphonation of 10.48 are 1.46×10^{-3} and 2.283×10^{-3} S/cm, respectively.

The results also show that as degree of sulphonation increases, the difference between the proton conductivities of the partially and fully hydrated membranes decreases due to ionic strength, as high degree of sulphonation equals high ion exchange capacity. This will inferably lead to high possibility of the membrane to be fully hydrated as the degree of sulphonation increases and therefore better ionic mobility. Figure 6.8 also illustrates the conductivities of the membrane at different degrees of sulphonation and temperatures. Results show that the proton conductivity of the membrane is in the order of 10^{-3} - 10^{-2} S/cm which increases as temperature and degree of sulphonation increase.

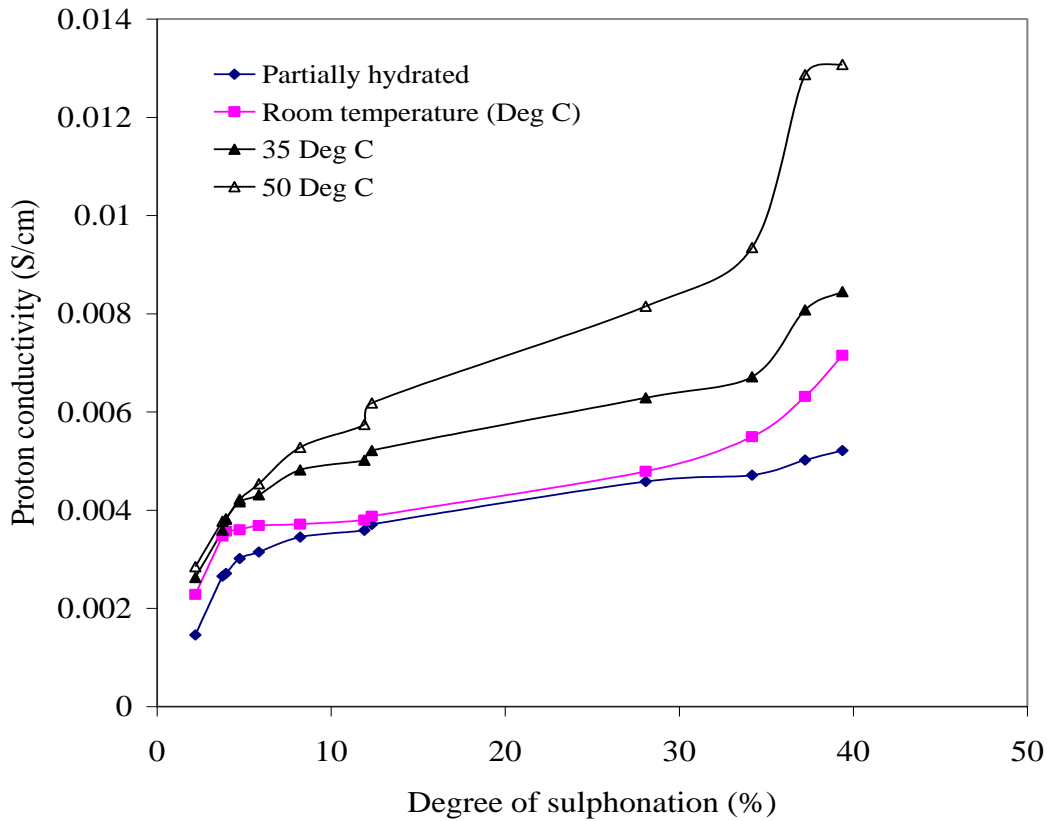


Figure 6.8: Protons conductivity of the membrane at different degree of sulphonation and temperature.

The fact that the proton conductivity increases as temperature increases, care must be taken not to dehydrate the membrane when it is used in fuel cell under high operating temperature because this can lead to a drop in fuel cell performance as ionic activities reduces due to drying out of the membrane. Therefore, proper humidification is necessary when using the membrane in PEM fuel cell to achieve good performance.

Figure 6.9 shows the membrane thickness dependence on proton conductivity of the membrane at different degree of sulphonation.

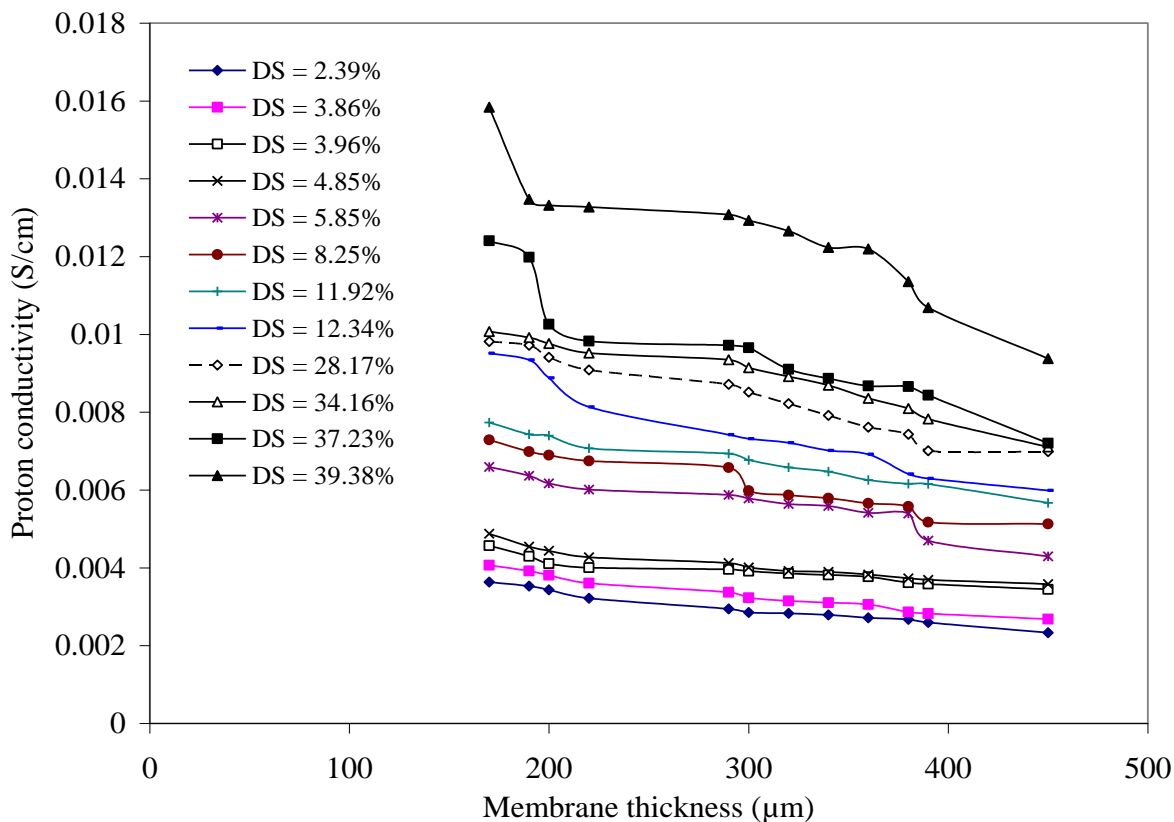


Figure 6.9: Effect of membrane thickness on the proton conductivity of the membrane at different degrees of sulphonation.

The conductivity of the membrane increases with an increase in degree of sulphonation and inversely proportional to the membrane thickness. For instance, membrane with the degree of sulphonation of 39.38 % achieved conductivity of 1.58×10^{-2} and 9.38×10^{-3} S/cm at membrane thickness of $170 \mu\text{m}$ and $450 \mu\text{m}$, respectively. The conductivity of the synthesised membrane is thus comparable with that of Nafion (10^{-2} S/cm).

It was reported that highly conducting membranes tend to be weak mechanically, and are often reinforced by a non conducting cloth or other similar structure (Chen et al., 2005; Chen et al., 2005; Mokirirn et al., 2006; Anilkumar et al., 2006; Jiang et al., 2006). Therefore, as the thinnest membrane yields the highest conductivity it is expected to exhibit the lowest

internal resistance. Therefore, membrane thickness must be considered so that slow molecular diffusion of gases is not only achieved but also for the membrane to be strong enough for fuel cells applications. A balance between membrane thickness and membrane conductivity must therefore be ascertained during membrane designing otherwise poor current efficiency and waste of fuel gas by diffusion may occur especially during long period of operation.

In order to confirm if the acidity of the membrane is due to loosely attached acid groups, the membrane samples were soaked in water for 30days and the proton conductivities were tested. Results obtained showed that conductance values were stable. This is an indication that there was no loss of sulphonic acid groups attached to the membrane. Therefore, the acid group in the synthesized membrane was strongly attached to the membrane to guarantee stable performance.

6.5 Porosity and Total Solvent Uptake

Membrane porosity often expressed as degree of swelling to solvent is a crucial issue in fuel cell technology as it affects fuel cell performance (Sageetha, 2005). Figure 6.10 depicts the overall uptake of methanol solution for different degrees of sulphonation, while Figure 6.11 presents the membrane porosity to methanol at different membrane thickness.

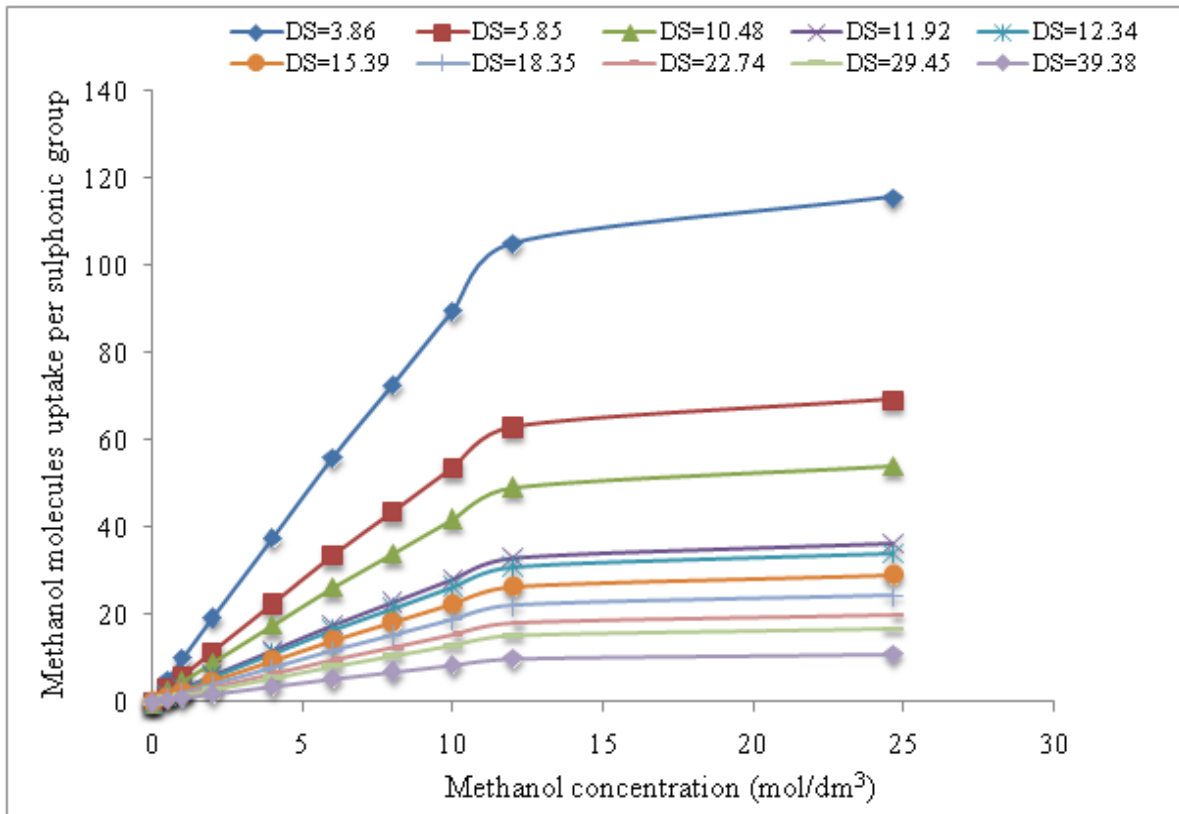


Figure 6.10: Methanol molecule uptake per sulphonic group at different concentration of methanol and degrees of sulphonation.

From the result it can be seen that the uptake of methanol per sulphonic group increases with increase in concentration of methanol. This can be attributed to the availability of the methanol at higher concentration than at lower concentration. This result is similar to that obtained by Sangetha (2005). Results also show that the methanol uptake per sulphonic group decreases with increase in degree of sulphonation. This can be attributed to the decrease in equivalent weight as the degree of sulphonation increases, which resulted in more sites for the distribution of the methanol within the membrane.

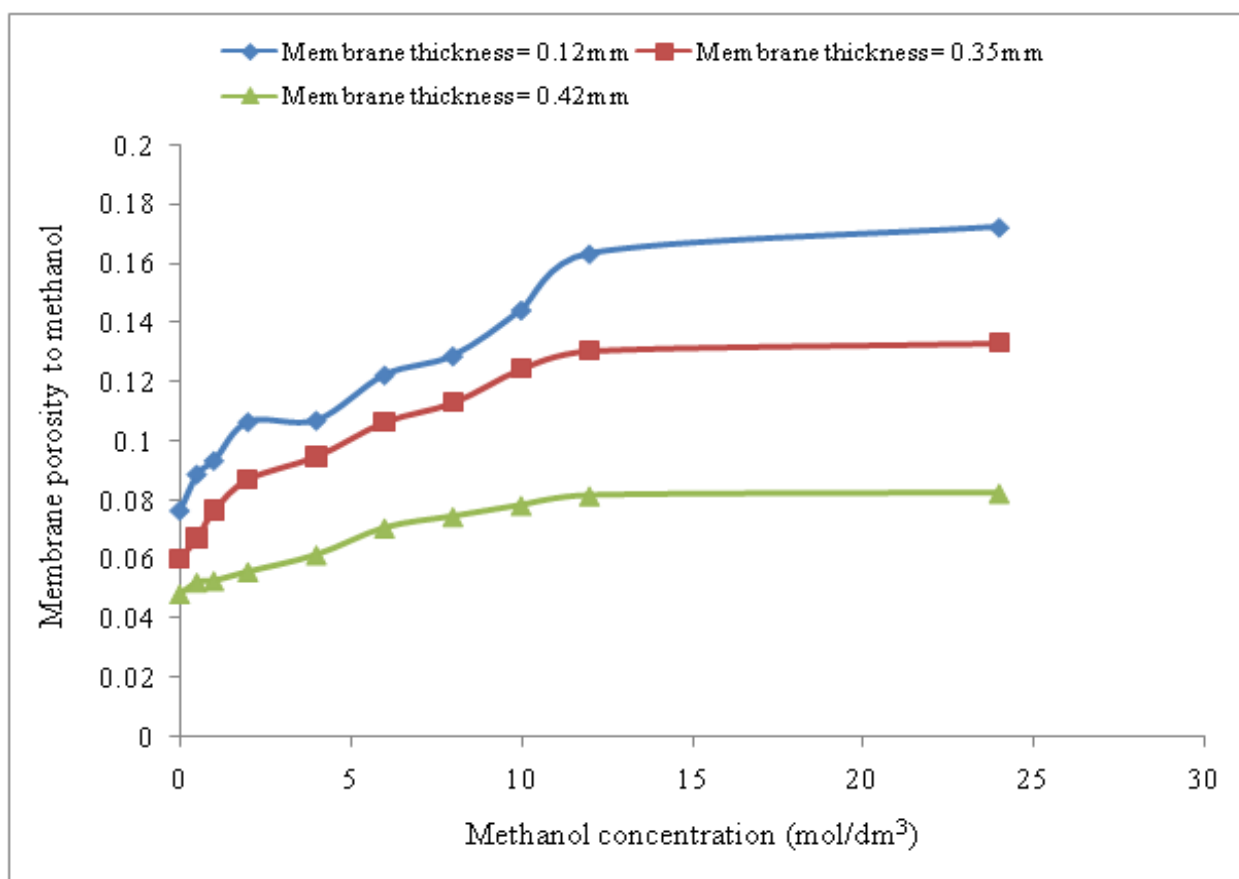


Figure 6.11: Effect of membrane thickness on the porosity of the membrane at different concentrations of methanol.

The results obtained on the porosity of the membranes show that porosity to methanol increases with decrease in membrane thickness. This can be attributed to the reduction in area of the site that is required to hold the methanol within the membrane matrix as the thickness of the membrane decreases. Consequently, this resulted in the diffusion of methanol through the membrane, which inferably resulted in high porosity of the membrane. Comparatively, porosity of the SPBR to methanol is less than that of Nafion[®], which is in the ranges of 0.40-0.51 depending on the concentrations of the methanol (Sangeetha, 2005).

The total uptake of methanol/water and water molecules per sulphonic acid group decreases with an increase in concentration of methanol as shown in Figure 6.12.

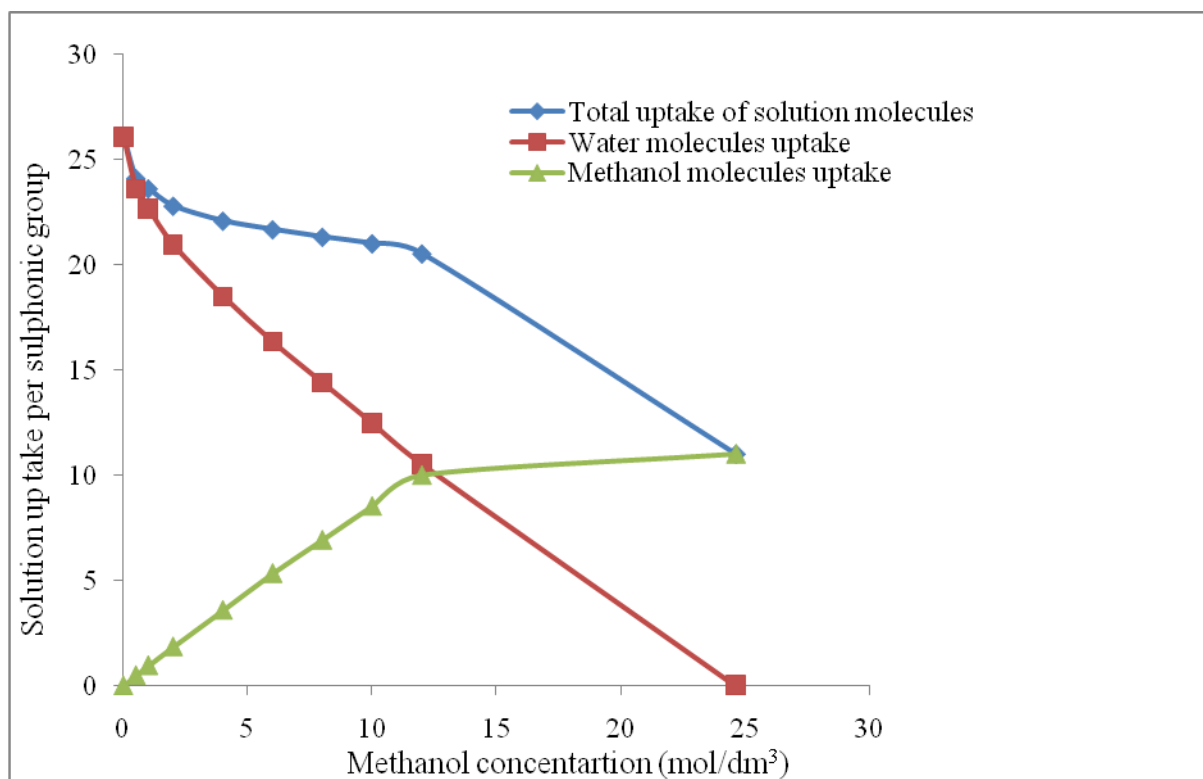


Figure 6.12: Uptake of solution molecule per sulphonic group.

Results also show that the water uptake per sulphonic acid group by the SPBR is higher than the methanol uptake per sulphonic group. Based on the results obtained from the porosity of the membrane to methanol and methanol uptake, it can be inferred that the membrane is less permeable to methanol than water. The water uptake per sulphonic group of Nafion[®] is almost constant (Sangeetha, 2005), while the membrane uptake increases with an increase in concentration of methanol with the sulphonated SPBR.

6.6 Methanol Crossover Study

Methanol crossover is considered as the inability of the membrane to block the methanol as fuel from going through the membrane (Han-Lang et al., 2006). It is important to mention here that the concept of methanol discussion in this project is for the purpose of characterising the synthesised membrane for other possible application such as Direct Methanol Fuel Cell (DMFC). The capacity of any membrane to methanol crossover is one of the major qualities of membrane that determines its performance in fuel cell applications. It has been recognized as a major obstacle which hinders the commercial availability of fuel cells that use solid electrolyte membrane (Hikita et al., 2001). Methanol crossover leads to decrease in the cathode potential and the energy efficiency (Hikita et al., 2001).

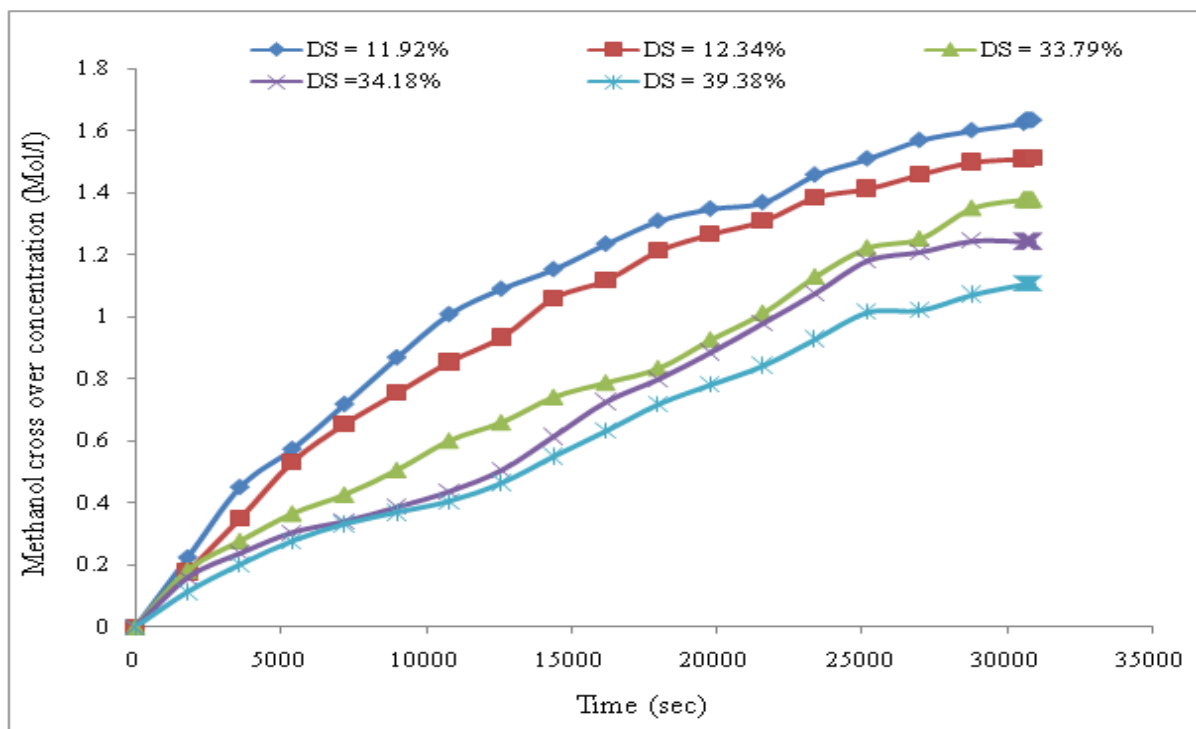


Figure 6.13: Methanol crossover concentration at different degrees of sulphonation

It is, therefore, important to synthesise a membrane with low methanol permeability in order to achieve and sustain a good fuel cell potential. Figure 6.13 shows typical concentration changes of methanol in aqueous solution at different degrees of sulphonation and membrane thickness of 220 μm to study the membrane permeability.

This was carried out using the method reported by Shen et al. (2005). Results show that at the same thickness, a membrane with a lower degree of sulphonation exhibited higher methanol crossover ($> 1.6 \text{ Mol/l}$), which decreases ($< 1.2 \text{ Mol/l}$) as the degree of sulphonation increases. This pattern of result could be linked to a decrease in equivalent weight as degree of sulphonation increases.

The reduction in equivalent weight resulted in more sites for the distribution of methanol within the membrane matrix, while the remaining methanol that the membrane could not hold crosses to the other side of the membrane. The results obtained from the methanol crossover were used to determine the overall diffusion coefficient and methanol permeability. The relation developed by Shen et al. 2005 was used to determine the methanol permeation on the following assumptions.

- Methanol solution diffuses through the membrane obeying Fick's law.
- Methanol solutions at both side of membrane are at equilibrium as a result of stirring.
- Proportional relationship exists between methanol concentration of bulk solution and membrane wall in contact with the solution.

Based on the assumptions stated above, diffusion due to a concentration difference across membrane, methanol diffuses from compartment A to B because $C_A > C_B$. Therefore, the methanol permeation will be obtained with the methanol concentration of the compartment B with relation to time using equation 6.1 (Shen et al., 2005).

$$\frac{dC_B}{dt} = A_m \frac{\rho_{AB} K^m}{d_m V_0} (C_{A0} - C_B) \quad (6.1)$$

where: C_A is the concentration of methanol in compartment A and C_B is the concentration of methanol in compartment B. $V_0 = V_A + V_B$, and where V_A and V_B are the methanol volume in compartment A and B, respectively, A_m is the area of the membrane while d_m is the membrane thickness.

Integration of Equation 6.1, the relationship between the changes in concentration as a function of time was obtained:

$$\frac{\frac{1}{2} \ln C_{A0}}{C_{A0} - 2C_B} = A_m \frac{\rho_{Am} K^m}{d_m V_0} t \quad (6.2)$$

where ρ_{Am} = diffusion coefficient, K^m = Proportional constant and $\rho_m K^m$ = overall

methanol diffusion coefficient. The slope of the plot of $\frac{\frac{1}{2} \ln C_{A0}}{C_{A0} - 2C_B}$ against time as presented

in Figure 6.14 is equal to $A_m \frac{\rho_{Am} K^m}{d_m V_0}$. The overall diffusion coefficient of the synthesized membrane was then determined from the slope. However, the linear variation of Figure 6.14 can be attributed to the effect of lag time and partition coefficient.

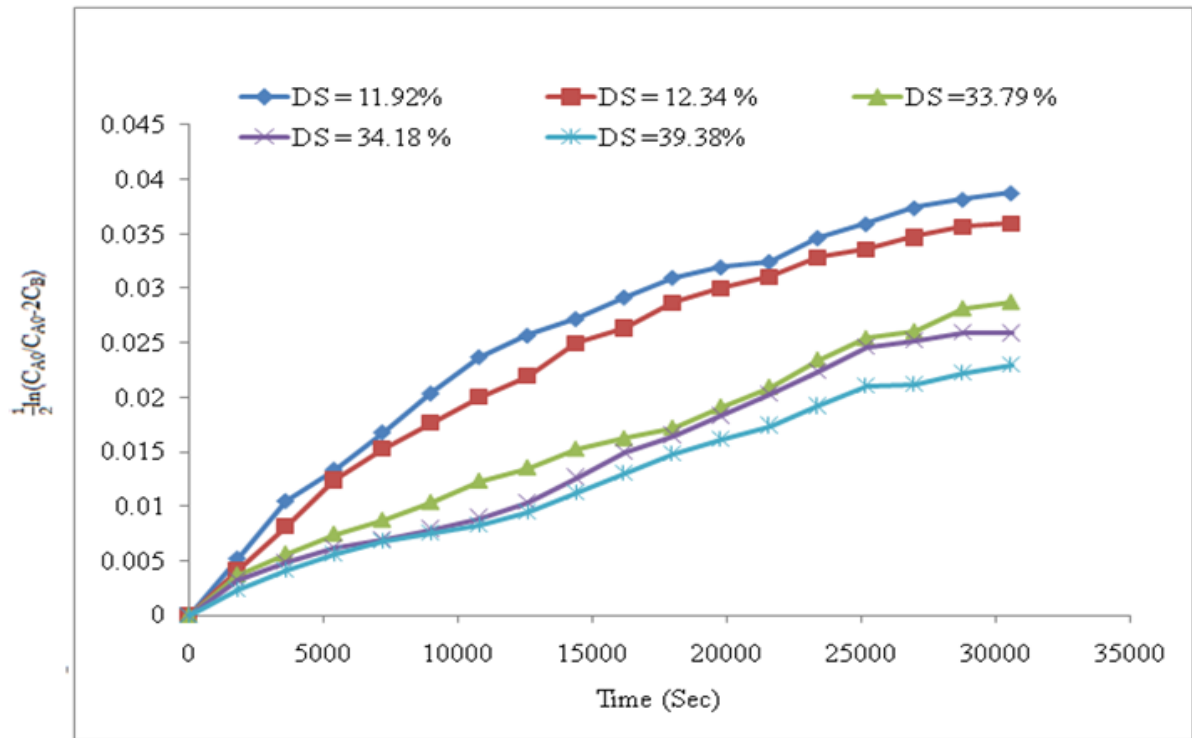


Figure 6.14: Plot of $\frac{1}{2} \ln \frac{C_{A0}}{C_{A0} - 2C_B}$ against time at different degree of sulphonation

The effects of degree of sulphonation on the measure of overall diffusion coefficients of the synthesised membrane at different membrane thickness are presented in Table 6.1. The results showed that the synthesised membrane from polystyrene-butadiene rubber exhibited lower methanol diffusion coefficient compared with Nafion 117 ($3.42 \times 10^{-6} \text{cm}^2/\text{s}$) (Shen et al, 2005). Relating the overall diffusion coefficient with degree of sulphonation of the synthesized membrane, it was observed that the membrane with lower degree of sulphonation had larger methanol overall diffusion coefficient than membrane with higher degree of sulphonation.

Table 6.1: Overall diffusion coefficient of the membrane at different thickness and degrees of sulphonation

DS	Overall diffusion coefficient (cm ² /s) 10 ⁻⁷					
	112 mm	115 mm	117 mm	220 mm	350 mm	420 mm
3.86	3.45	3.42	3.41	4.51	5.37	5.12
5.89	3.33	3.31	3.29	4.36	5.19	4.96
15.39	2.62	2.61	2.60	3.46	4.12	4.32
29.45	2.57	2.55	2.54	3.39	4.04	4.23
39.38	2.19	2.18	2.17	2.9	3.46	3.63

The Overall diffusion coefficient determined from the slope of the graph shown in Figure 6.14 was used to evaluate the methanol permeation using equation 6.3, and the results obtained at different degree of sulphonation and membrane thickness are shown in Figure 6.15.

$$J = \rho_{Am} \frac{dC_m}{dm} \quad (6.3)$$

where: ρ_{Am} is the Overall diffusion coefficient, dC_m is the concentration of methanol and J is the methanol permeation

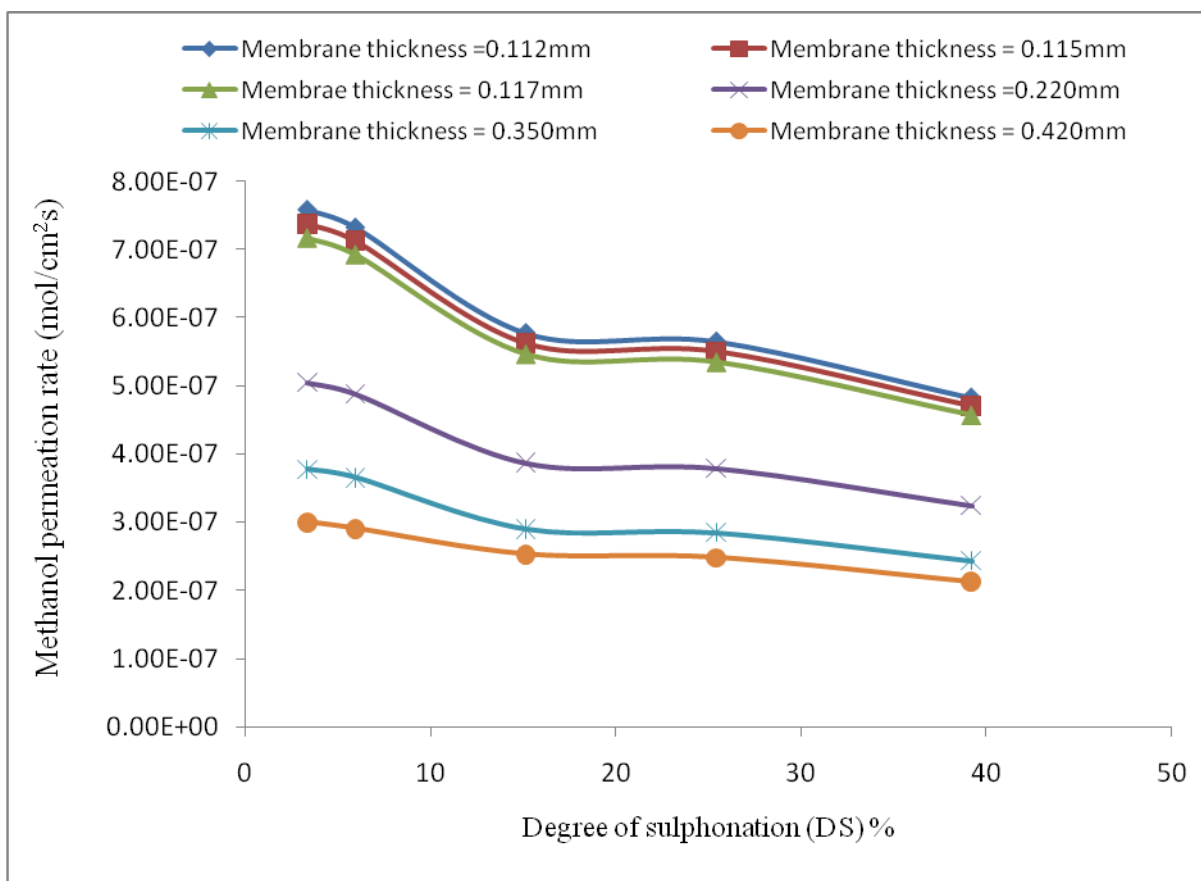


Figure 6.15: Methanol permeation at different degree of sulphonation and membrane thickness

The results presented in Figure 6.16 showed that methanol permeability increases with decreasing thickness. This is expected because thickness is proportional to permeability across the membrane. The methanol permeability of the synthesized membrane is considerably lower than that of Nafion[®] 115 membrane ($3.15 \times 10^{-6} \text{ cm}^2/\text{s}$). The methanol permeability of the synthesized membrane ranges from $2.13 \times 10^{-7} - 7.18 \times 10^{-7} \text{ cm}^2/\text{s}$, which was lower than that of Nafion[®]. The low methanol permeability values of the synthesised membrane point to the fact that the methanol crossover rate for the synthesised membrane would be drastically reduced. This will, however, improve the performance of fuel cells using direct methanol when the synthesised membrane is used instead of Nafion[®] membrane. Membrane with high permeability resulted in a high methanol permeates from anode to

cathode where it directly reacts with oxygen, causing oxidation of the fuel and thus opposing energy production. This is a phenomenon which leads to efficiency reduction in fuel cell (Matsunguchi and Takahashi, 2006) which is considered as a challenge in fuel cell technology. In fuel cell applications, the methanol permeation per unit area can be evaluated theoretically from Equation 6.3. Figure 6.16 thus presents typical theoretical evaluated methanol permeation at different degree of sulphonation, membrane thickness and methanol concentration at 2 Mol/l.

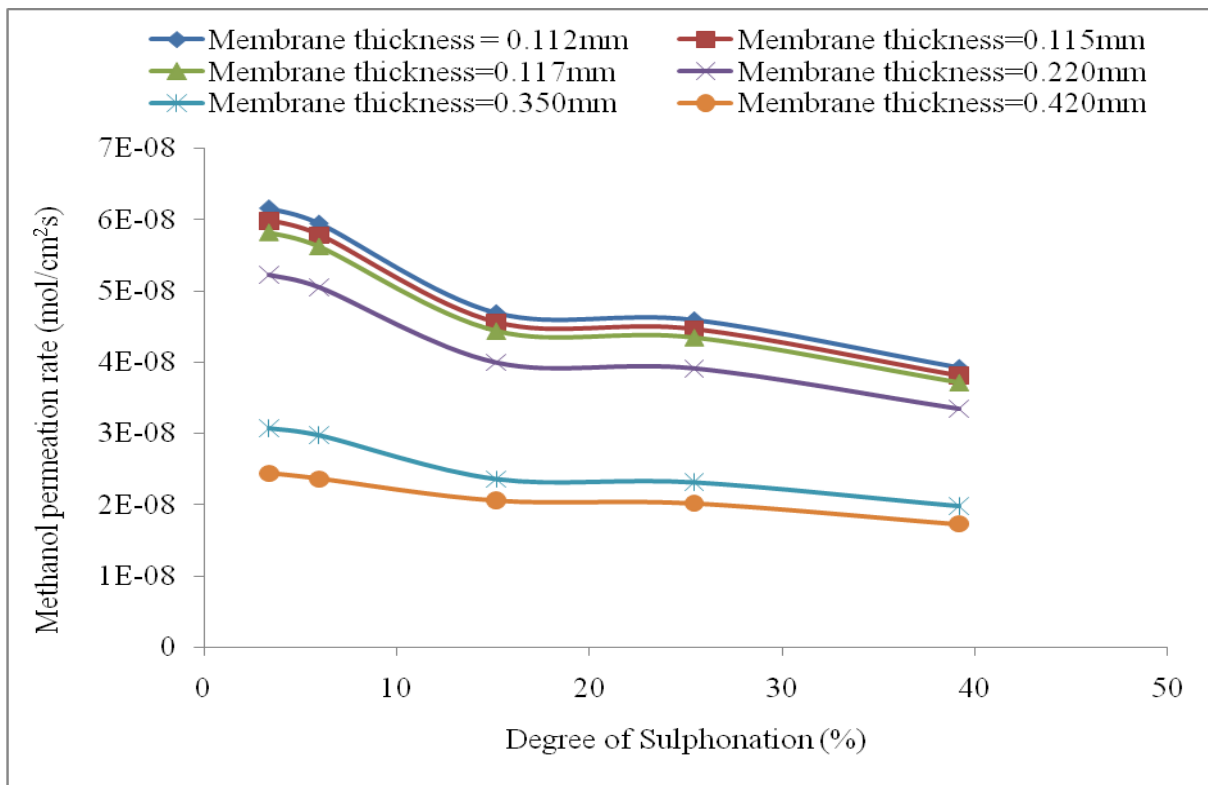


Figure 6.16: Theoretically calculated methanol permeation

6.7 Water Uptake and Water Desorption Capacity of the Membranes

Water uptake is the weight percent of water absorbed by the membrane with respect to the weight of dry membrane (Sangeetha, 2005). Water molecules are necessary in the membrane because it provides the medium for the movement of ions, but excess uptake of water can result in swelling of the membrane and consequently affect the mechanical and conductivity properties. Considering electro-osmotic transport of water by the conduction ion and back diffusion of water once gradient is established, water uptake and physical dimension of membrane become important among the special properties of the ion exchange membrane in fuel cell applications. In this work a thin film of membrane of various thicknesses, devoid of air, was casted using a laboratory scale casting machine. The water uptake and desorption capacity of the membrane at different thickness and temperature was investigated and the results obtained are presented.

The results obtained on the water uptake at different degrees of sulphonation are shown in Figure 6.17. The results show that as degree of sulphonation increases, the water uptake per gramme of dry membrane increases. This is expected as high degree of sulphonation results in high ion exchange capacity.

At a degree of sulphonation of 39.38 % an approximately 70 % of water uptake per gram of dry membrane was realised as against < 20 % with a membrane of 5.85 % degree of sulphonation. All the membranes investigated show an initial rapid uptake of water which decreases with time until saturation was reached forming a plateau.

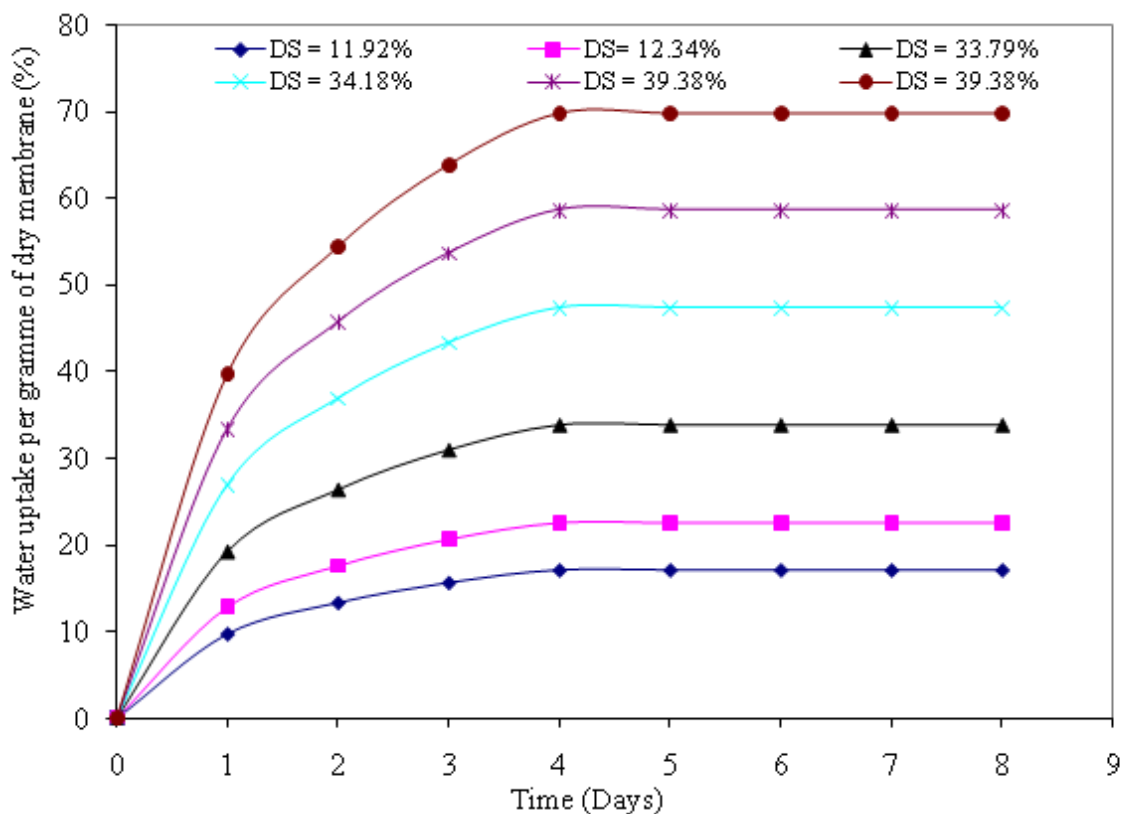


Figure 6.17: Water uptake at different degree of sulphonation

The degree of sulphonation (resulting from the ion exchange capacity of the membrane) and water uptake contribute to the proton transport through the dense membrane (Basile et al., 2006). Better water uptake encourages better proton conductivity of the membrane (Constamagna and Srinivasan, 2001). For a sulphonic acid based membrane, the proton conductivity depends on the number of available acid groups best expressed as degree of sulphonation and water contents in the membrane (Mokrini et al., 2006). Therefore, the higher the degree of sulphonation, the better the ability of the membrane to absorb water and causes proton dissociation and mobility. It is, therefore, important to note that proton conduction in sulphonic acid membranes is due to proton hopping from one sulphonic group to another (Grothus mechanism) (Costamagna and Srinivasan, 2001). In the presence of water, both the proton and the sulphonic groups are in the solvated form, and it is recognized to greatly facilitate the hopping mechanism, for instance a specific conductivity of about 0.1

S/cm has been reported for a fully hydrated Nafion membrane at 80°C (Costamagna and Srinivasan, 2001). Thus maximum water uptake by the membrane electrolyte is vital for proton exchange membrane fuel cell to attain its highest performance (Costamagna and Srinivasan, 2001).

The results obtained on the variation of water uptake at different thickness of the membrane at 9.4 % degree of sulphonation as shown in Figure 6.18 showed that water uptake increases as the thickness of the membrane decreases.

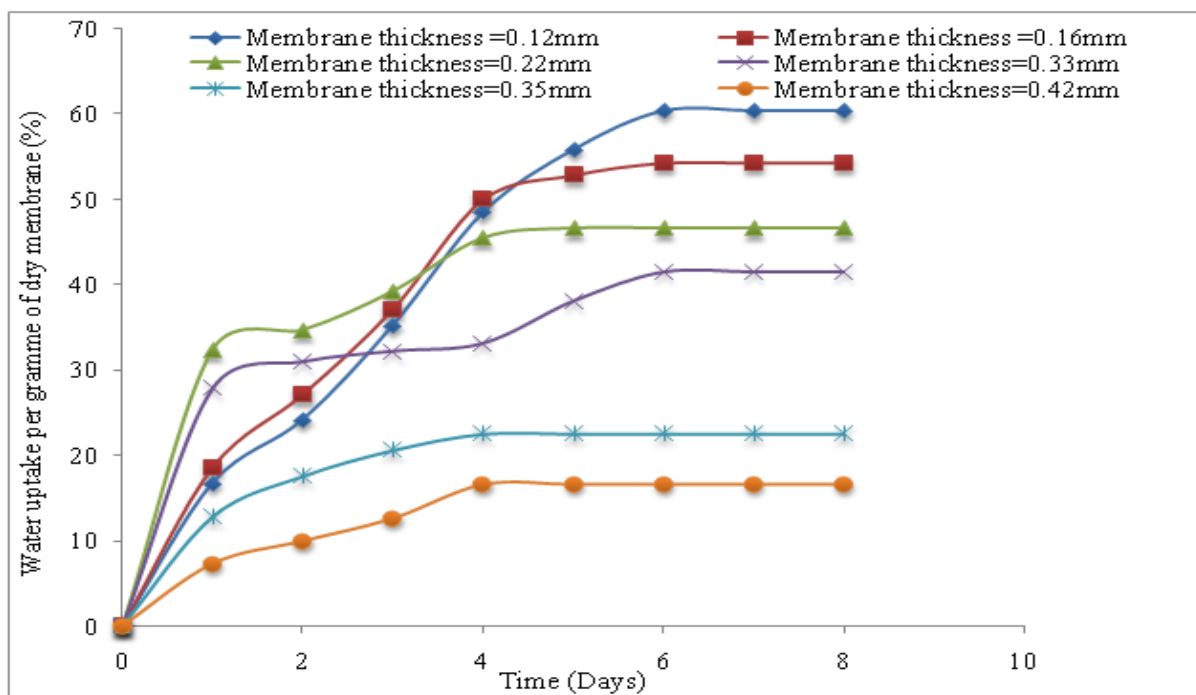


Figure 6.18: Water uptake at different membrane thickness

The maximum water uptakes at different thickness of membrane are 60.33 % for membrane thickness of 0.12mm, 54.29 % for 0.16 mm, 46.59 % for 0.22 mm, 41.49 % for 0.33 mm and 16.67 % for membrane of thickness of 0.42 mm. Results also show that all the membrane

attained their saturation point on the fifth day except for the membrane with thickness 0.12 and 0.16 mm, which attained their water saturation point on the sixth day. The membrane ability to absorb water was high for the first day and followed by gradual water uptake towards saturation point. This trend of results is in agreement with the one obtained by Sangeetha (2005), while investigating the conductivity and solvent uptake of polystyrene triblock polymer.

The result obtained on the effects of temperature on the water uptake ability of the membrane is presented in Figure 6.19. Results revealed that as the temperature increases, the percentage of water uptake also increases, but the time required by the membrane to attain its saturation decreases as the temperature increases.

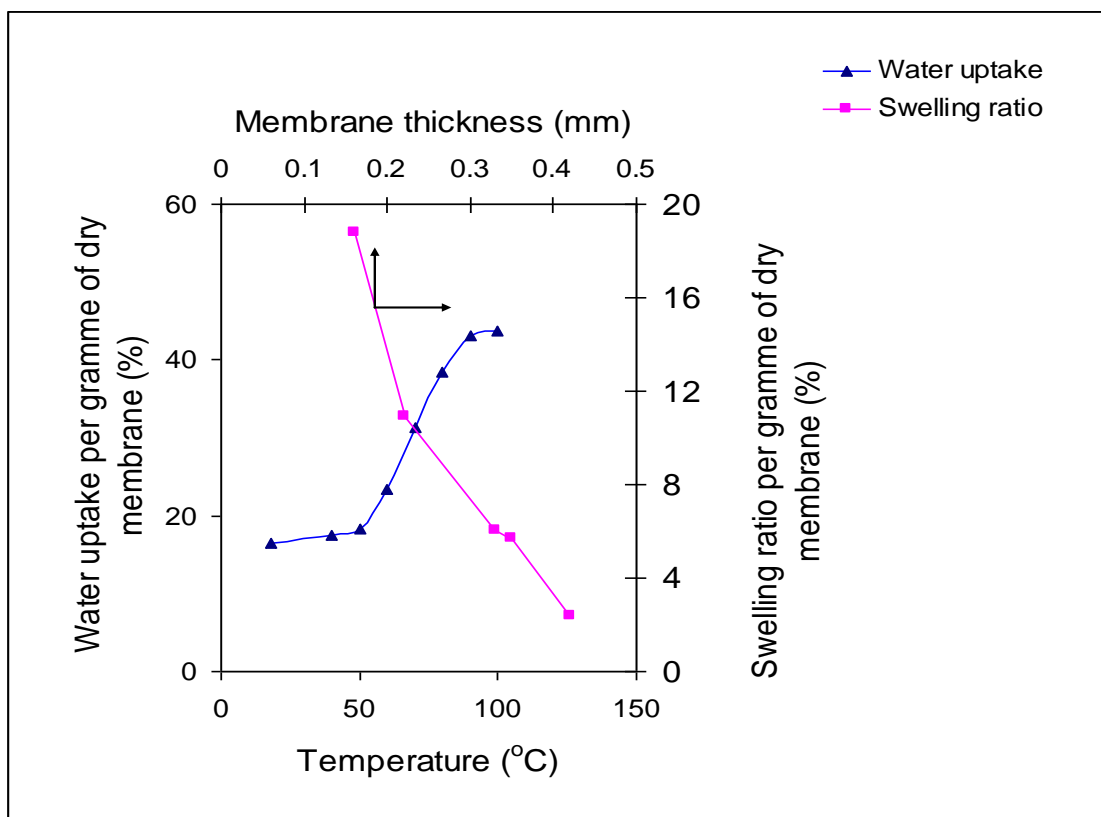


Figure 6.19: Effect of temperature and membrane thickness on water uptake and swelling ratio

A comparison of the water uptake ability of the synthesised membrane with that of Nafion[®] shows that the synthesised membrane has better water uptake ability than Nafion[®] which was reported to be the ranges of 30 - 36 % by weight (Sangeetha, 2006; Ni et al., 2006). Though excess water uptake by the membrane could lead to swelling of the membrane and thus affect the thermal and morphological strength of the membrane. But the synthesised membrane shows a moderate water uptake when compared to the values reported in literature for synthesized membrane from other sources (Sangeetha, 2005; Gu et al., 2006; Ni et al., 2006). Therefore, a synthesized membrane form PSBR has a moderate water uptake, which makes it a good candidate for fuel cell applications.

The moderate water uptake of the synthesised membrane could be attributed to the chain flexibility in comparison to Nafion[®]. The main chain of both the polystyrene-butadiene rubber and Nafion[®] are well organised. The branched chains attached to the polystyrene-butadiene are aromatic and flexible, where as the Nafion[®] membrane has a rigid linear fluorinate chain (Woo et al., 2003).

Desorption results which measure the rate at which the membrane becomes dehydrated was investigated at various temperatures and time and the results obtained are presented in Table 6.2. Results show that the membrane can hold up water to 100°C for one hour. At room temperature, the percentage of water desorption by the membrane was increasing gradually with time and retain some of the water after 12 hours. At 40°C and 50°C, the membrane lost all its water content after 3 hours, while water retention time at 60°C was 2 hours and 1 hour at 70, 80 and 100°C. Therefore, the higher the temperature, the lower the water retention time of the membrane and consequently the lower will be the performance of the membrane.

Hence, it can be inferred that the membrane will require humidification especially if the fuel cell where the membrane will be used is operating above room temperature.

Swelling ratio is the percentage change in membrane thickness per gramme of dry membrane. The result in the same Figure 6.19 shows that the swelling ratio is inversely proportional to the membrane thickness, i.e. the smaller the thickness the higher the swelling ratio. This pattern of results is in agreement with the results obtained earlier on the water uptake capacity of the membrane at different thickness as shown in Figure 6.18, where the water uptake ability of the membrane is higher at smaller thickness.

Table 6.2: Effect of time and temperature on the water desorption capacity of the membrane

Water desorption of the membrane (%)							
Time (H)	25°C	40°C	50°C	60°C	70°C	80°C	100°C
1	85.47	97.83	98.96	99.19	99.30	99.5	99.6
2	92.33	98.91	98.96	99.19	100.00	100.00	100.00
3	94.62	98.91	98.96	100.00	100.00	100.00	100.00
4	94.62	98.91	100.00	100.00	100.00	100.00	100.00
5	98.06	100.00	100.00	100.00	100.00	100.00	100.00
6	98.06	100.00	100.00	100.00	100.00	100.00	100.00
7	98.06	100.00	100.00	100.00	100.00	100.00	100.00
8	99.20	100.00	100.00	100.00	100.00	100.00	100.00
9	99.20	100.00	100.00	100.00	100.00	100.00	100.00
10	99.20	100.00	100.00	100.00	100.00	100.00	100.00
11	99.20	100.00	100.00	100.00	100.00	100.00	100.00
12	99.20	100.00	100.00	100.00	100.00	100.00	100.00

6.8 PSBR Related Problem of Brittleness and Cure

The SEM study which shows that the base material has porous, coarse characteristics was found to show element of brittleness after being cast into thin film. This could be associated with the plastic domain of the polymer as polystyrene often time exhibits crosslink characteristic. Polymer crosslink tends to constrain polymer network thereby inducing rigidity and restriction of water absorption. This problem of brittleness was solved via sulphonation. It was observed from analysis that the brittleness reduces as degree of sulphonation increases until it is completely overcome. This, is therefore, means that as degree of sulphonation increases, it in turn reduces the porous, coarse nature of the starting polymer to a dense polymer material. Its mechanical property was found to be correspondingly enhanced. At degree of sulphonation > 2.5 % membrane brittleness was completely overcome, up until degree of sulphonation of 55 % (Figure 6.20 a – d) but membrane showed signs of brittleness again at highest degree of sulphonation (DS > 55 %) though with the highest level of conductivity. Since PEM is required to balance conductivity property with mechanical properties, membrane having DS > 55 % is considered unfit for PEM fuel.

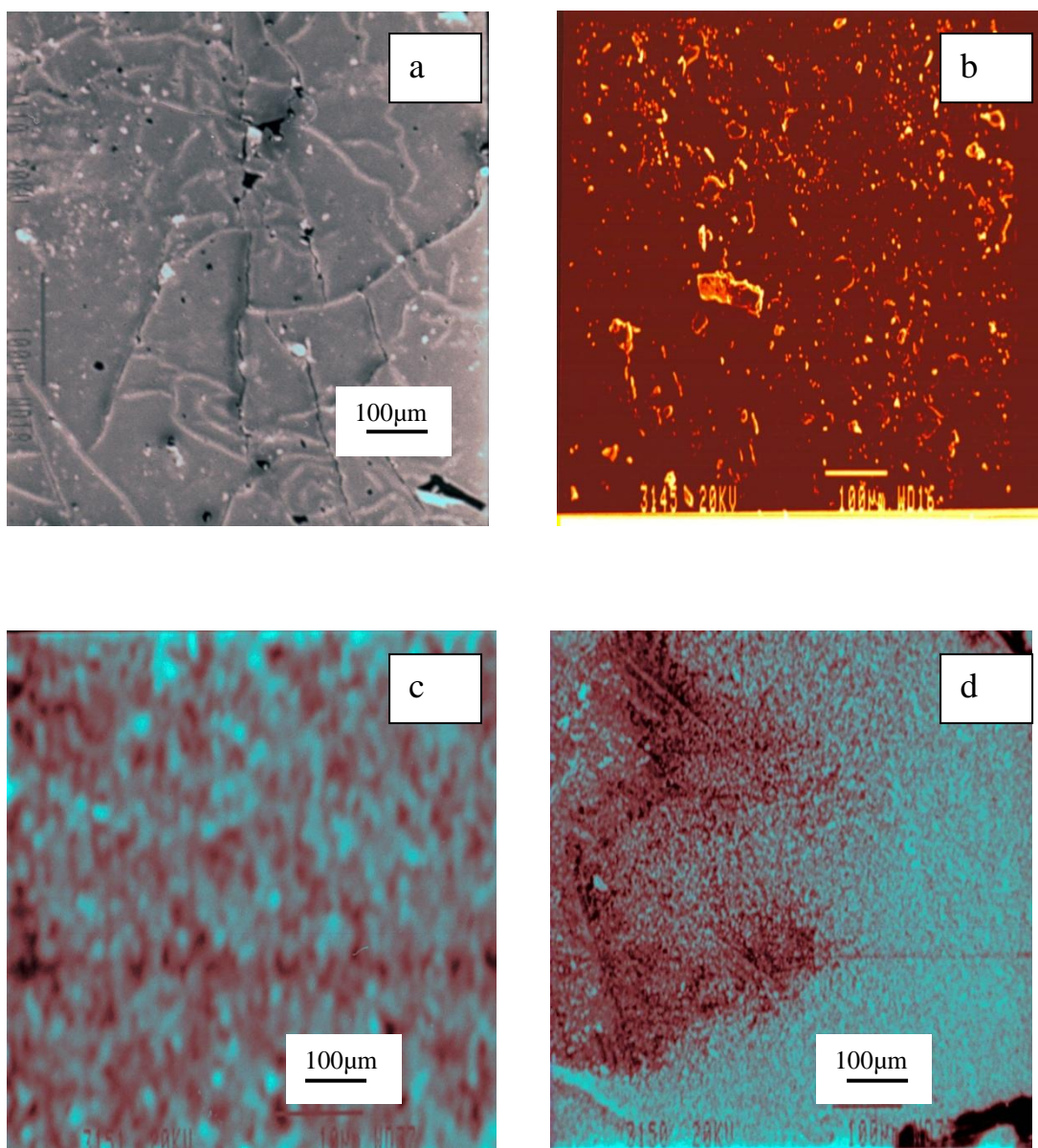


Figure 6.20: SEM images of (a) DS < 2.5 %; (b) DS = > 7 %; (c) DS > 10 %; (d) DS > 55 %, respectively.

6.9 Performance Testing of Synthesised Membrane in PEMFC

An electrochemical activity test of a fuel cell involving the synthesised membrane was carried out along with a commercial state-of-the-art membrane. Figure 2.2 shows the schematic of the operation of single cell in fuel cell test apparatus. The fuel gases (hydrogen and oxygen) were allowed to diffuse through the porous backing layer while at the gas/electrolyte interface the gases dissolved and then diffused to the electrolyte/electrode

interface. Electro catalytic reaction on the catalyst layer preceded the gas adsorption at the electrode surface while ionic transport occurs in the electrolyte, but electronic transport takes place in the electrode. Prior to installing the membrane electrode assembly (MEA) in the fuel cell stack, the MEA was hydrated for ~ 48 hrs with demineralised water.

The single cell was then installed in a fuel cell testing apparatus equipped with gas sources, temperature control, and gas flow–rate control rotameters, back pressure regulators for both hydrogen and oxygen, and a load of resistant box. Hydrogen and oxygen (Afrox, South Africa, 97-98 % purity) were the reactants used in this PEM fuel operation. Fuel cell tests were carried out with Pt/C catalyst (Afolabi, 2009) in order to determine the distribution of reaction products which involved passing hydrogen through a humidifier to wet the gas and were fed into the anode at a flow rate of 712 ml/min and 20 kPa. Oxygen entered the fuel cell through the cathode at a flow rate of 433 ml/min and 15 kPa. The electrons generated from the anode were connected to a digital multimeter (1906 Competing Multimeter), with an external variable resistance to measure the current and voltage produced by the cell. The polarisation tests were started when the open circuit voltage (OCV) stabilised. Figure 6.21 shows the polarisation curve where a performance of an OCV of 718.75 mV (approximately 0.72 V) was achieved with the synthesised membrane of constant degree of sulphonation (39.38 %) with 40 wt % catalyst loading. At different catalyst loadings, results showed that the electrical performance decreases with decrease in wt % catalyst loading. The result also showed that as current density increases the electrical performance decreases at current densities between 50 to 220 mA/cm², there was a linear fall in voltage as the current density increases. This effect was due to the fact that there was a resistance to current flow within the fuel cell.

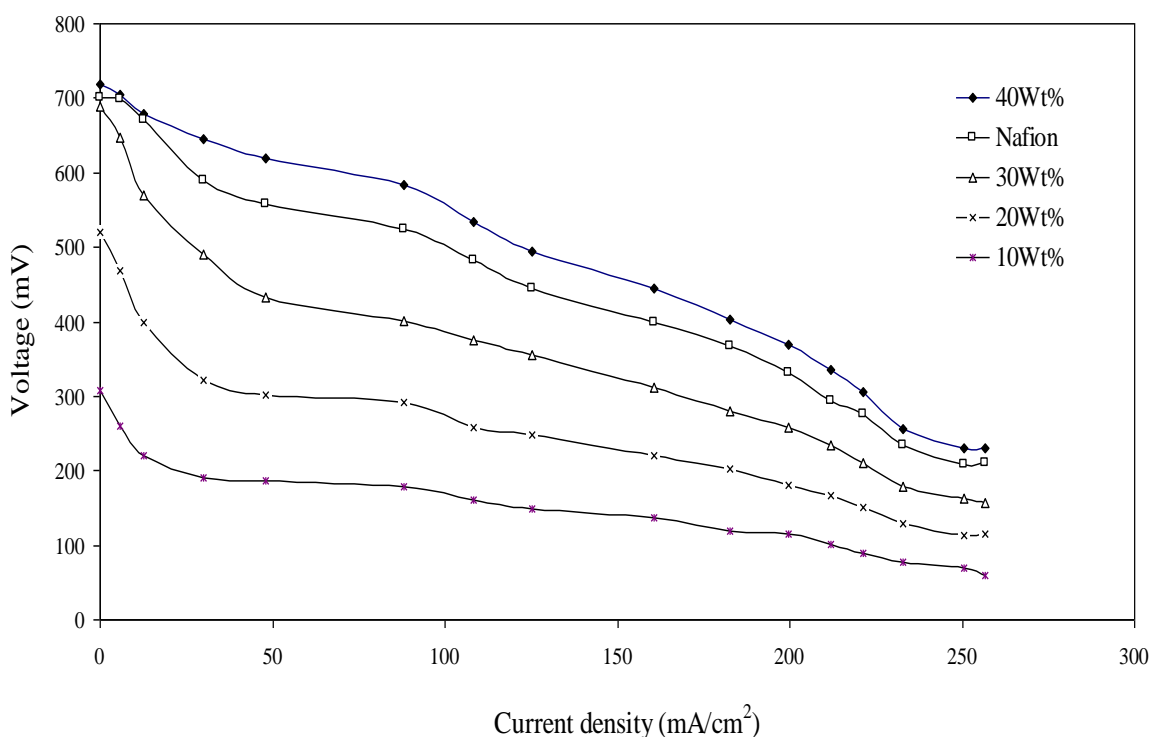


Figure 6.21: Cell potential Vs current density for a single cell (25 cm^2) for electrodes operated at 25°C with $\text{H}_2:\text{O}_2$ ratio of 1:2

Comparatively, a state-of-the-art membrane, Nafion[®] (Nafion 112) having the same concentration of catalyst loading was also investigated. Result showed that an OCV of 700.89 mV (approximately 0.7V) was achieved, which is slightly lower than (0.2 %) that of the synthesised membrane with the same catalyst loading. But on the average it could be considered to be equal in performance. The 0.2 % increase in performance differences should be expected as the synthesised membrane has a better hydration property under the same condition. However, for all the membranes considered, the performance has the same trend, that is, the lower the current density the higher the performance. This observation is consistent with literature (Chaojie et al 2007; Staita et al., 1997; Xianguo, 2006; Larminie and Dicks, 2000; Denver and Norman, 2006; Horsfall and Lovell, 2001). In the low current

density region where performance is higher, the contribution from mass transfer polarisation can be negligible, and the electrode charge transfer and membrane polarisations are significant (Chaojie et al 2007).

Figure 6.22 is the polarisation curves obtained from the electrochemical activity of the cell. The results showed that increasing current density correspondingly increased the power density of the cell system.

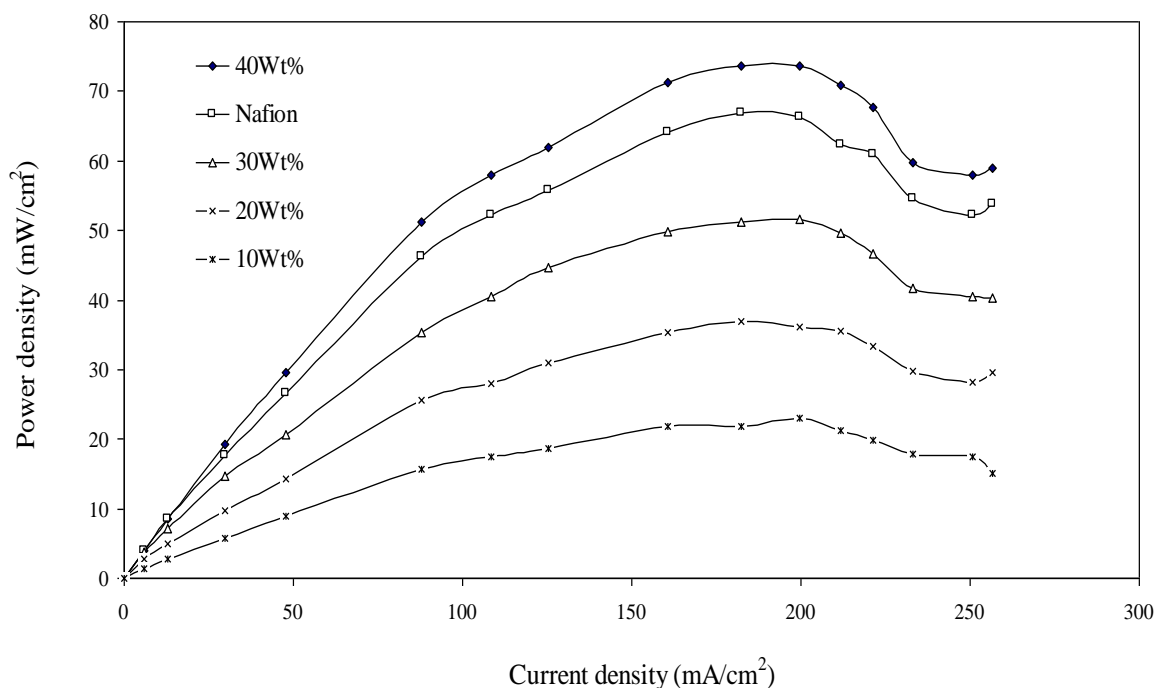


Figure 6.22: Power density Vs current density for a single cell (25 cm²) for electrodes operated at 25°C with H₂:O₂ ratio of 1:2

This showed that at high current densities (199.68 mA/cm²), the hydrogen reaction rate was high. A maximum power density of 73.68 mW/cm² was recorded at 199.68 mA/cm². After this point the performance dropped even at higher current density considered. The drop could be associated to several factors such as decrease in catalyst active surface, drying of both the

membrane and the catalyst layer ionomer, decrease in O₂ and H₂ partial pressures (Chaojie et al 2007). The highest fuel cell performance was obtained with the synthesised membrane (73.68 mW/cm²) as against the state-of-the art membrane (66.85 mW/cm²) having the same catalyst loading. The result also showed that as catalyst loading decreases, the power density decreases. A percentage decrease of 34.58 % was obtained between the 40 – 10 % catalyst loading considered.

6.9.1 Effect of degree of sulphonation on the SPSBR membrane performance

The effect of the degree of sulphonation on the membrane performance of the fuel cell was also investigated. Figure 6.23 shows the polarisation curve at different degree of sulphonation. The result showed that the cell potential of the fuel cell is a function of the degree of sulphonation of the membrane.

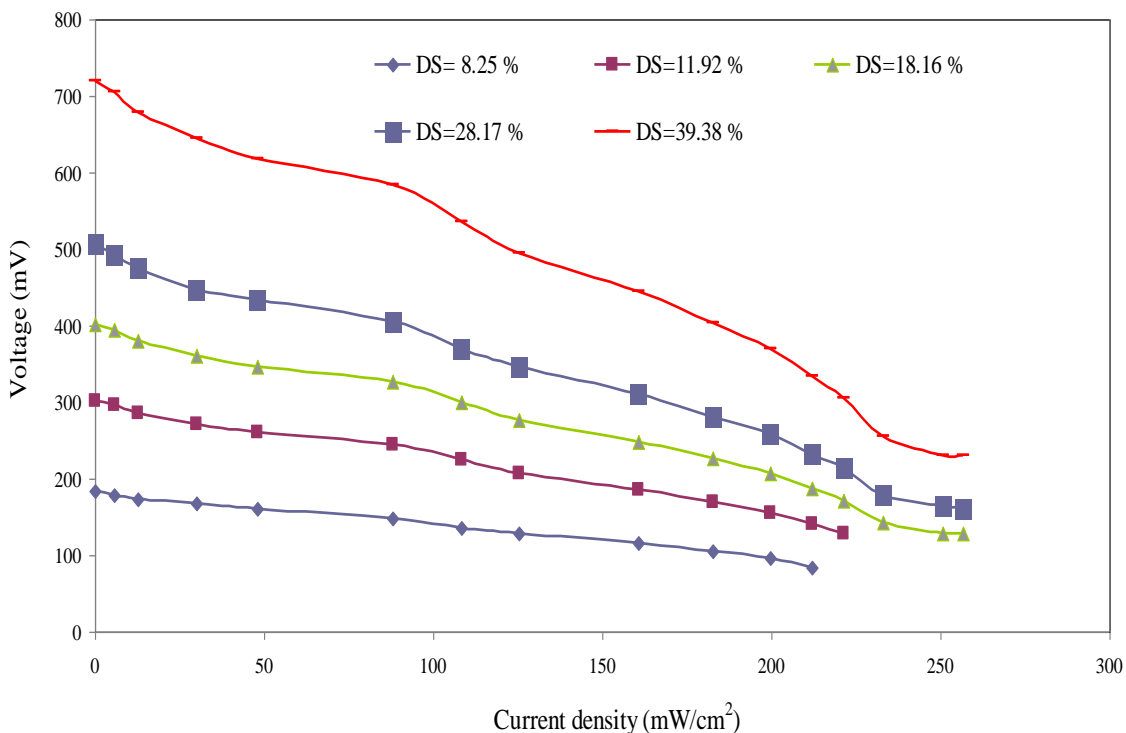


Figure 6.23: plot of cell potential as a function of current density drawn from experimental data

The membrane with 39.38 % degree of sulphonation achieved an OCV performance of 7.18 mV while that with the least degree of sulphonation (8.25 %) achieved the poorest OCV performance of 186.88 mV. This is a 3.8 fold decrease in performance. The cell potential falls drastically as the current density is increased for the membrane with the least degrees of sulphonation (8.25 and 11.92 %). However, membranes with higher degrees of sulphonation show better performance across the entire current density range.

Figure 6.24 is the result of the power density as a function of current density. Result also showed that power density which is a major resistance to current flow of the fuel cell is dependent on the membrane's degrees of sulphonation.

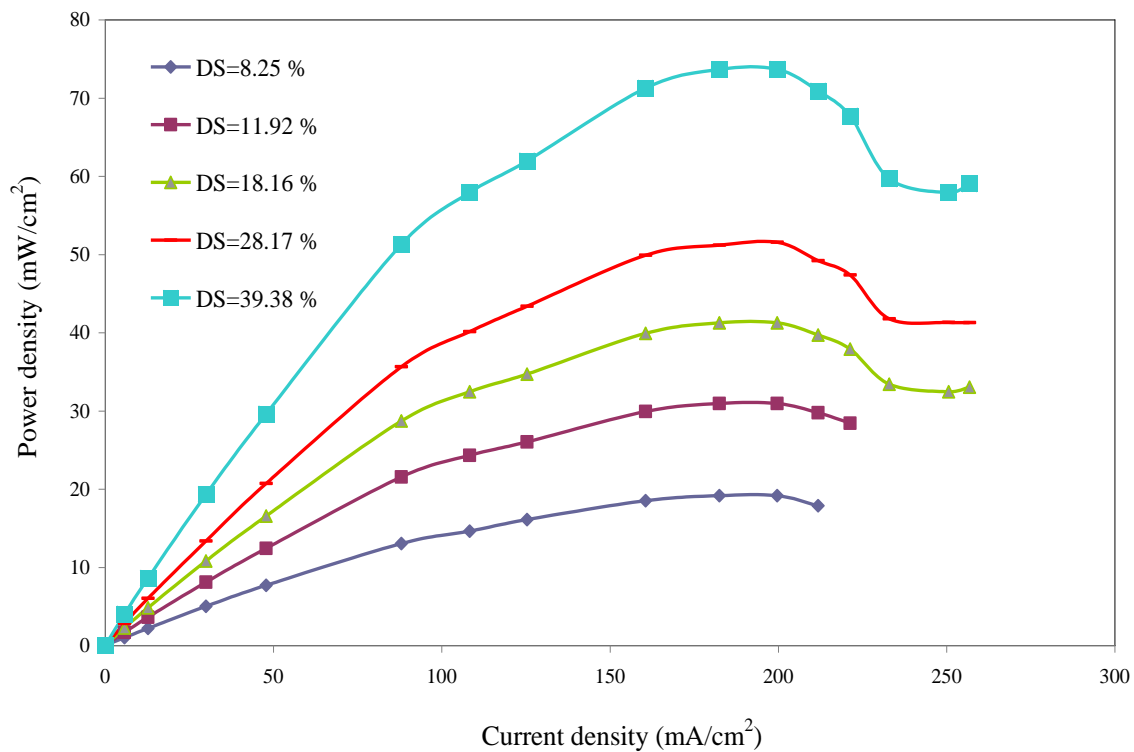


Figure 6.24: plot of the power density as a function of current density drawn from experimental data and calculated

The membrane with the highest degree of sulphonation achieved maximum power density of 73.68 mV/cm², while the membrane with the least degree of sulphonation achieved a maximum power density of 19.16 mV/cm², being the poorest performance. The highest performance was achieved at current density of 199.68 mA/cm² and after this region, the fuel cell performance dropped. The drop could be attributed to any of numerous factors such as; decrease in catalyst active surface, drying of both the membrane and the catalyst layer ionomer, H₂ crossover effect, decreases in O₂ and H₂ partial pressures (Chaojie et al 2007). The membranes with higher degrees of sulphonation achieving superior performance over the membranes with lower degrees of sulphonation is traceable to their high ion exchange capacity and equivalent weight capacity and therefore absorb water easily and better. This enables them to achieve a much better comparative performance (Horsfall and Lovell, 2001) especially in a water-starved environment or situation.

6.9.2 SPSBR membrane durability test

Fuel cell performance and stacks usually undergo degradation over time (Xianguo, 2006; Larminie and Dicks, 2000; Borup et al., 2006). The durability of fuel cell membrane-electrode-assembling (MEA) is recognised to play a vital role in the overall lifetime that is achieved by a stack in field application (Borup et al., 2006). The fuel cell durability test in this study was conducted with a synthesised membrane of 39.38 % degree of sulphonation. Figure 6.25 shows the performance durability for a single cell (25 cm²) for electrode operated at 25°C. A performance of an OCV of 718.75 mV was achieved at initial time of operation. The result also showed that the MEA performance underwent degradation between initial operation times up until 7 hrs before maintaining a constant performance of 438.49 mV. The loss can be attributed to materials, fabrication and operating conditions (Borup, et al., 2006). However, start up/shut down of any fuel cell can lead to membrane degradation and carbon

corrosion, which are known to affect the durability of a fuel cell (Borup et al., 2006). From Figure 6.25 it can be seen also that performance decay rate is not uniform and the data under analysis suggests initial losses of cell potential to be ~ 0.06 V/hr. This is quite high, probably due to a decrease in catalytic activity of the fuel cell.

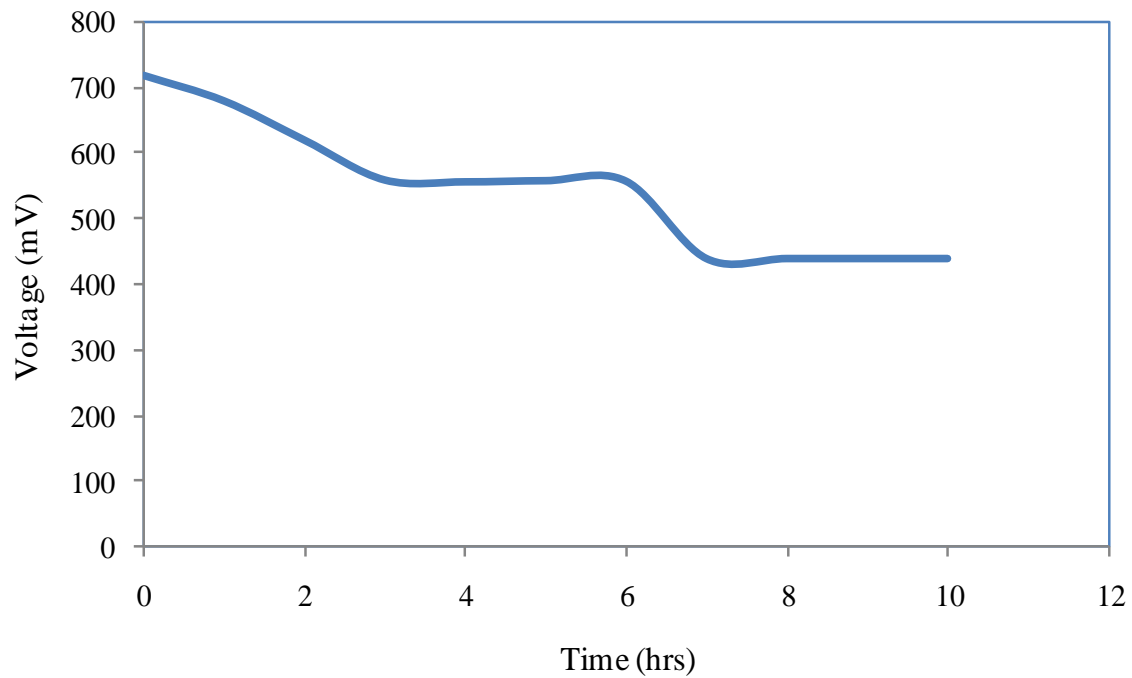


Figure 6.25: Performance durability for a single cell (25 cm^2) for electrode operated at 25°C

Also envisaged as a possible cause of high performance decay was the problem of electrode creepage (deformation of the particulate structure of the electrode under compression) and sintering (coarsening of the particulate) (Xianguo, 2006). However, achieving longer lifetime is possible if the fuel cell performance decay rate is reduced.

CHAPTER SEVEN

7.0 CONCLUSION AND RECOMMENDATION

7.1 Conclusion

The process of chemically modifying the structure of PSBR, which is originally an insulator to a conductor via sulphonation, was carried out using chlorosulphonic acid. The effect of weight of the rubber, concentration of sulphonating agent, reaction time, stirring speed and temperature were found to be very relevant parameters in the sulphonation of PSBR. An optimum degree of sulphonation (39.38 %) and ion exchange capacity (2.074) at room temperature was achieved using 1.6 M ml⁻¹ of chlorosulphonic acid at 24 hrs of reaction time and a stirring speed of 1500 rpm. The use of IR and ¹HNMR confirmed the attachment of the SO₃H group on the polymer matrix. The presence of the SO₃H on the rubber was found to create a hydrophobic and hydrophilic phase on the sulphonated rubber making it useful to serve the purpose of fuel cell application.

The sulphonation kinetic of PSBR was studied in 0.0016 mol L⁻¹ of chlorosulphonic acid where first-order kinetic model; without the effect of HCl and the effect of HCl were investigated. The reaction rate was found to obey the first-order model with the HCl produced having a desulphonation effect on the reaction. A predictive model was developed and is able to predict the degree of sulphonation at different initial concentrations of acid. The thermodynamic study showed that the reaction is non-spontaneous, and as temperature increases the reaction system experienced phase change from liquid to solid at temperature above 328 K, as the entropy of the system started reducing gradually with increasing temperature.

A thin film membrane was latter cast from a solution of the sulphonated PSBR of about 15-30 % wt, onto a clean polymer paper support using a laboratory doctor blade casting machine. The thermal analysis of the membranes was carried out. The results from DSC showed a highly thermo stable sulphonated polystyrene-butadiene rubber with a glass transition temperature (T_g) of about 198°C. The TGA results also showed that the sulphonated rubber main chain only decompose at a temperature range of 402°C- 475°C. The TGA curves were able to reveal that a drop in weight at these temperature ranges reduced as the degree of sulphonation increased, which was an indication that the attached SO_3H group improved the strength of the rubber. This result was further justified using DTA, and the result was found to be consistent. However, the original PSBR was found to be brittle in an unsulphonated state and at a very low degree of sulphonation of < 2.5 % due to its porous and coarse morphology. But as the degree of sulphonation increased the brittleness was overcome when the sulphonated PSBR turned a dense material. However, membranes with a degree of sulphonation above > 55 %, were found to show possible signs of brittleness and solubility in water.

The proton conductivities of the synthesised membranes were measured at different temperatures and membrane thickness. Result showed that conductivity in the order of 10^{-3} – 10^{-2} S/cm was achieved, and it was found that the conductivity increased with temperature and decreased as membrane thickness increased.

The results on uptake of methanol per sulphonic group show that the methanol uptake per sulphonic group increases with increase in concentration of methanol. This is attributable to the availability of the methanol at higher concentration than at lower concentration. Results also showed that the methanol uptake per sulphonic group decreased with increase in the

degree of sulphonation. This was due to a decrease in equivalent weight as the degree of sulphonation increases, which resulted in more sites for the distribution of the methanol within the membrane. However, results on water uptake show that the water uptake per sulphonic acid group by the sulphonated PSBR was higher than the methanol uptake per sulphonic group, and the synthesised membranes exhibited moderate water adsorption and desorption capacity both at room temperature and at a higher temperature (100°C). The results obtained on the porosity of the membranes show that porosity to methanol increased with decrease in membrane thickness, a situation that was associated with reduction in the area of the site required to hold the methanol within the membrane matrix as the thickness of the membrane decreased. Consequently this resulted in the diffusion of methanol through the membrane, which inferably resulted in high porosity of the membrane. Comparatively, porosity of the SPBR to methanol was found to be less than that of Nafion[®], which was in the range of 0.40-0.51, depending on the concentrations of the methanol.

On methanol crossover at same thickness, membrane with lower degree of sulphonation exhibited higher methanol crossover (> 1.6 Mol/l), which decreases (< 1.2 Mol/l) as the degree of sulphonation increased. The results were able to show that the synthesized membrane from polystyrene-butadiene rubber exhibited lower methanol diffusion coefficient (10^{-7}) compared with Nafion 117 ($3.42 \times 10^{-6} \text{ cm}^2/\text{s}$).

The electrochemical test of the MEA achieved a performance of an OCV of 718.75 mV with the synthesised membrane (39.38 %) with 40 wt % catalyst loading. At different catalyst loading result showed that the electrical performance decreased with decrease in wt % catalyst loading. Comparatively, a state-of--the art membrane, Nafion[®] (Nafion 112) having the same concentration of catalyst loading was also investigated. The result showed that an

OCV of 700.89 mV was achieved, which was slightly lower than (0.2 %) that of the synthesised membrane with the same catalyst loading. A maximum of power density of 73.68 mW/cm² was recorded at 199.68 mA/cm². The investigation of effect of degree of sulphonation showed that the cell potential was a function of the degree of sulphonation of the membranes. The membrane with 39.38 % degree of sulphonation achieved an OCV performance of 7.18 mV while that with the least degree of sulphonation (8.25 %) achieved the poorest OCV performance of 186.88 mV, which represents a 3.8 fold decrease in performance.

Finally, the durability of the MEA was also studied and result showed that the MEA performance underwent degradation between initial operation times up until 7 hrs before maintaining a constant performance of 438.49 mV. The cause of the initial high performance decay was envisaged as probable electrode creepage and sintering. However, longer lifetime performance can be achieved. This study, therefore, shows that a novel alternative PEM to Nafion[®] that will be efficient for fuel cell application can be synthesised from a locally commercially available polystyrene-butadiene rubber.

7.2 Recommendation

Blend of PSBR with well selected hard materials or composites (such as carbon nanotubes or nanoballs, clay e.t.c) can probably help to reinforce the sulphonated rubber better especially to overcome dissolution in water at a higher degree of sulphonation (> 55 %).

REFERENCES

- Adams, R (2002). Organic reactions. Vol. III. John Wiley & Sons, Inc. New York. Pp 142-164.
- Aflabi, A. S (2009). Development of carbon nanotubes platinum electro catalytic electrodes for proton exchange membrane fuel cell. PhD Thesis, University of the Witwatersrand, South Africa. Unpublished.
- Akovali, G and Özkan, A (1998). Converting waste polystyrene into a polymer flocculant for waste water treatment. *Polymer*, **27**:1277.
- Akovali, G and Özkan, A (1986). Notes on modification of polystyrene by sulphonation: some properties of poly(styrenesulphonic acid). *Polymer*, **27**: 1277-1280.
- Allam, C., Liu, K. J and Mohanty, D. K (1999). Preparation and properties of novel aromatic poly(thioethers) derived from 4,4'-thiobisbenzenethiol. *Macromolecular Chemistry and Physics*, **200**:1854-1862.
- Anikumer. G.M., Nakazawa. S., Okubo. T and Yamaguchi. T (2006): Proton conducting phosphated zirconia-sulfonated polyether sulfone nano hybrid electrolyte for low humidity, wide-temperature PEMFC operation. *Electrochemistry communication*, **8**: 133-136.
- Atkinson, S (2005). Fuel cells for mobile devices. *Membrane Technology Feature*, December, 2005.

- Bailly, C., Williams, D., Karasz, F. E and Macknight, W. J (1987). The sodium salts of sulphonated poly(aryl-ether-ether-ketone) (PEEK): Preparation and Characterization. *Polymer*, **28**: 1009-1016.
- Balkin, A. R (2002). Modelling a 500 W polymer electrolyte membrane fuel cell. Thesis, University of Sidney, Faculty of Engineering. Pp 4-25.
- Bashir, H., Linares, A and Acosta, J. L (2001). Heterogeneous sulfonation of blend systems based on hydrogenated poly(butadiene-styrene) block copolymer. Electrical and structural characterization. *Solid State Ionics*, **139**:189-196.
- Basile, A., Paturzo, L., Lulianelli, A., Gatto, I and Passalacqua, E (2006). Sulfonated PEEK-WC membranes for proton – exchange membrane fuel cell: Effect of the increasing level of sulfonation on electrochemical performances. *Journal of Membrane Science*, **281**: 377- 385.
- Bebin, P., Caravanier, M and Galiano, H (2005). Nafion/Clay –SO₃H membrane for proton exchange membrane fuel cell application, *Journal of Membrane Science*, **278**: 35- 42.
- Behre, H., Blnak, H. U., Kohler, W., Muller, N., Schnegg, P (1989). Process for the sulphonation of aromatic compound with sulphur trioxide. U. S. Patent 4859372.
- Biemark, K., Brand, J. C., Cole, A. R. H., King, J. F., Edward, L., Mcquillin, F. J., Karl, H. O., Scott, A. I., Stothers, J. B., Swan, G. A and Valenta, Z (1963), Elucidation of

structures by physical and chemical methods. John Wiley & Sons, Inc. USA. 1963, pp 142-211.

Bigi, F., Casiraghi, G., Casnati, G., Sartori, G., Gasparri G. Fava and Belicchi, M. F (1985). Asymmetric electrophilic substitution on phenols in a Friedel-Crafts hydroxyalkylation. Enantioselective ortho-hydroxyalkylation mediated by chiral alkoxyaluminum chlorides. *Journal of Organic Chemistry*, **50**: 5018-5022.

Bishop, M. T., Karasz, F. E., Russo, P. S and Langley, K. H (1985). Solubility and properties of a polyarylether keton in strong acids. *Macromolecules*, **18**: 86-93.

Blackwell, R. I. and Mauritz, K. A (2004). Dynamic mechanical properties of annealed sulfonated poly(styrene-b-[ethylene/butylene]-b-styrene) block copolymers. *Polymer*, **45**: 3457 – 3463.

Blanco, J. F., Nguyen, Q. T and Schaetzel, P (2001). Novel hydrophilic membrane materials: sulphonated polyethersulfone Cardo. *Journal of Membrane Science*, **186**:267-279.

Bockris, J and Srinivasan, S (1969). Fuel cells, their electrochemistry, 1st Ed., McGraw-Hill, New York, USA. Pp 659.

Borup, R. L., Davey, F. H., Garzon, D. L., Welch, P. M, and More, K, Wood, (2006). Polymer electrolyte membrane (PEM) fuel cell durability. Los Alamos National Laboratory, an affirmative action/equal opportunity employer, operated by Los Alamos National Security, LLC, for the National Nuclear Security Administration of the U.S.

Department of Energy under contract DE-AC52-06NA25396. A U.S. Department of Energy Laboratory. Summer 2006.LALP-06-108

Brandon, N. P., Skinner, S and Steele, B. C. H (2003). Recent advances in materials for fuel cells. *Annual Review of Material Research*, **33**: 183.

Campbell, C. J (2004). Oil and gas liquids 2004 scenerion. Uppsala hydrocarbon depletion group. Pp 1

Canter, N. H (1969). Ger. Offen. 1 (915) 236. In: Smitha, B., Sridhar, S., Khan, A. A (2003). Synthesis and characterization of proton conducting polymer membranes for fuel cells, *Journal Membrane Science*, **225**: 63-76.

Carratta, N., Tricoli, V and Picchioni, F (2000). Ionomeric membranes based on partially sulfonated poly(styrene): synthesis, proton conduction and methanol permeation. *Journal of Membrane Science*, **166**:189-197.

Cerfontain, H (1968). Mechanistic aspects in aromatic sulphonation and desulphonation. Wiley Interscience, New York. Pp 10-200.

Chaijie, S., Yanghua, T., Jian, L. Z., Jiujun Z., Haijiang W., Jun S., Scott, M, Jing, L and Paul, K (2007). PEM fuel cell reaction kinetics in the temperature range of 23 – 120°C. *Electrochimica Acta*, **52**: 2552-2561.

- Chen, J., Asano, M., Yamaki, T and Yoshida, M (2005). preparation of sulfonated cross linked PTFE graft-poly (alkyl vinyl ether) membranes for polymer electrolyte membrane fuel cells by radiation processing. *Journal of membranes science*, **256**: 38-45.
- Cheng, S., Krishnan, L., Srinivasan, S., Benziger, J and Bocarsley, A.B (2004). Ion exchange resin/polystyrene sulfonate composite membranes for PEM fuel cells. *Journal Membrane Science*, **243**: 327-333.
- Clauwaert, P., Aelterman, P., Pham, H. T., De Schamphelaire, L., Carballa, M., Rabaey, K. and Verstraete, W (2008). Minimizing losses in bio-electrochemical systems: the road to applications. *Applied Microbiology Biotechnology*, **79**: 901.
- Gottesfield, S and Zawodzinski, T, A (1997). Polymer electrolyte fuel cells. *Advances in Electrochemical Science and Engineering*, eds., Alkire, A. C, Gerischer, H., Kolb, D. M and Tobias, C. W. 5, Wiley – VCH, New York. Pp 195-301.
- Cremllyn, R. J (2002). Chlorosulphonic acid- a versatile reagent. Royal Society Chemistry, Great Britain. Pp 181-267.
- Dahr, H. P (2005). Medium term stability testing of proton exchange membrane fuel cells stacks as independent power units. *Journal of Power Sources*, **143**: 185-190.
- Daoust, D., Devaux, J and Godard, P (2001). Mechanism and kinetics of poly(ether ether ketone) (PEEK) sulphonation in concentrated sulphuric acid at room temperature. Part

1. Quantitative comparison between polymer and monomer model compound sulphonation. *Polymer International*, **50**: 917-924.
- del Río, C., Jurado, J.R and Acosta, V (2005). Hybrid membranes based on block copolymer ionomers and silica gel. Synthesis and characterization. *Polymer*, **46**: 3975-3985.
- Denver, F. C and Norman, D. H. M (2006). Three dimensional modelling of high temperature PEM fuel cells. *Journal of Power Sources*, **160**: 215- 223.
- Desjardins, A and Eisenberg, A (1991). Colloidal properties of block ionomers. 1. Characterization of reverse micelles of styrene-b-metal methacrylate diblocks by size-exclusion chromatography. *Macromolecules*, **24**:5779-5790.
- Dimitrova, P., Friedrich, K. A., Stimming, U and Vogt, B (2002). Modified Nafion-based membranes for use in direct methanol fuel cells. *Solid State Ionics*, **150**: 115
- Ehrenberg, S. G., Serpico, J. M., Wnek, G. K and Rider, J. N (1995). Fuel cell incorporating novel ion-conducting membrane. US Patent No. 5. 468,574.
- Ehrenberg, S. G., Serpico, J. M., Wnek, G. K and Rider, J. N (1997). Fuel cell incorporating novel ion-conducting membrane. US Patent No. 5. 679,482.
- Farrell, C. P. O and Serniuk, G. E (1974). Process for preparing lattices of sulfonated elastomers. US Patent No. 3,836,511.

- Fogler, H. S (1992). Elements of chemical reaction engineering. 2nd Edition. Prentice Hall P T R. Pp 1 – 90.
- Gao, Y., Gilles, P. R., Guiver, M. D., Jian, X., Mikhailenko, S. D., Wang, Kaliaguine, S (2006). Low-swelling proton-conducting copoly(aryl ether nitrile)s containing naphthalene structure with sulfonic acid group meta to the ether linkage. *Polymer*, **47**: 808-816.
- Gao, Y., Gilles, P. R., Guiver, M. D., Jian, X., Mikhailenko, S. D., Wang, Kaliaguine, S (2003). Sulfonation of poly (phthalazinones) with fuming sulfuric acid mixtures for proton exchange membrane materials. *Journal of Membrane Science*, **227**, 39-50.
- Gauthier, S and Eisenberg, A (1987). Vinylpyridinium ionmers. 2. Styrene – based ABA block copolymer. *Macromolecules*, **20**: 760-767.
- Genies, C., Mercier, R., Sillion, B., Cornet, N., Gebel, G and Pineri, M (2001). Soluble sulfonated naphthalenic polyimides as materials for proton exchange membranes. *Polymers*, **42**:3 59-373.
- Ghenciu, A. F (2002). Review of fuel processing catalysts for hydrogen production in PEM fuel systems. *Current Opinion on Solid State Matter Science*, **6**: 389-399.
- Gottesfield, S and Zawodzinski, T, A (1997). Polymer electrolyte fuel cells. Advances in Electrochemical Science and Engineering, eds., Alkire, A. C, Gerischer, H., Kolb, D. M and Tobias, C. W. 5, Wiley – VCH, New York. Pp 195-301.

Gu. S., He. G., Wu. X., Li. C., Liu . H., Liu. C and Li . X (2006) Synthesis and characteristics of sulfonated poly (phtali zinone ethet sulfone ketone) (SPESK) for direct methanol fuel cell (DMFC). *Journal of Membrane science*, **21**: 121-129.

Han-Lang, W., Che-Chi, M. M., Chia-Itsun, L.; Tzong-Ming, L., Chih-Yuan, C., Chin-Lung, C and Chen, W (2006). Sulfonated poly(ether ether keton)/poly(amide imide). Polymer blends for proton conducting membrane. *Journal membrane Science*, **280**: 501-508.

Haubold, H. G., Vad, T., Jangbluth, H and Hiller, P (2001). Nano structure of Nafion: a SAXS study. *Journal of Electrochemical Acta*, **48**: 1559-1563.

Hays, D. G (2005). Testing of an axial in a turn charger system for polymer electrolyte membrane fuel cells. MSc Thesis, Georgia Institute of Technology. Pp 1-129.

Heijden, J and Baarle (2002). Natural rubber. Newsletter of the Rubber Foundation Information Center for Natural Rubber. 28, 4th quarter 2002. Pp 1.

Hickner, M. A., Ghasseni, H., Kim, Y. S., Einsla, B. R and McGrath, J. E (2004). Alternative polymer systems for proton exchange membranes (PEMs). *Chemical Review*, **104**: 4587.

Hikita, S., Yamane, K and Nakajima, Y (2001). Measurement of methanol crossover in direct methanol fuel cell. *JSAE review*; **22**: 151-156.

Horsfall, J. A and Lovell, K. V (2001). Fuel cell performance of radiation grafted sulphonic acid membranes. *Fuel Cells*, **1**: 3-4.

- Honma, I., Nomura, S and Nakajima, H (2001). Proton conducting organic/inorganic nanocomposite for polymer electrolyte membrane. *Journal of Membrane Science*, **185**: 83-94.
- Huange, R. Y. M., Shao, P., Burns, C.M and Feeng, X (2001). Sulfonation of poly(Ether Ether Ketone) (PEEK): Kinetic study and characterization. *Journal. Applied Polymer Science*, **82**: 2651-2660.
- Inzelt, M., Pineri, M., Schlitz, J. W and Vorotyntsev, M. A (2000). Electron and proton conducting polymers: recent development and prospects. *Electrochemical Acta*, **45**: 2403.
- Ihm, C. D and Ihm, S. K (1995). Pervaporation of water-ethanol mixtures through sulfonated polystyrene membranes prepared by plasma graft-polymerization. *Journal of Membrane Science*, **98**: 89-96.
- Jang, W., Lee, C., Sundar, S., Shul, Y. G and Han, H (2005). Thermal and hydrolytic stability of sulfonated polyimide membranes with varying chemical structure. *Polymer Degradation*, 90: 431-440
- Jian-Li, W., Myong-Hoon, L and Jun, Y (2005). Synthesis and characterisation of sulphonated polymer derived from 6FDA-ODA polyimide. *Polymer Bulletin*, 55: 357-365.

- Jelcic, Z., Holjevac-Grguric, T and Rek, V (2005). Mechanical properties and fractal morphology of high-impact polystyrene/poly(styrene-b-butadiene-b-styrene) blends. *Polymer Degradation and Stability*, **90**: 295-302.
- Jia, L., Xu., X., Zhang, H and Xu, J (1996). Sulfonation of polyetheretherketone and its effect on permeation behaviour to nitrogen and water vapour. *Journal of Applied Polymer Science*, **60**: 1231-1237.
- Jiang. R., Kunz. H.R and Fenton. J.M (2006): Composite silica/ Nafion membrane prepared by tetra ethyl ortosilicate sol-gel reaction and solution casting for direct methanol fuel cells. *Journal of membrane science*, **272**: 116-124.
- Jones, D. J., and Rozière, J (2001). Recent advances in the functionalization of polybenzimidazole and polyetherketone for fuel cell applications. *Journal of Membrane Science*, **185**: 73-81.
- Kaliaguine, S (2004). Synthesis and characterization of sulfonated poly (ether ketone) for proton exchange membrane. *Journal of Membrane Science*, **229**: 95-106.
- Kapias, T and Griffiths, R. F (2001). Spill behaviour using REACTPOOL Part 1. Results for accidental releases of chlorosulphonic acid (HSO_3Cl). *Journal of Hazardous Materials*, **A81**: 19-30.
- Kerres, J.A (2001). Development of ionmer membrane for fuel cells. *Journal of Membrane Science*, **185**: 3-27.

Kibler, C. J and Lappin, G. R (1973). Sulfopolyesters having improved clarity in water. Dispersible formulations and products made therefrom. US Ptent No. 3,734,874.

Kobayashi, T., Rikukawa, M., Sanui, K and Ogata, N (1998). Proton conducting polymers derived from polymers derived from poly(ether-etherketone) and poly(4-phenoxybenzoyl-1-4-phenylene). *Solid State Ionics*, **106**: 219-225.

Kreuer, K. D (2001). On the development of proton conducting membrane for hydrogen and methanol fuel cells. *Journal of Membrane Science*, **185**: 29-39.

Kruczek, B and Matsuura, T (2000). Effect of metal substitution of high molecular weight sulfonated polyphenylene oxide membranes on their gas separation performance. *Journal of Membrane Science*, **167**: 203-216.

Larminie, J and Dicks, A (2003). Fuel cell systems explained, 2nd Edition. John Wiley & Sons, Ltd, New York. Pp 1-120.

Larminie, J and Dicks, A (2000). Fuel cell systems explained. John Wiley & Sons, Ltd, England. Pp 1-50.

Lee, H. C., Hong, H. S., Kim, Y. M., Choi, S. H., Hong, M. Z., Lee, H. S and Keen, K (2004). Preparation of sulfonated-fluoronated poly (arylene ether) membranes for a proton exchange fuel cell. *Journal of Electro Chemical Arts*, 49: 252-260.

- Li, W. S., Lu, D. S., Luo, J. L and Chyang, K. T (2005). Chemical and energy co-generation from direct hydrocarbon oxygen proton exchange membrane fuel cell. *Journal of Power Sources*, 145: 376-382.
- Liebhafsky, H. A and Cairns, E. J (1968). Fuel cells and batteries. John Wiley and Sons, Inc., New York. Pp 7.
- Liversage, J. H (2004). An enhancement of the mechanical properties in functionally graded liquid-phase sintered SiC-TiC ceramic composites. PhD Thesis, University of the Witwatersrand, Johannesburg. Unpublished.
- Matsunguchi, M and Takahashi, H (2006). Methanol permeability and proton conductivity of a semi-interpenetrating polymer networks (IPNs) membrane composed of Nafion[®] and cross-linked DVB. *Journal Membrane Science*, **281**: 707-715.
- McNicol, B. D, Rand, D. A. J and Williams, K R (1999). Direct methanol-air-fuel cells for road transportation. *Journal of Power Sources*, **83**: 15-31
- Mokrini, A., Huneault, M. A and Gerard, P (2006). Partially fluorinated proton exchange membranes based on PVDF-SEBS blends compatibilized with methylmethacrylate block copolymers. *Journal of Membrane Science*, **283**: 74-83.
- Mokrini, A and Acosta, J. L (2001). Studies of sulfonated block copolymer and its blends. *Polymer*, **42**: 9-15.

Nazan, G (2001). Synthesis and characterization of sulfonated polyimides as proton exchange membranes for fuel cells. Desertation, Virginia Polytechnic and State University, Blacksburg, VA. Pp 75-185.

Ni. H., Li. Z., Dou. H., Li . H and Zhao . C (2006): Synthesis and characterization of fluorinated ionomer P-perfluoro – [1-2-sulfonic ethoxy] ethylated polystyrene ionirile-styrene. *Journal of Fluorine chemistry*, **127**: 1036-1041.

Nick A. P and David W. C. M (2001). New Strategies in Organic Catalysis: The First Enantioselective Organocatalytic Friedel-Crafts Alkylation. *Journal of Americal Chemical Society*, **123**: 4370-4371.

Nobuhiro, S and Roger, S. P (1994). A reconsideration of the kinetics of aromatic sulfonation by sulphuric acid. *Macromolecules*, **27**: 6267-6271.

Nobuhiro, S and Roger, S. P (1992). Kinetics of PEEK Sulfonation in concentrated sulphuric acid. *Macromolecules*, **25**: 6495-6499.

Okada, O and Yokoyama, K (2001). Development of polymer electrolyte fuel cell cogeneration systems for residential applications. *Fuel Cells*, **1**: 72.

Paturzo, L Basile, A., Iulianelli, A., Jansen, J. C., Gatto, I., and Passalacque, E (2005) High temperature proton exchange fuel cell using a sulphonated membrane obtained via H₂SO₄ treatment of PEEK-WC, *Journal Catalysis Today*, **104**: 213-218.

- Peixiang, X., Gilles, P., Robertson, A., Michael, D., Guiver S. D., Mikhailenko, K., Wang, B and Serge, K (2004). Synthesis and characterization of sulfonated poly(ether ether ketone) for proton exchange membranes. *Journal of Membrane Science*, **229**: 95-106.
- Ralp, T, R (1997). Proton exchange membrane fuel cells. Progress in cost reduction of the key components. *Plantinum Metals Review*. **41**:102-113.
- Ren, X. M., Wilson, M. S and Gottesfeld, S (1996). High-performance direct methanol polymer electrolyte fuel cells. *Journal of Electrochemical Society*, **143**: 12-15
- Rikukawa, M and Sanui, K (2000). Proton-conducting polymer electrolyte membranes based on hydrocarbon polymers. *Progress in Polymer Science*, **25**: 1463.
- Robertson, G. P., Mikhailenko, S. D., Wang, K., Xing, P., Guiver, M. D., Kaliaguine, S (2003). Casting solvent interactions with sulfonated poly(ether ether ketone) during proton exchange membrane fabrication. *Journal of membrane Science*, **29**: 113.
- Rusanov, A. L and Bulycheva, E. G (1991). Polyimides and other high temperature polymers. In: Abadie, M. J. M and Sillion, B (eds.), Elsevier, Mercier, R French Patent: Ponomarev, I. I., Nikol'skii, O. G, Volkova. Pp 125-149.
- Sageetha, D (2005). Conductivity and solvent uptake of proton exchange membrane based on polystyrene(ethylene-butadiene)polystyrene triblock polymer. *European polymer Journal*, **41**: 2644-2652.

Samuelson, L. A., Anagnostopoulos, A., Alva, K. S., Kumar, J and Tripathy, S. K (1998).
Micromolecules, **31**: 4376.

Savadogo, O and Mater, J. N (1998). Emerging membranes for electrochemical systems: (1)
solid polymer electrolyte membrane for fuel cell systems. *Electrochemical Systems*, **1**:
47-66.

Scherer, G. G and Bunsenges, B (1990). Acid-based polymer blends and their application in
membrane processes. *Physical Chemistry*, **94**: 1008.

Sheng-Li, C., Krishnan, L., Srinivasan, S., Benziger, J and Bocarsly, A. B (2004). Ion
exchange resin/polystyrene sulfonate composite membranes for PEM fuel cells. *Journal
of Membrane Science*, **243**: 327-333.

Shen, M., Roy, S., Kuhlmann, J. W., Scott, K., Lovell, K and Horsfall, J. A. (2005). Grafted
polymer electrolyte membrane for direct methanol fuel cells. *Journal of Membrane
Science*; **251**: 121-130.

Smitha, B., Sridhar, S., Khan, A. A (2003). Synthesis and characterization of proton
conducting polymer membranes for fuel cells, *Journal Membrane Science*, **225**: 63-76.

Smitha, B., Stridhar, S and Khan, A. A (2005). Solid polymer electrolyte membrane for fuel
cell application- a review. *Journal of membrane Science*, **259**: 10-26

Sopian, K and Wan Daud, W (2006). Challenges and future developments in proton exchange
membrane fuel cells. *Journal of Renewable Energy*, **31**: 719-727

Song, C (2002). Fuel processing for low-temperature and high-temperature fuel cells challenges, and opportunities for sustainable development in the 21st century. *Catalysis Today*, **77**: 17-49.

Song, S., Dovatzides, S and Tsiakaras, P (2005). Energy analysis of an ethanol fueled proton exchange membrane fuel cell system for automobile applications. *Journal of Power Sources*, **145**: 123-134.

Srinivasan, S., Omourtag, A. V., Arvind, P., David, J. M and John, A. A (1991). High energy efficiency and high power density proton exchange membrane fuel cells-electrode kinetics and mass transport. *Journal of Power Sources*, **36**: 299-320.

Staiti, P., Hocevar, S and Giordano, N (1997). Fuel cells with H₃PW₁₂O₄₀.29H₂O as solid electrolyte. *International Journal of Hydrogen Energy*, **22**: 809 – 814.

Staiti, P., Lufrano, F., Aricò, A. S., Passalacqua, E and Antonucci, V (2001). Sulfonated polybenzimidazole membranes-preparation and physico-chemical characterization. *Journal of Membrane Science*, **188**: 71-78.

Staiti, P., Aricò, A. S., Baglio, V, Lufrano, F., Passalacqua, E and Antonucci, V (2001). Hybrid Nafion-silica membranes doped with heteropolyacids for application in direct methanol fuel cells. *Solid State Ionics*, **145**: 101-107.

Steele, B. C. H and Heinzel, A (2001). Materials for fuel-cell technologies. *Nature*, **414**: 345-352

- Ueda, M., Toyota, H., Ouchi, T., Sugiyama, J and Yonetake, K (1993). Synthesis and characterization of aromatic poly(ether sulfone)s containing pendant sodium sulfonate groups. *Journal of Polymer Science*, **31**: 853-858.
- Wang, S., Sun, G., Wang, G., Zhou, Z., Zhao, X., Sun, H., Fam, X., Yi, B and Xin, Q (2005). Improvement of direct methanol fuel cell performance. *Electrochemistry Communication*, **7**: 1007-1012.
- Wang, F., Hickner, M and Mcgrath, J. E (2002). Direct polymerization of sulfonated poly(arylene ether sulfone) random (statical) copolymers: candidates for new proton exchange membranes. *Journal of Membrane Science*, **197**: 231-242.
- Wang, F; Li, J Chen, T and Xu, J (1998). Sodium sulfonate-functionalised poly(ether ether ketone)s. *Macromolecular, Chemistry and Physics*, **199**: 1421-1426.
- Warshay, M and Prokopius, P. R (1990). "The fuel cell in space: yesterday, today and tomorrow". *Journal of power Source*, **29** (1&2): 193-200.
- Wasmus, S and Kuver, A (1999). Methanol oxidation and direct methanol fuel cells: a selective review. *Journal of Electroanalytical Chemistry*, **461**: 14-31.
- Watkins, D, Dirck, K., Epp, E and Harkness, A (1986). Proceedings of the 32nd international power sources symposium. *The Electrochemical Society Inc., Pennington, N J*. Pp 590.

Weiss, R. A., Sen, A L., Pottick, A., and Wallis, C. L (1991). Block copolymer ionomers:2. Viscoelastic and mechanical properties of sulphonated poly(styrene-ethylene/butylene-styrene), *Polymer*, **32** (15): 2785-2792.

Weiss, R. A., Sen, A., Wallis, C. L and Pottick, L. A (1991). Block copolymer ionomers:1. Synthesis and physical properties of sulphonated poly(styrene-ethylene/butylene-styrene), *Polymer*, **32** (10): 1867-1874.

Weiss, R. A., Sen, A., Pottik, L. A and Willis, C. L (1990). Block copolymer ionomers. Thermoplastic elastomers possessing two distinct physical networks. *Polymer Communications*, **31**: 220-223.

William, L, H (2002). Sythesis and characterization of sulfonated poly (arylene ether sulfone) copolymers vis direct copolymerization: candidates for proton exchange membrane fuel cells. Dissertation, Virginia Polytechnic Institute and State University, Blacksburg.Pp 1-15.

Wilson, M. S and Gottesfeld, S (1992). Thin film catalyst for polymer electrolyte fuel cell electrode. *Journal of Applied Electrochemistry*, **22**: 1-7

Wonbong, J., Choonkeun, L., Saimani, S., Yong, G. S., and Haksoo, H (2005). Thermal and hydrolytic stability of sulfonated polyimide membranes with varying chemical structure. *Polymer degradation and Stability*, **90**: 431-440.

- Wonbong, J., Saimani, S., Seunghyuk, C., Yong-Gun, S and Haksoo Han (2006). Acid-base polyimide blends for the application as electrolyte membrane for fuel cells. *Journal of Membrane Science*, **280**: 321-329.
- Woo, Y., Oh S.E., Kang Y.S and Jung B (2008): Synthesis and Characterization of sulfonated polyimide membrane for direct methanol fuel cell. *Journal of Membrane Science*, **220**: 31-45.
- Wycisk, R and Pintauro, P. N (1996). Sulfonated polyphosphazene ion-exchange membranes. *Journal of Membrane Science*, **199**: 155-160.
- Xianguo, L (2006). Principles of fuel cells. Taylor and Francis group, LLC, New York. Pp 1-147.
- Xing, P, Robertson, G. P., Guiver, M. D., Mikhailenko, S. D., Wang, K and Kaliaguine, S (2004). Synthesis and characterization of sulfonated poly (ether ketone) for proton exchange membrane. *Journal of Membrane Science*, **229**: 95-106.
- Xu, T (2005). Ion exchange membrane: State of their development and perspective, *Journal of Membrane science*, **263**: 1-29.
- Zawodzinski, T. A., Smith, V. T and Gottesfeld, S (1993). Water uptake by the transport through Nafion 117 membranes. *Journal Electrochemical Society*, **140**: 1041

- Zhou, Z., Peifer, D and Chu, B (1994). Light scattering studies of block ionomer aggregation characteristics in nonpolar solvent. *Macromolecules*, **27**: 1428-1433
- Zongwu, B, Michael, F. D., and Thuy, D. D (2006). Proton conductivity and properties of sulfonated polyarylenethioether sulfones as proton exchange membranes in fuel cells. *Journal of Membrane Science*, **281**: 508-516.
- Yan, G., Gilles, P. R., Micheal, D. G., Serguei, D. M., Xiang, L. and Serge K (2006). Low-swelling proton-conducting copol(aryl ether nitrile)s containing naphthalene structure with sulphuric acid group meta to the ether linkage. *Polymer*, **47**: 808-816.
- Yeager, A. L and Steck, A (1981). Proton transport in polymer electrolyte fuel cell membranes: an overview over the recent experimental, theoretical and simulation studies. *Electrochemical Society*, **128**: 1880-1884.
- .
- Yeo, R. S and Yeager, H. L (1985). Structural and transport properties of perfluorinated ion – exchange membrane. *Modern Aspects of Electrochemistry*, eds., Conway, B. E., White, R. E and Bockris, J. O. M. Plenum Press, New York. No 16.
- Yu, S. K., Feng, W. M. H., Thomas A. Z and James E. M (2003). Fabrication and characterization of heteropolyacid (H₃PW₁₂O₄₀)/directly polymerized sulfonated poly(arylene ether sulfone) copolymer composite membranes for higher temperature fuel cell applications. *Journal of Membrane Science*, **212**: 263 – 282.

Zawodzinski, T. A., Smith, V. T and Gottesfeld (1993). Water uptake by the transport through Nafion 117 membrane. *Journal of electrochemical Society*, **140**:1041.

APPENDIX 1

Table i : Effect of Acid Concentration on the DS and IEC of PSBR

Acid Concentration (M/ml)	% S	DS (%)	Ion Exchange Capacity (mmol/g)
0.4	1.32	6.73	0.412
0.6	1.76	9.13	0.552
0.8	2.27	11.92	0.711
1	2.35	12.34	0.735
1.2	2.49	13.13	0.779
1.4	2.88	15.39	0.903
1.6	3.68	20.04	1.15
1.8	3.39	18.35	1.062
2	3.13	16.76	0.977

where IEC = Ion Exchange Capacity; DS = Degree of Sulphonation

Table ii: Effect of Acid Concentration on DS, IEC and Viscosity on PSBR

IEC (mmol/g)	DS (%)	Viscosity dl/g
0.412	6.73	0.58
0.552	9.13	0.63
0.711	11.92	0.68
0.735	12.34	0.68
0.779	13.13	0.69
0.903	15.39	0.74
1.15	20.04	0.8

where IEC = Ion Exchange Capacity; DS = Degree of Sulphonation

APPENDIX 2

Table iii: Effect of Time on DS and IEC of PSBR

Time (hrs)	% S	Degree of Sulphonation (%)	Ion Exchange Capacity (mmol/g)
2	2.50	13.22	0.784
4	2.79	14.84	0.873
6	3.36	18.16	1.052
8	4.12	22.74	1.289
10	4.96	28.07	1.553
12	5.16	29.35	1.615
14	5.44	31.17	1.701
16	5.65	32.6	1.768
18	5.89	34.18	1.841
20	6.06	35.34	1.894
22	6.33	37.23	1.979
24	6.64	39.38	2.074
36	4.23	23.45	1.325
48	4.15	22.93	1.299

where IEC = Ion Exchange Capacity; DS = Degree of Sulphonation

Table iv: Effect of Time on the DS and Viscosity of PSBR

Time (hrs)	Degree of Sulphonation (mmol/g)	Viscosity (dl/g)
2	13.22	0.69
4	14.84	0.72
6	18.16	0.78
8	22.74	0.87
10	28.07	1.03
12	29.35	1.09
14	31.17	1.13
16	32.6	1.19
18	34.18	1.37
20	35.34	1.4
22	37.23	1.53
24	39.38	1.61
36	23.45	0.95
48	22.93	0.84

APPENDIX 3

Table v: Effect of Stirring Speed on DS and IEC

Stirring Speed (rpm)	% S	Degree of Sulphonation (%)	Ion Exchange Capacity (mmol/g)
250	0.96	4.76	0.3
500	1,08	5.37	0.3375
750	1.24	6.17	0.388
1000	1.36	6.77	0.425
1250	1.48	7.65	0.4625
1500	4.04	20.45	1.263

APPENDIX 4

Table vi: Effect of Temperature on % Sulphure (S)

Time (hrs)	22oC	35oC	55oC	65oC	75oC
0	0	0	0	0	0
3	1.408202	2.143371	2.977546	3.513272	3.775285
6	2.107106	3.058746	4.797217	4.951298	6.941577
9	3.008686	3.908978	5.412984	6.914031	7.871987
12	3.335885	4.842494	6.435684	7.494845	8.655902
15	3.638915	5.259958	6.934695	8.350321	9.295689
18	3.938551	5.61391	7.567814	8.896086	9.747181
21	4.448251	5.998544	7.936784	9.216129	10.27214
24	4.772186	6.589657	8.490763	9.594708	10.53808

Table vii: Effect of Temperature on IEC

Time (Hrs)	Temperature °C				
	22	35	55	75	85
3	0.44	0.66	0.93	1.09	1.18
6	0.65	0.95	1.49	1.54	2.16
9	0.94	1.22	1.69	2.16	2.45
12	1.04	1.51	2.01	2.34	2.70
15	1.13	1.64	2.16	2.60	2.90
18	1.23	1.75	2.36	2.78	3.04
21	1.39	1.87	2.48	2.88	3.21
24	1.49	2.05	2.65	2.98	3.29

Table viii: Effect of Temperature on DS

Time (Hrs)	Temperature °C				
	22	35	55	75	85
3	7.21	11.9	15.9	19.04	20.61
6	10.99	16.37	26.96	27.95	41.58
9	16.08	21.42	30.97	41.38	48.84
12	17.99	27.25	37.96	45.67	54.73
15	19.79	29.96	41.53	52.69	60.02
18	21.6	32.31	46.22	59.69	63.89
21	24.75	34.92	49.04	59.35	68.54
24	26.8	39.05	53.4	62.57	70.86

APPENDIX 5

Table ix: Kinetics of PSBR Conversion at Different Concentrations of Acid

Time (hrs)	Concentration (M/ml)				
	0.4	0.8	1.0	1.4	1.6
0	0	0	0	0	0
2	0.0201	0.0301	0.0468	0.0705	0.1322
4	0.0329	0.0479	0.0643	0.1007	0.1484
6	0.0438	0.0623	0.0925	0.1279	0.1816
8	0.0529	0.0795	0.1029	0.1389	0.2274
10	0.0639	0.0913	0.1192	0.1549	0.2805
12	0.0657	0.1037	0.1295	0.1773	0.2935
14	0.0782	0.1102	0.1463	0.1823	0.3117
16	0.0813	0.1187	0.1523	0.1955	0.326
18	0.0882	0.1313	0.1598	0.2167	0.3418
20	0.0921	0.1407	0.1832	0.2261	0.3534
22	0.0978	0.1419	0.1864	0.2417	0.3723
24	0.1024	0.1503	0.1934	0.259	0.3938
36	0.1279	0.1857	0.2299	0.2301	0.2345
48	0.1475	0.2119	0.2519	0.2287	0.2293

Table x: $-\ln(1-X)$ as a Function of Time

Time (hrs)	0.4 M/ml	0.8 M/ml	1.0 M/ml	1.4 M/ml	1.6 M/ml
0	0	0	0	0	0
2	0.020304753	0.0305623	0.0479305	0.0731085	0.141794
4	0.033453376	0.0490852	0.0664604	0.1061386	0.1606383
6	0.044788183	0.0643252	0.0970617	0.1368512	0.2004041
8	0.054350595	0.0828383	0.1085879	0.1495446	0.2579938
10	0.066032971	0.0957403	0.1269247	0.1683003	0.3291988
12	0.067957693	0.1094801	0.1386875	0.1951637	0.3474321
14	0.081426999	0.1167586	0.1581754	0.2012598	0.3735305
16	0.084795652	0.1263572	0.1652285	0.2175343	0.3945252
18	0.092334611	0.1407574	0.1860886	0.2442395	0.4182464
20	0.096621039	0.1516372	0.202361	0.2563126	0.4360274
22	0.102919054	0.1530346	0.2062864	0.2766762	0.4656929
24	0.108030744	0.1628719	0.2149274	0.2997547	0.5005453
36	0.136851183	0.2054264	0.2612349		
48	0.15958207	0.2381303	0.2902186		

Table xi: $C_0\{-X\ln(1-X)\}$ as a function of Time

Time (hrs)	0.4 M/m	0.8 M/ml	1.0 M/ml	1.4 M/ml	1.6 M/ml
0	0	0	0	0	0
2	1.40215E-05	3.166E-05	7.7419E-05	0.0001786	0.000657
4	3.78952E-05	8.116E-05	0.000147942	0.0003724	0.0008381
6	6.76708E-05	0.0001387	0.000312386	0.000613	0.0012877
8	9.93367E-05	0.0002286	0.00038951	0.0007289	0.0020951
10	0.000146066	0.0003041	0.000528987	0.0009177	0.0033349
12	0.000154607	0.0003958	0.000629161	0.0012233	0.0036933
14	0.000220985	0.0004491	0.00081323	0.0012984	0.0042342
16	0.000239382	0.0005244	0.000885342	0.0015089	0.0046926
18	0.000283138	0.0006476	0.001115446	0.0018859	0.0052351
20	0.000309601	0.000749	0.001312146	0.002069	0.0056583
22	0.000350553	0.0007625	0.001361823	0.0023952	0.0063955
24	0.000385593	0.0008609	0.001474196	0.0027909	0.0073099
36	0.000612977	0.0013509	0.002145814		
48	0.00082738	0.0017963	0.002624059		

Table xii: Model data

Time (hrs)	0.4 M/ml	0.8 M/ml	1.0 M/ml	1.4M/ml	1.6 M/ml
0	0	0	0	0	0
2	0.0276393	0.0366815	0.0438548	0.0720176	0.1060574
4	0.0410327	0.0543326	0.0648396	0.1057132	0.1543021
6	0.0516261	0.0682356	0.0813135	0.1318151	0.1910563
8	0.0607106	0.080117	0.0953531	0.1538153	0.2216091
10	0.068804	0.0906701	0.1077927	0.1731192	0.2480926
12	0.0761788	0.1002595	0.1190714	0.1904671	0.2716305
14	0.0829996	0.109106	0.129455	0.2063079	0.2929045
16	0.0893756	0.1173558	0.1391196	0.2209391	0.3123664
18	0.0953835	0.1251116	0.1481891	0.2345703	0.3303344
20	0.1010799	0.1324494	0.156755	0.247356	0.3470432
22	0.1065078	0.139427	0.164887	0.2594141	0.3626718
24	0.111701	0.1460898	0.1726398	0.2708374	0.3773606
36	0.1391629	0.1811055	0.2131833		
48	0.1622707	0.2102828	0.2467036		

APPENDIX 6

Table xiii: Water Uptake at Different Degrees of Sulphonation and Constant Membrane Thickness of 350 μ m

Time (Days)	DS=5.85	DS=9.4	DS=18.16	DS=28.07	DS=37.23	DS=39.38
0	0	0	0	0	0	0
1	9.7356	12.81	19.215	26.901	33.306	39.711
2	13.3456	17.56	26.34	36.876	45.656	54.436
3	15.6712	20.62	30.93	43.302	53.612	63.922
4	17.1304	22.54	33.81	47.334	58.604	69.874
5	17.1304	22.54	33.81	47.334	58.604	69.874
6	17.1304	22.54	33.81	47.334	58.604	69.874
7	17.1304	22.54	33.81	47.334	58.604	69.874
8	17.1304	22.54	33.81	47.334	58.604	69.874

Table xiv: Water Uptake at Different Membrane Thickness and Constant Degree of Sulphonation (9.4%)

Time (Days)	Membrane Thickness (120 μ m)	Membrane Thickness (160 μ m)	Membrane Thickness (220 μ m)	Membrane Thickness (330 μ m)	Membrane Thickness (350 μ m)	Membrane Thickness (420 μ m)
0	0	0	0	0	0	0
1	16.75	18.57	32.39	27.86	12.81	7.33
2	24.18	27.14	34.66	30.96	17.56	10
3	35.24	37.14	39.21	32.2	20.62	12.67
4	48.45	50	45.46	33.13	22.54	16.67
5	55.78	52.86	46.59	38.08	22.54	16.67
6	60.33	54.29	46.59	41.49	22.54	16.67
7	60.33	54.29	46.59	41.49	22.54	16.67
8	60.33	54.29	46.59	41.49	22.54	16.67

APPENDIX 7

Table xv: Effect of Hydration and Temperature on Proton Conductivity at Different Degrees of Sulphonation

Degree of Sulphonation (%)	Partially hydrated (20oC)	Fully hydrated (20oC)	Fully Hydrated (35oC)	Fully hydrated (50oC)
2.2	0.001461	0.002283	0.002427	0.00265
3.76	0.002655	0.00347	0.003792	0.003973
3.96	0.002712	0.00357	0.003821	0.004139
4.75	0.003014	0.003601	0.004171	0.004218
5.85	0.00315	0.003687	0.004314	0.004536
8.23	0.003451	0.003714	0.004817	0.005279
11.92	0.003589	0.003798	0.005016	0.005745
12.34	0.00371	0.003877	0.005213	0.00618
28.07	0.004586	0.004791	0.006288	0.00815
34.18	0.004714	0.005493	0.006714	0.009346
37.23	0.005019	0.006312	0.008076	0.01287
39.38	0.005213	0.008154	0.009449	0.016076

Table xvi: Effect of Membrane Thickness on the Proton conductivity of the Membrane
at Different degrees of Sulphonation

Membrane Thickness (μm)	DS =2.2	DS =3.76	DS =3.96	DS =4.75	DS =9.4
170	0.003632	0.0040663	0.00457126	0.0048743	0.00773332
190	0.003531	0.0039169	0.00429489	0.004544715	0.00742887
200	0.003433	0.0038082	0.00410792	0.004436695	0.00739656
220	0.003218	0.0036034	0.00400206	0.004274426	0.00707421
290	0.002942	0.0033701	0.00395628	0.004121	0.00693632
300	0.00285	0.0032299	0.00391534	0.004009	0.00676791
320	0.002831	0.0031483	0.00385387	0.003917	0.00658318
340	0.002789	0.003105	0.00381363	0.003894	0.00647464
360	0.002714	0.0030547	0.00377255	0.003827	0.00625721
380	0.002673	0.0028624	0.0036142	0.003732	0.00616228
390	0.002595	0.0028216	0.0035846	0.003692	0.00615621
450	0.002332	0.0026819	0.00344433	0.003584	0.00567058

Membrane Thickness (μm)	DS =12.23	DS =25.49	DS =39.38
170	0.0095125	0.009817	0.015839
190	0.0093416	0.009716	0.013474
200	0.0088775	0.00941	0.01332
220	0.0081335	0.009086	0.013275
290	0.0074182	0.008716	0.013076
300	0.007319	0.008513	0.012928
320	0.007216	0.008218	0.012654
340	0.007016	0.007914	0.012234
360	0.006917	0.007612	0.012195
380	0.006413	0.007432	0.011355
390	0.006298	0.007009	0.010688
450	0.005987	0.006985	0.009379

APPENDIX 8

Table xvii: Methanol Molecule Uptake Per Sulphonic Group at Different Concentration of Methanol

Methanol Concentration (mol/dm ³)	DS= 3.86	DS =5.85	DS =10.48	DS =11.92	DS =12.34
0.00	0.0000	0.0000	0.0000	0.0000	0.0000
0.50	5.1398	3.0839	2.4043	1.6220	1.5157
1.00	10.0694	6.0417	4.7103	3.1776	2.9694
2.00	19.4384	11.6631	9.0929	6.1342	5.7322
4.00	37.6620	22.5973	17.6174	11.8850	11.1062
6.00	56.0599	33.6360	26.2236	17.6909	16.5316
8.00	72.7127	43.6277	34.0134	22.9460	21.4424
10.00	89.5724	53.7436	41.9000	28.2665	26.4142
12.00	105.0249	63.0152	49.1284	33.1429	30.9711
24.63	115.5975	69.3590	54.0743	36.4797	34.0892

Methanol Concentration (mol/dm ³)	DS =15.39	DS =29.45	DS =39.38
0.00	0.0000	0.0000	0.0000
0.50	1.2980	0.7390	0.4894
1.00	2.5428	1.4477	0.9588
2.00	4.9088	2.7947	1.8510
4.00	9.5107	5.4148	3.5862
6.00	14.1567	8.0599	5.3381
8.00	18.3620	10.4542	6.9239
10.00	22.6196	12.8782	8.5293
12.00	26.5219	15.0999	10.0008
24.63	29.1922	16.6205	11.0081

APPENDIX 9

Table xviii: Effects of Membrane Thickness on the Porosity of the Membrane at Different Concentration of Methanol

Methanol Concentration (mol/dm ³)	Membrane Thickness =120 μ m	Membrane Thickness =350 μ m	Membrane Thickness =420 μ m
0	0.076356	0.0601132	0.048337
0.5	0.088663679	0.067029051	0.052224476
1	0.093280682	0.076316171	0.052810627
2	0.106368665	0.086842255	0.05583182
4	0.106857702	0.094534219	0.061504716
6	0.12218445	0.106189076	0.070628831
8	0.128650031	0.112710566	0.074434512
10	0.144161253	0.124128014	0.078209697
12	0.163187455	0.130270188	0.08146747
24	0.172151978	0.132897537	0.082340744

APPENDIX 10

Table xix: Uptake of Solution Per Sulphonic Group

Methanol Concentration (M)	Total uptake of solution molecule	Total uptake of water molecule	Methanol molecule uptake
0	26.1013	26.1013	0
0.5	24.11007322	23.62063874	0.489434486
1	23.61641358	22.65758719	0.958826391
2	22.79510162	20.94413937	1.850962252
4	22.08273879	18.49650201	3.586236779
6	21.67330371	16.33516901	5.338134705
8	21.31730825	14.39344653	6.923861721
10	21.00816944	12.47885265	8.529316793
12	20.52703337	10.52626271	10.00077066
24.63	11.00805917	0	11.00805917

APPENDIX 11

Table xx: Methanol Crossover Concentration at Different Degree of Sulphonation

Time	DS=3.37	DS=5.97	DS=15.17	DS=25.45	DS=39.2
0	0	0	0	0	0
1800	0.224455	0.17808	0.1827	0.1596	0.1134
3600	0.450765	0.350595	0.2772	0.2373	0.2016
5400	0.573195	0.532385	0.3654	0.3045	0.2772
7200	0.717885	0.654815	0.4263	0.3402	0.3318
9000	0.86814	0.754985	0.5061	0.3864	0.3696
10800	1.007265	0.855155	0.6006	0.4368	0.4053
12600	1.088885	0.93492	0.6594	0.5061	0.4641
14400	1.151955	1.06106	0.7413	0.6153	0.5502
16200	1.233575	1.118565	0.7875	0.7266	0.6321
18000	1.307775	1.21317	0.8337	0.8001	0.7182
19800	1.34673	1.266965	0.9261	0.8862	0.7812
21600	1.367135	1.30963	1.0122	0.9807	0.8421
23400	1.456175	1.385685	1.1298	1.0773	0.9282
25200	1.508115	1.41351	1.2222	1.1823	1.0143
27000	1.567475	1.459885	1.2516	1.2096	1.0206
28800	1.59901	1.49884	1.3503	1.2453	1.071
30600	1.623125	1.50997	1.3776	1.2432	1.1052
30660	1.63141	1.51114	1.3776	1.2432	1.1052
30720	1.63162	1.51119	1.3776	1.2432	1.1052
30780	1.63165	1.51201	1.3776	1.2432	1.1052
30840	1.63164	1.51203	1.3776	1.2432	1.1052
30900	1.63164	1.51203	1.3776	1.2432	1.1052

APPENDIX 12

Table xxi: Performance of MEA at Different Weight of Catalyst, Constant Membrane DS (39.38%) and Nafion 112.

Current density	Voltage 40 Wt%	voltage Nafion	Voltage 30 Wt%	Voltage 20 Wt%	Voltage 10 Wt%
0	718.75	700.89	689.79	520.48	307.45
5.72	704.5	698.89	647.54	469.24	259.76
12.688	678.9	669.98	569.87	398.56	220.45
29.952	645.15	588.634	489.99	322.575	191.545
47.84	618.7	556.83	433.09	300.78	185.61
87.984	583.05	524.745	400.56	291.525	178.914
108.316	534.9	482.45	374.43	258.56	160.47
125.32	494.5	445.05	355.65	247.25	148.35
160.576	443.9	399.51	310.73	219.78	136.023
182.52	403.65	366.286	280.55	201.825	119.098
199.68	369	332.1	258.3	180.78	115.8
211.848	334.65	294.25	234.255	167.325	100.395
221.312	305.9	275.31	210.67	150.95	89.78
232.96	256.15	234.54	179.305	128.075	76.845
250.64	231.15	208.035	161.805	112.567	69.89
256.8	229.85	209.87	156.89	114.925	58.955

where Current density is in mA/cm² and Voltage in mV

Table xxii: Power Density at Different Weight of Catalyst, Constant Membrane DS (39.38%) and Nafion 112.

Current Idensity	P - density 40 Wt%	P – density Nafion	P - density 30 Wt%	P - density 20 Wt%	P – density 10 Wt%
0	0	0	0	0	0
5.72	4.02974	3.9976508	3.7039288	2.6840528	1.4858272
12.688	8.6138832	8.50070624	7.23051056	5.05692928	2.7970696
29.952	19.3235328	17.63076557	14.67618048	9.6617664	5.73715584
47.84	29.598608	26.6387472	20.7190256	14.3893152	8.8795824
87.984	51.2990712	46.16916408	35.24287104	25.6495356	15.74156938
108.316	57.9382284	52.2570542	40.55675988	28.00618496	17.38146852
125.32	61.97074	55.773666	44.570058	30.98537	18.591222
160.576	71.2796864	64.15171776	49.89578048	35.29139328	21.84202925
182.52	73.674198	66.85452072	51.205986	36.837099	21.73776696
199.68	73.68192	66.313728	51.577344	36.0981504	23.122944
211.848	70.8949332	62.336274	49.62645324	35.4474666	21.26847996
221.312	67.6993408	60.92940672	46.62379904	33.4070464	19.86939136
232.96	59.672704	54.6384384	41.7708928	29.836352	17.9018112
250.64	57.935436	52.1418924	40.5548052	28.21379288	17.5172296
256.8	59.02548	53.894616	40.289352	29.51274	15.139644

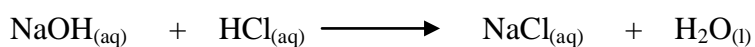
where $P - \text{density} = \text{power density in } \text{wM}/\text{cm}^2$ and $\text{Current density in } \text{mA}/\text{cm}^2$

APPENDIX 13

TITROMETRIC QUANTIFICATION OF HCl CONCENTRATION IN AQUEOUS SOLUTION

Considering 60 ml of $3.9 \times 10^{-5} \text{ mol L}^{-1}$ NaOH neutralising 25 ml of HCl

The balance chemical equation for the acid-base reaction is;



NaOH Volume (V) = 60 ml, Concentration (M) = $3.9 \times 10^{-5} \text{ mol L}^{-1}$

HCl Volume (V) = 25 ml, Concentration (M) = ?

Under standard condition, checking data for consistency;

NaOH $V = 60 \times 10^{-3} \text{L}$, $M = 3.9 \times 10^{-5} \text{ mol L}^{-1}$

HCl $V = 25 \times 10^{-3} \text{L}$, $M = ?$

Mole of NaOH

$n(\text{NaOH}) = M \times V = 2.3 \times 10^{-6} \text{ moles}$

From balance chemical equation, mole ratio is;

NaOH : HCl

1 : 1

Moles of HCl therefore;

$n(\text{NaOH}) = (\text{HCl}) = 2.34 \times 10^{-3} \text{ moles}$

Concentration of HCl is obtained;

$$M = n/V$$

$$n = 2.34 \times 10^{-4} \text{ moles, } V = 25 \times 10^{-3} \text{L}$$

$$M(\text{HCl}) = 2.34 \times 10^{-3} \text{ moles}/25 \times 10^{-3} \text{L}$$

$$= 9.36 \times 10^{-5} \text{ M or } 9.36 \times 10^{-5} \text{ mol L}^{-1}$$

APPENDIX 14

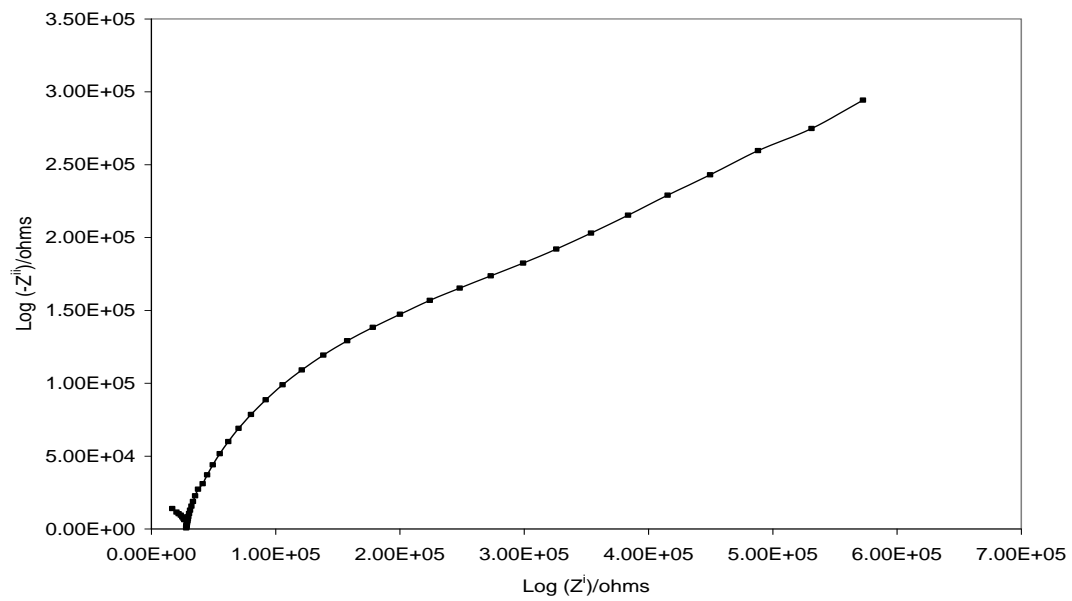
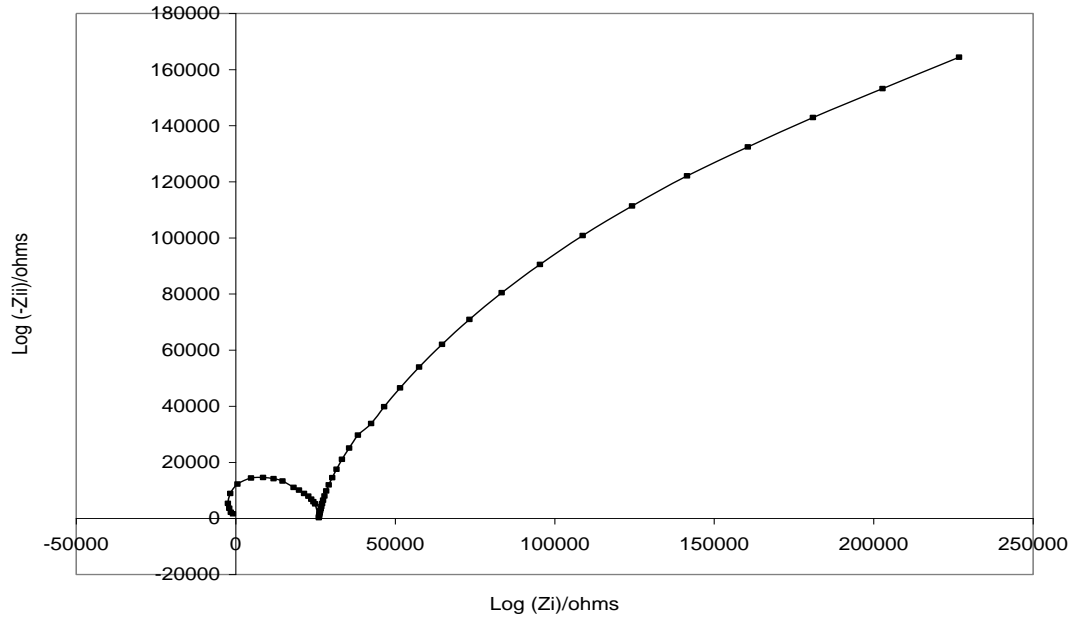


Figure i: A graph of Proton Conductivity Measurement of the Synthesised Membrane from Impedance Spectroscopy